Damping of Power Oscillations in Large Power Systems

Eliasson, Bo

1990

Document Version:
Publisher's PDF, also known as Version of record

Damping of Power Oscillations in Large Power Systems

Bo Eliasson

Lund 1990

To

Ingalill,
Johan,
Sandra
and
Nina

Department of Automatic Control
Lund Institute of Technology
Box 118
S-221 00 LUND
Sweden

Published 1990
Printed in Sweden by Studentlitteratur AB

Abstract

Many of the power systems of today are probably the largest MIMO-systems (Multi Input Multi Output) ever built by mankind. A lot of research has been done during the last twenty years about tuning of damping equipment in power systems. Damping equipment of concern in this thesis are PSSs (Power System Stabilizers), SVCs (Static Var Compensators), and HVDC (High Voltage Direct Current) links. A large number of design techniques have been presented, from conventional SISO-design (single input–single output), root-loci design to modern techniques such as LQ-design and MIMO-techniques (multi input–multi output). Unfortunately, the existing control design techniques cannot cope with large power systems, which models typically have more than 2000 states. Either the techniques are too time consuming for the designer or the computational demand is far beyond the capacity of modern computers. Another important feature, which seldom is included in the models or the design procedures, is the characteristics of the load. Especially the voltage dependence of the load has a major impact on the performance and tuning of parameters concerning the PSSs and the SVCs. The frequency dependence of the load becomes important in connection with HVDC links.

This thesis focuses on four major topics: (1) Modelling of a large power system with respect to slow oscillations (two states/generator); (2) Aggregation of large power systems with preservation of the slow dynamics; (3) Finding proper feedback structures for the different damping equipment for the siting and tuning analysis; (4) Formulation of an optimization problem for tuning of control parameters applicable to damping equipment in a large power system.

Only slow and system wide modes are of concern in this thesis, i.e. modes with a frequency less than about 0.8 Hz. Faster modes are rather well damped due to the damper windings in the generators. At the most a three state concept for damping is enough. For slow modes, though, a two state concept is enough, which is also pointed out in this thesis. The optimization problem is tested for 200 parameters and the tuning works well. This amount of parameters covers the need of tuning of slow modes in a large power system.

Contents

Preface

The goals of this thesis were formulated during the first half of 1986. During this period a guest professorship was funded by Sydkraft AB and Vattenfall. David Hill from the University of Newcastle in Australia held this professorship. An ultimate question, which we tried to answer, was how to tune damping equipment with respect to slow oscillations in a large power system. This led to the research results which are reported here.

During 1987 a research program was presented for the Nordic Fund for Technology and Industrial Research. The decision was that the project should go on for another two years period. Most of the educational program was also planned at this stage. Courses concerning control theory and mathematics were read at Lund Institute of Technology. Power system theory was examined at the Technical University of Denmark, DTH. An essential period of experiences shall also be added to the basic knowledge. The author has worked 3 years at Network Control, ABB, three years at HVDC, ABB, and eight years at Sydkraft AB, of which five years at the operational department.

This thesis points out some interesting research fields concerning control of large (power) systems, e.g. modeling with respect to interesting dynamics, analysis of inherent structures, application of modern numerical and mathematical methods, synthesis of a MIMO-system. The universities have a great opportunity to develop new methods and tools concerning large systems. Therefore the industry of concern should make long term investments in this field and support research institutes so new tools can be foreseen in the future. The joint research between DTH, LTH and Sydkraft AB must be considered successful. Hopefully the reader get interested in the combination of large power system and automatic control.

Acknowledgement

I wold like to thank my superiors at Sydkraft for their support. Especially, a heartily thank goes to my superior Sture Lindahl, Sydkraft AB, for his great support, guidance and enthusiastic discussions during this period of research. I am also grateful to Karl Johan Åström for his initiative to start this project. A special thank goes to Björn Wittenmark and Per Hagander for reading and commenting my thesis. Their experiences and suggestions have greatly improved the verification of the model and the optimization part of this thesis.

A warm thank goes to Jan Rönne-Hansen and his staff at DTH, Denmark, for their hospitality and interesting courses. Jan has been an interested reader and commentator of my thesis. I also would like to express my gratitude to David Hill, University of Newcastle, Australia, for our interesting discussions and guidance at the start of this project, especially the siting analysis. David Hill has also improved many parts of my thesis and the layout.

A special thank goes to my colleagues at LTH and especially to Magnus Akke. He has been a good friend and an enthusiastic collaborator during our common studies at DTH and LTH.

This thesis has been supported by the Nordic Fund for Technology and Industrial Research and administrated by the Danish Academy of Technical Sciences, ATV. Birgitte Rolf Jacobsen has done a honourable administratión of this project (NIFU 6).

Finally, a heartily thank to my family and especially to my wife, Ingalill.

1

Introduction

1.1 Aims of the Thesis

A power system is probably the largest MIMO-system ever built by mankind. A lot of control activities take place every moment. This thesis focus on control of slow Electro Mechanical Oscillations (EMO) or power oscillations in large power systems, e.g. several hundreds of generators.

The EMOs can be illustrated by the following mechanical analog. A number of masses, representing the inertia of the generators in the electric system, are suspended from a "network" consisting of elastic strings, the latter representing the electric transmission lines. The system is in a static steady state, with each string loaded below its break point (corresponding to the fact that each transmission line is operated below its static stability limit). At this point one of the strings is suddenly decoupled and recoupled after a short period of time, representing a breaker operation after e.g. a hit of lightning on a certain line. As a result the masses will experience coupled motions, and the forces in the strings will fluctuate. The system will settle down to the same equilibrium state, characterized by the same set of string forces (i.e. the same line powers in the electric case).

In a power system the machine angles will start to oscillate relatively to each other. The amplitudes are regarded to be within the limits for linear analysis, i.e. Small Disturbance Stability Analysis (SDSA). These oscillations can also start spontaneously and are not due to elements with highly nonlinear characteristics. When these spontaneous oscillations appear the damping will be the critical factor for power transfer. The limit of the transfer capacity is set by damping demands. In other cases the transfer limit of power can be set by transient

conditions or thermal demands of the components in the power system. The EMOs are in general damped by PSSs. Also SVCs and HVDC links are used for this purpose.

The dominant control activities in a power system are to keep the frequency and the magnitude of the voltage within certain stipulated limits. The frequency control is executed by the turbine regulators. These regulators change the active power input to the generators dedicated for frequency control. The frequency deviation is the input signal. Also Automatic Generation Control (AGC) is used for frequency control, higher up in the control hierarchy. The AGC control is mainly used when several big power areas are interconnected, e.g. the Nordel power system. The voltage control in a large power system is executed by several devices, such as: shunt capacitors, shunt reactors, tap changers on the transformers and thyristor controlled SVCs and AVRs.

The terminal voltage of the generator is controlled by changing the magnetization of the synchronous machine. This is arranged by an Automatic Voltage Regulator (AVR). A lot of control activities are also taken place in the power plants, such as: control of pressure, temperature and heat flows.

The EMOs caused large problems during the 1960's when interconnection of power system was a new challenge for power engineers. Many medium-sized power systems were connected to large power systems using tielines. In order to run the system with a reasonable stability margin it was necessary to set power limitations on certain branches or cut sets. These limitations were determined through simulations. In the early sixties an intensive research period started in order to master the EMOs. Figure 1.1 shows the distribution of the EMOs in the Nordel power system. After 1973 the EMOs occurred rather seldom. The explanation is that the first 400 kV cable between Zealand and Sweden was installed. In the early 1970's also the ties between Sweden and Norway were strengthened. Some serious EMOs have occurred during the 1980's. Damping equipments of concern at this time were PSSs (Power System Stabilizers) and HVDCs (High Voltage Direct Current links). Many different design techniques were presented for the PSSs. The HVDC links had already been used for damping purposes (Pacific Intertie). In the early eighties also SVCs (Static Var Compensators) were taken into operation for damping of EMOs. The PSSs are added on devices to the regular AVR systems of the generators. Some overall questions arise:

- Which are the important generators, i.e. generators which have a major impact on the energy of the slow system wide modes?
- How to tune the parameters of different control laws corresponding to PSS-, SVC- and HVDC-equipment coordinated in a large power system?

Previous analytical methods of power systems concerning EMOs are not applicable to large power systems. The models are too detailed and demand super computers for being used.

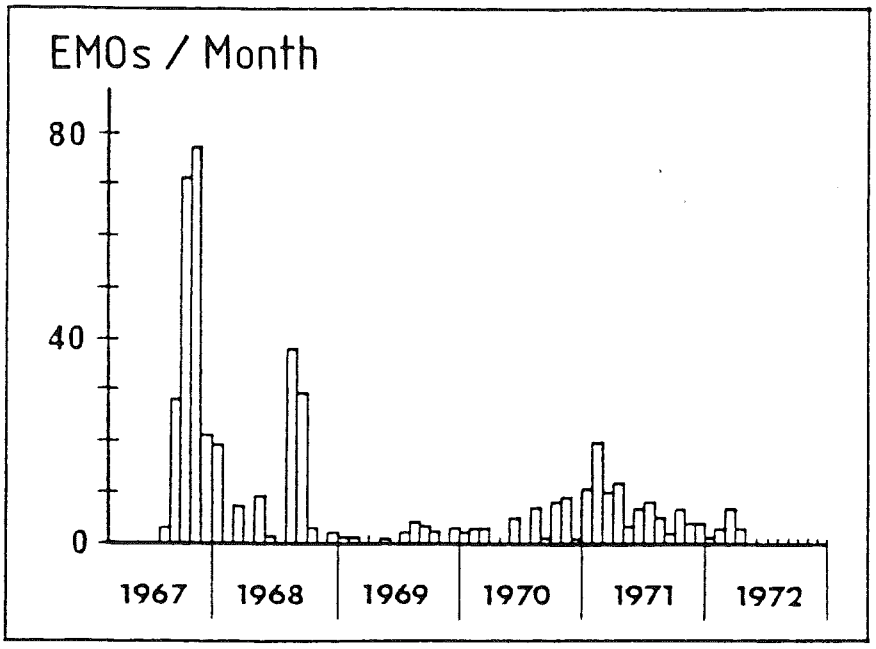

Figure 1.1 Distribution of the EMOs/month in the Nordel power system.

Also the design techniques of today can not be applied to a large power system, except the SISO-concept. The SISO-concept covers one generator swinging against an infinite bus, but in slow and system wide oscillations the interaction between the generators is significant. The formulation of the optimization problem is also very crucial for successful selection of control parameters. In generally all optimization based on linear quadratic theory (LQ) and pole placement are not applicable to large power systems due to the computer time needed.

After an extensive study of state of the art concerning EMOs, it was clear that the dynamic damping problem of large power systems need further research, especially on the methodology side and development of new tools. These tools must be tailor made for the EMO problem and with special attention to the slow EMOs. The aim of this thesis can now be summarized in the following items:

1. Development of a model that well describes the slow dynamics of large power system. The model must also include important characteristics of the load. Only small disturbance stability analysis (SDSA) is considered.
2. A numerical reliable model is of great importance.
3. In a coordinated way include all kinds of damping equipment for siting and tuning analysis.
4. The result will be graphically presented.
5. All methods used must be numerical stable and fast in terms of CPU-time.

6. Important results of the research will be verified against complex nonlinear models accepted by power engineers throughout the world (PSS/E or SIMPOW). In this thesis special attention is paid to the verification of the model and the augmented damping introduced by the developed methodology.

1.2 Previous Work

Introduction to power system stability, nonlinear (transient) stability and steady-state stability can be found in Anderson and Fouad (1977), Elgerd (1971, 1983) and Akke (1989). A nice survey of dynamic stability problems and techniques for introduction of damping is given in Yu (1983). This book also describes different kinds of equivalencing techniques (dynamic equivalents based on coherency).

Generally it can be stated, that tools and methodology available today hardly can be used for design and analysis of inherent quality of large power systems. The methods are too time consuming.

Firstly, time simulations with nonlinear models is not a tool for synthesis of control strategies of large power systems. Secondly, eigenvalue and eigenvector analysis of a linear model, with all kinds of control devices included, of a large power system is unrealistic with computers available of today.

Eigenvalue and eigenvector analysis, though, seems to be a successful way if the number of non important states are drastically reduced with respect to slow power oscillations.

None of the modern MIMO-concepts can be applied to a large power system. The largest number of machines included in a coordinated design technique, in the literature, covers 16 generators. See Akke (1989). Only PSSs are considered and integrated with the AVR system. Intercommunication between PSSs are also established. LQ-design is used in a MIMO-concept and three states per generator is used. Twenty-two hours were needed for the LQ-design on a modern workstation (SUN).

Other authors are using LQ- and pole placement techniques. The methods are applied to a three-machine system in average. See, e.g., Arnautovic *et al.* (1987), Lefebvre (1983), Siwakumar (1985) and Wilson and Aplevich (1986). The SISO-concept can always be applied, but for slow and system wide modes it can hardly lead to a successful design for a large power system, see deMello *et al.* (1980).

Generally, it must be emphasized that only important dynamics shall be modeled due to the control problem and especially for large power systems. A three-state model per generator (Akke (1989)) will cover most of the need for EMO analysis. For slow modes it is enough with a two state concept, which is pointed out in this thesis. Most of the designers of today use too many state. See, e.g., Abdalla *et al.* (1984), Lefebvre (1983), Siwakumar *et al.* (1985), Vournas

et al. (1987) and Wilson *et al.* (1986). deMello *et al.* (1980) and in discussion Abdalla *et al.* (1984) clearly points out that a two-state model is enough for study of the eigenvectors concerning the dynamics of the generators.

A crucial thing is therefore to find a proper model describing the EMOs in a large power system and allow nonlinear loads. Another important question is how to include important system properties, e.g. load characteristics.

Important system properties to include are the frequency and voltage dependence of the load. Especially the voltage dependence of the load is very important to include. Power system stabilizers (PSSs) and Static Var Compensators (SVCs) affect the voltage to introduce damping.

Modern numerical differentiation techniques used for linearization of the systems, have the disadvantage that the designer loses insight of the modeling and the structure of the system. Many of designers never talk about, e.g., voltage dependence of load, see Castro *et al.* (1988), Chow *et al.* (1989), Abdalla *et al.* (1984), Arnautovic *et al.* (1987), deMello *et al.* (1980), Lefebvre *et al.* (1983), Nolan *et al.* (1976), Rudnick *et al.* (1983), Siwakumar *et al.* (1985), Vournas *et al.* (1987), and Wilson *et al.* (1986). The siting of damping equipment depends strongly on the voltage dependence of the load and actual load flow conditions.

The most common siting techniques of today use the sensitivity analysis of the eigenvalues with respect to control parameters. See, e.g., Lefebvre (1983), Nolan *et al.* (1976), Vournas *et al.* (1987) and deMello *et al.* (1980).

The author strongly recommend the use of sensitivity derivatives for siting analysis, because the derivatives depend on the assumptions about the voltage characteristic of the load and the actual load flow. Some designers use the components of the eigenvectors for selecting the most important sites for PSSs, see deMello *et al.* (1980). The author do not believe in these techniques because it doesn't necessarily imply that the real part of the sensitivity derivative also has the largest negative value for selected machine.

It is better to use the mass-scaled eigenvector in this case, but still the last statement is not necessarily fulfilled. deMello *et al.* (1975) do mention the properties of the load concerning dynamic stability but it is not used in the design, deMello *et al.* (1980). This can be explained by the models used. The most commonly used models are generator oriented (Anderson and Fouad (1977)), rather than network oriented (Bergen and Hill (1981)).

To consider analytical aspects of power system dynamics and security, it is of utmost importance to use a structure preserving model. A structure preserving model is used throughout this thesis. This model also gives a technique to robustly site PSSs and SVCs with respect to the voltage dependence of the load. No papers mention these robustness aspects of damping equipment. No overall siting technique for SVCs in a large power system can be found. Only local criteria are analyzed, see Ledwich *et al.* (1982), Ledwich (1983), Kinoshitu (1979), Fujiwara *et al.* (1981) and Padiyar *et al.* (1986).

The HVDC links, in general, are not sited from a damping point of view. Until now the links have been used to damp inter-area oscillations and improve the transfer capacity of power in an AC-system.

This thesis presents a technique to determine alternative points for measurement of the frequency deviation to improve the damping of HVDC-links. No paper presented of today describes a model of a large power system and models of PSSs, SVCs and HVDC links integrated. This implies that no one has described a tuning procedure for these equipments.

Optimization techniques specifying constraints on the eigenvalues can hardly lead to a successful solution, see Siwakumar *et al.* (1985). The inherent aim of modern optimization routines is to take the largest possible step in the best direction for reaching an optimal solution. The eigenvalues are, in general, also a highly nonlinear function of the control parameters. The Jacobian matrix must therefore be updated numerically, which will overload any modern computer. From a numerical point of view it is also bad to calculate the eigenvalues.

The whole analysis is focused on slow and system wide modes of large power systems. Many machines participate in the system wide modes. Therefore a multi-input and multi-output concept must be used, see Brockett (1970), Friedland (1986) and Kailath (1980). The optimization technique must include tuning of all damping equipments dedicated to damp system wide modes. In this thesis one way of a successful optimization is presented.

When developing new software for large power systems it is also of great importance to have a technique to reduce large power systems. The aggregation technique presented in this analysis preserve the dynamics in the low frequency range of power oscillations. This method is based on finding coherent machines among the chosen modes. A new definition is introduced. Another very important aspect of this new definition of coherent machines is, that the grouping of the machines do not depend on any kind of disturbance. Only Geeves (1988) uses a similar technique. The other authors (Gallai *et al.* (1982), Germond and Podmore (1978), Wu *et al.* (1983), Young *et al.* (1988) and Zhou *et al.* (1985)) use different kinds of performance indices. This index-technique is applied to reasonable large power systems (approximately 20 machines) and only large disturbance stability (LDSA) is considered.

Oshawa *et al.* (1978) uses Liapunov-function analysis for definition of coherency. None of this methods can be applied to a large power system. Podmore (1978), though, has applied his technique to 295 generators. The method seems to be time consuming.

The coherency technique in this thesis only demands that the user specify a certain frequency window in the low frequency range and then the computer will present the coherent groups within a couple of minutes for a power system of 250 machines. The low frequency dynamics is preserved during the aggregation.

1.3 Contributions of the Thesis

At an early stage it was clear that the development of a model for slow dynamics should be an important factor throughout the research. After a serious analysis of models, available in the literature, it could be stated that in general too many states are included in the models in terms of computational time needed for our research. A linear model was developed and verified against a detailed non-linear model. The outcome was that a two-state/generator model is enough to model slow oscillations. The AVR-system can be considered fast and the dynamics of the governor systems can be considered as slow in comparison with slow power oscillations. The frequency and voltage dependence of the loads are included in the model. These properties are free to vary in the model.

During 1986 also an embryo to a siting program was developed, but this program could not be applied to a large power system. Early in the start of this project, it was clear that a tool for aggregation of large power systems was needed. The states in the developed linear model are easy to interpret physically. Using this insight into the physical interpretation and the analogy with coherent light sources, it was straightforward to define a new coherency technique. This technique doesn't depend on any applied disturbances, which other coherence techniques do. The need for aggregation was twofolded:

1. Reduce the time for development and testing of programs.
2. Possibilities to reduce the number of free control parameters during the coordinated tuning.

The basic demand of the aggregation was that the characteristics of the slow modes should be preserved during the aggregation. This is also shown in the thesis.

In the early 1987 it was clear from the results, that it should be possible to develop a program for siting of damping equipment in a large power system. At this stage, it also was clear that graphical presentation of the result was the only way to deal with the presentation of results. The siting program can handle 250 generators connected to a power system. A new and important insight of the siting problem was how different load characteristics affect the result.

A cluster point of problems occurred when the optimization problem should be formulated. For a large power system, it is a question of tuning about 200 parameters with constraints and other constraints functions. The Jacobian matrix for the constraint functions must, in general, be updated numerically due to incidents between the damping equipments. This implies that the introduced constraint function must be reasonably easy to update. By investigation of papers written about this problem, e.g., specifying constraints on the eigenvalues, can hardly lead to a successful solution. Reasonable demands on the values of the control parameters may be:

1. The parameters of the controller must vary when the process gain varies, i.e. (in our case) during heavy and light load conditions.
2. The characteristics of the load must affect the values of the parameters.
3. The tuning must guarantee specified damping at least for the slow and system wide modes.
4. The natural frequencies of the power system must be affected as little as possible. Especially, the frequencies must not be decreased in low frequency range during the tuning. The inherent damping of the generators are poor in the low frequency range.

The computational time must also be reasonable from practical point of view. The method must also be numerical stable. These demands were fulfilled by introduction of a new constraint function aimed for large power systems. The verification of the designed PSS-controller, clearly shows that the optimized values have a significant impact on the damping of slow modes. A multivariable theory is used throughout the thesis, because many generators are interacting during slow and system wide oscillations.

The analysis covers the following issues:

1. Design and verification of a model aimed for slow modes. The model is simple enough to allow states for very large power systems, but includes nonlinear loads, PSS, SVC and HVDC.
2. Qualitatively definition of slow and system wide and slow local modes.
3. Definition of a new coherency concept. This procedure can reliably produce a reduced order model within given bandwidth.
4. Sensitivity analysis of PSSs, SVCs and HVDC links with respect to slow and system wide modes and voltage dependence of load. Theoretical insights into network conditions favoring improved damping from various damping devices. Also the speed of calculation is improved by theoretical insights. The left eigenvectors are known when the right eigenvectors are known for the uncontrolled system.
5. Coordinated tuning of PSSs, SVCs and HVDC links with respect to slow and system wide modes and voltage dependence of load. The optimization procedure does not involve repeated calculations of eigenvalues and the procedure is extremely fast. Two cpu-hours for tuning of roughly 200 parameters.
6. Robustness against load characteristics, change of load flow and topology.
7. Improved methodology for presenting mode and sensitivity information for very large systems by graphical means.
8. All results from the different sections are applied to the Nordel power system.

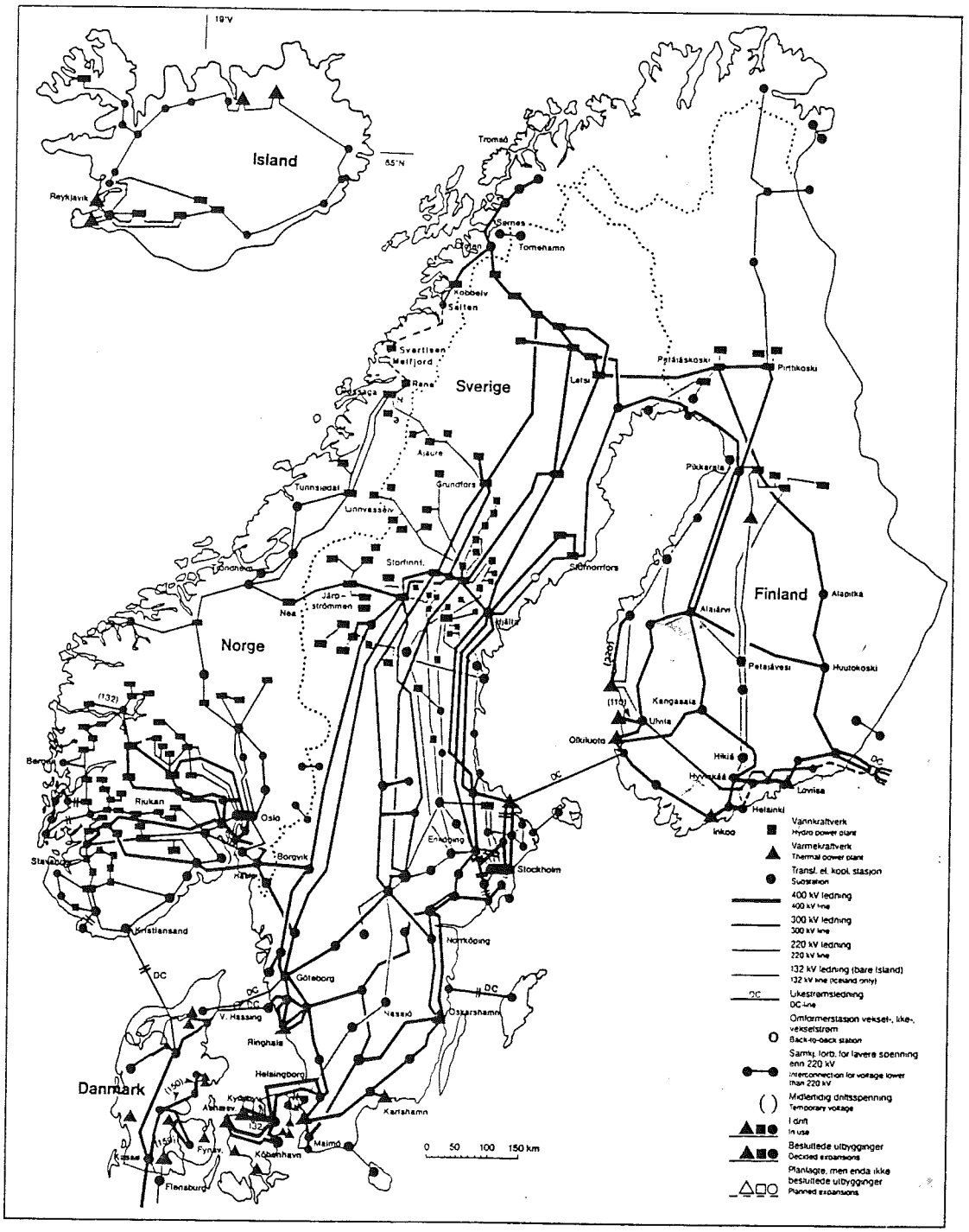

Figure 1.2 The Nordel main grid, 1988.

Table 1.1 Transmission lines in service 1988 (KM).

	400 KV	220–300 KV	110, 132, 150 KV
Sweden	10 051	5 192	15 000
Norway	1 687	5 231	9 600
Denmark	924	247	3 500
Finland	3 259	2 477	13 650

Table 1.2 Installed net capacity (MW) in 1988.

(MW)	Sweden	Norway	Denmark	Finland
Hydro power	16 112	15 647	10	2 648
Wind power	8	0	200	0
Thermal power	17 561	314	7 929	9 620
Total	33 681	25 961	8 139	12 268

1.4 The Nordel Power System

Figure 1.2 shows a map of the Scandinavian countries with the Nordel main grid included. The grid covers a huge area (1300 km in the east-west direction and 1740 km in the south-north direction). Iceland is excluded in this presentation of the Nordel power system.

The trunk line system in service Dec. 31, 1988, is shown in Table 1.1. The net installed capacity in Nordel was bout 80 000 MW during 1988. Table 1.2 shows the distribution of the installed capacity per country. The main idea by the interconnection of power systems is to create the possibilities to utilize the installed capacity more economicly and increase the availability of electric energy. The transfer of power between the Nordic countries is therefore of great importance. Table 1.3 shows the exchange of electric energy in 1988. All figures in the tables are fetched from Nordel 1988, annual report.

The dynamic model of this huge interconnect power system in terms of constants, states etc. is given in Case 3 below. More complex models are used today for analysis of different stability phenomenon. At the start of this research, the 224-machine case was a commonly used simulation model of the Nordel power system.

All calculations in the different parts of the thesis have been applied to three different cases. The original system consists of 224 machines representing the Nordel power system. This system has been reduced with respect to preservation of the slow dynamics. The new coherence technique has made this possible and two other systems have been created, 44 and 21 machines.

Table 1.3 Exchange of electric energy in 1988 (GWh).

Export from	Import to			
	Sweden	Norway	Denmark	Finland
Sweden	–	1 138	3 475*	3 058
Norway	4 466	–	2 287	5
Denmark	189	27	–	–
Finland	409	–	–	–

* From southern Sweden to Zealand/reverse: 2814/156 GWh.
From southern Sweden to Jutland/reverse (HVDC): 661/33 GWh.

Data for the non-linear models including generators, governors, AVRs etc. and the corresponding simplified model used in the thesis:

Case 1: 21 machines
766 constants
81 variables
265 states
Corresponding simplified two-state/generator model consists of 42 states.

Case 2: 44 machines
1388 constants
88 variables
480 states
Corresponding simplified two-state/generator model consists of 88 states.

Case 3: 224 machines
7329 constants
617 variables
2518 states
Corresponding simplified two-state/generator model consists of 448 states.

If everything of interest should be presented for all three cases, the thesis should be very thick. The result of interest will therefore be presented for a mix of all cases. Due to the coherently aggregated models, it does not matter which case is shown in principle. These cases are used throughout the thesis for exemplifying the result of the developed methods.

The verification of the two-state/generator model in Chapter 2 uses Case 2 as a reference. Especially the calculated eigenfrequencies of the two-state/generator model are compared with resonances in the much more complex model of Case 2.

To show the result from the new coherency technique in Chapter 3, all cases are naturally used. The slow and system wide modes are compared in all cases. The eigenvector components are compared and must describe the same swing pattern in all cases. Otherwise, the dynamic properties are not preserved during the aggregation. Only the two-state/generator model is used in Chapter 3 to exemplify the developed method.

The robust siting technique in Chapter 4 is exemplified by the simplified model of Case 2 and Case 3. The result from the coordinated tuning of control parameters corresponds to the simplified model of Case 1 and Case 3 (Chapter 5). Finally, the verification of the introduced damping by using the result from Chapter 5 is simulated on the complex models of Case 1 and Case 3.

1.5 Outline of the Thesis

Chapter 2 describes the design of the model and special emphasis is paid to important system parameters and assumptions behind the choice of model.

Through physical interpretation of the state representing the model, it is possible to define a new coherence technique. Chapter 3 describes this subject.

Chapter 4 gives information about the siting problem associated to the different damping equipments. Important system parameters are varied in order to get robust sites. The siting technique uses sensitivity analysis.

The coordinated tuning and formulation of the optimization problem was the last, but not the easiest, crucial task to solve. Chapter 5 describes this subject. The choice of a proper constraint function is motivated in terms of an example, but it is also motivated to some extent in Chapter 4. The gradient of the trace of the system matrix is related to the sensitivity derivatives as shown in Chapter 4.

Chapter 6 summarizes all knowledge found in the earlier chapters and the theory is tested on complex nonlinear models. These simulations show that the augmented damping is significant.

2

A Structure Preserving Multimachine Model

2.1 Introduction

The first goal of the thesis is to create a simplified linear *structure preserving* model for slow oscillations of a large power system, i.e. a model for small disturbance stability analysis, SDSA. A structure preserving model preserves the topology of the network. P- and Q-injections are used at the nodes when the model is derived. This makes it easy to include non-linear loads. The basic demands of the model are:

- The low frequency dynamics of the model must be well modelled.
- Possibilities to vary the load characteristics must be included.
- Possibilities to include control laws for PSSs, SVCs and HVDC links.

As earlier mentioned the model used for EMOs requires a system wide rather than a single generator view. In Appendix A a general structure preserving model is derived. For slow and system wide modes it is possible to make some approximations or assumptions, which simplifies the model in Appendix A. The validation shows that the assumptions are motivated. Generator oriented models are described in Anderson and Fouad (1977), Elgerd (1971, 1983). Structure preserving models are discussed in Berger and Hill (1981) and in Hill and Bhatti (1987).

More generalized models, including detailed AVR representation in a multimachine concept, can hardly be used to analyze a large power system.

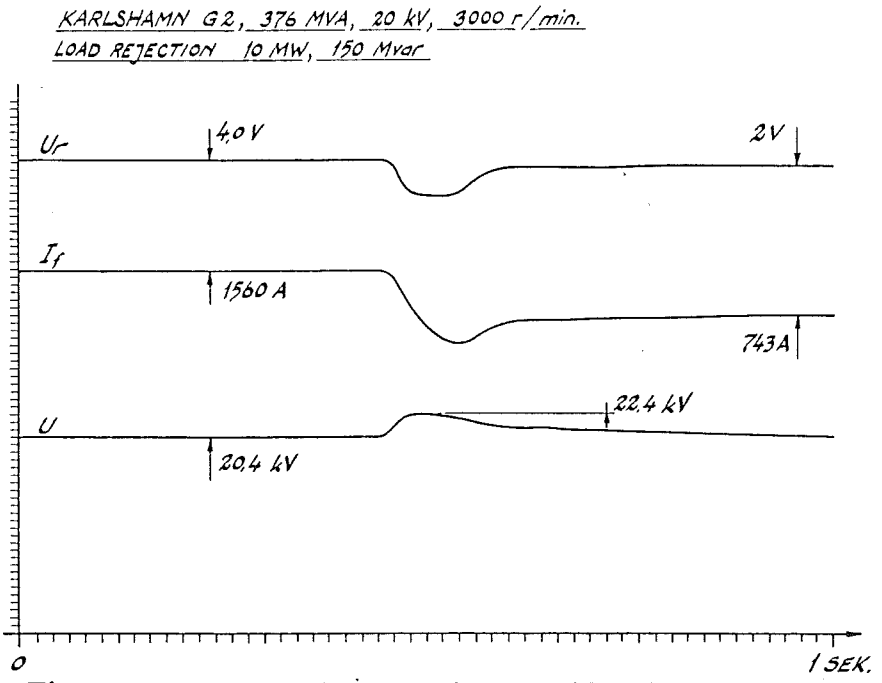

Figure 2.1 Changes of U_r, I_f and U caused by a load rejection.

2.2 Assumptions for the Derived Model

The mathematical tools for small mechanical oscillations are well known from the theory of classical mechanics, see Goldstein (1970) and Uhlhorn (1986). The model (KM) is derived below, where K stands for synchronous stiffness matrix and M stands for mass matrix of the power system. The model (KM) is the most simplified model we can use. It takes into account the inertia of the generator/turbine and the stiffness of the network.

The basic assumptions are:

1. Constant mechanical torque.
2. Neglection of all electrical generator dynamics, i.e the dynamics of the voltage control are fast compared to dynamics of power swings.
3. Lossless transmission network.
4. Algebraic (nonlinear) models of load with respect to frequency and voltage from local quantities (mainly used for siting and coordinated tuning studies) at generator/load buses.
5. The rotor angles for each generator are stiffly connected to the angles of the terminal voltage of each generator.

6. The network is in sinusoidal steady-state with transmission lines represented by series impedances.

All assumptions except items 2 and 5 are natural to do when working with slow power oscillations. Figure 2.1 shows three quantities, setpoint of the terminal voltage (V_r), field current (I_f) and terminal voltage (U) as a function of time. The load is changed by 10 MW and 150 MVar. The quantities are changed according to Fig. 2.1. This is a real field test of a generator. We can see that the transient is over after 5 to 6 periods, i.e. 100 to 120 ms. The AVR-system is a very fast system. This is needed when a short circuit occurs close to the generator in order to keep the generator in synchronism. We are working with oscillations of a period time of 2 to 4 seconds. In this perspective it is reasonable to assume item 2 above.

Item 5 is motivated by the knowledge that the load angels of the generators vary little in the low frequency range when the amplitude of the disturbance is less than 0.1 Hz.

It can be shown that the relative angle deviation ($\Delta\delta$) is:

$$\Delta\delta = \frac{\Delta f}{f_0} \cdot \tan(\delta_0)$$

where

f_0 = nominal value of the frequency

δ_0 = the angle deviation of $|E|$ and V_T at steady-state operation

Δf = frequency deviation from nominal value

$|V_T|$ = the magnitude of the terminal voltage of the generator

$|E|$ = the magnitude of the emf of the generator

Typical values of the quantities:

$$f_0 = 50 \text{ Hz}, \qquad \delta_0 = 30^\circ, \qquad \Delta f = 0.1 \text{ Hz}$$

The calculation of $\Delta\delta$ gives:

$$\Delta\delta \approx 0.1^\circ$$

Simulations show that normally the value of Δf is less than 0.1 Hz.

When the stiff connection of the rotor angle to the angle of the terminal voltage is introduced, an error in the relative angle is less than about 1% in the operative range of the generator. In this perspective it is reasonable to assume item 5 above.

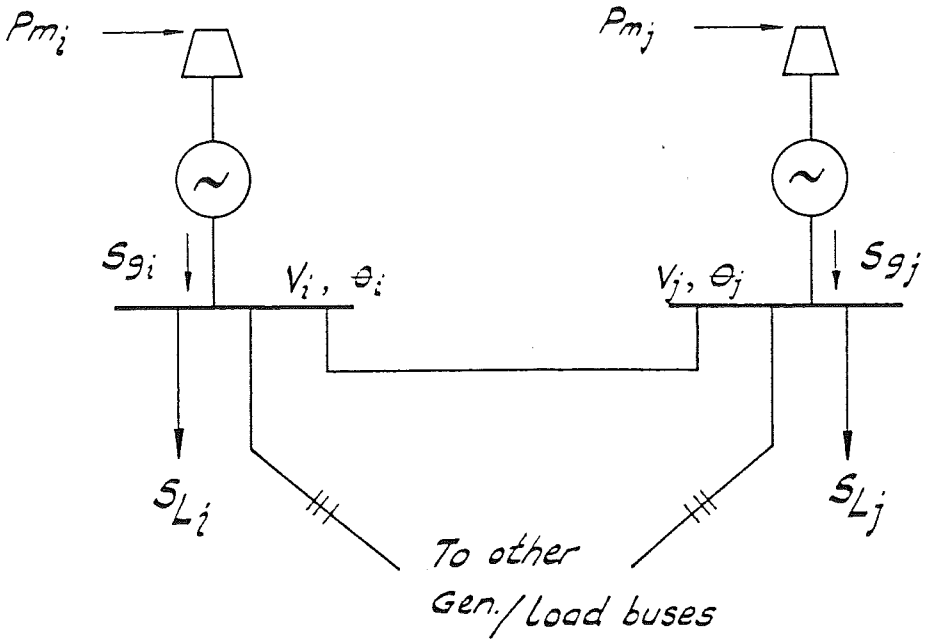

Figure 2.2 No machine reactances included in the aggregation.

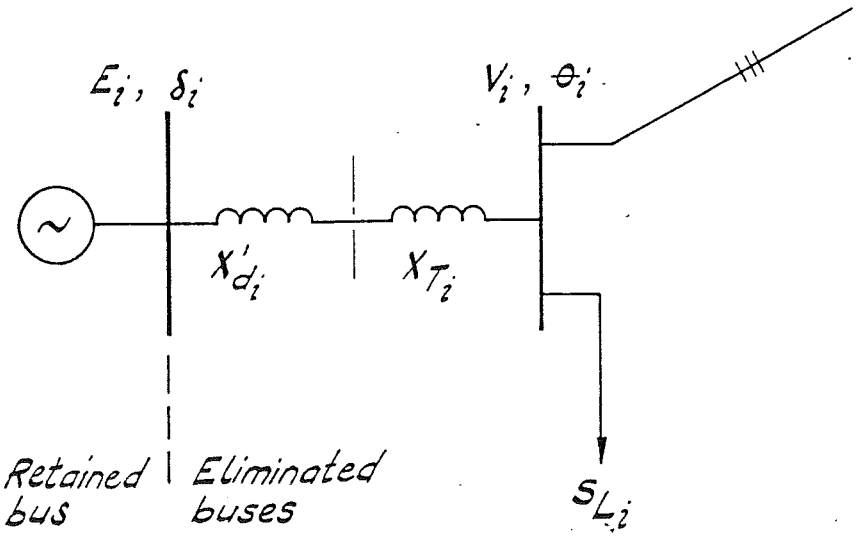

Figure 2.3 x'_d included in the aggregation.

2.3 Basic Equations of the Nonlinear Model

In this section the model used throughout the thesis will be derived. The structure of the system matrices are also discussed. As seen from Fig 2.2 all load buses have been eliminated in a regular manner. A power system can always be written in this way, even if nonlinear load is introduced. This is shown later in this chapter. If x'_d (transient reactance) shall be included, it can be done as shown in Fig. 2.3, which is equivalent to Fig. 2.2 after introduction of a new loadbus for each machine. From now on we just consider the system structure as in Fig. 2.2.

From the theory of power systems (Anderson and Fouad (1977), Elgerd (1971, 1983), Lysfjord *et al.* (1982), deMello and Concordia (1969), Heffron and Phillips (1952), Vournas and Fleming (1978), Hill and Bhatti (1987)) the model used is derived as described below. List of notations is given in Appendix C.

Consider bus i. We define the net injection S_i to bus i as:

$$S_i \triangleq S_{g_i} - S_{L_i} = P_{g_i} - P_{L_i} + j\,(Q_{g_i} - Q_{L_i}) \quad i = 1, 2, \ldots, n$$

The total active and reactive powers leaving the i:th bus via the transmission lines can be written as (Elgerd (1983, Chapter 7)):

$$P_i = \sum_{j=1}^{n} \frac{V_i V_j}{x_{ij}} \cdot \sin(\theta_i - \theta_j) \tag{2.1}$$

$$Q_i = -\sum_{j=1}^{n} \frac{V_i V_j}{x_{ij}} \cdot \cos(\theta_i - \theta_j) \tag{2.2}$$

where

$$x_{ij} = x_{ji} \qquad i \neq j$$

$$x_{ii}^{-1} = \sum_{j \neq i} -\frac{1}{x_{ij}}$$

x_{ij} is the serial reactance of the line between buses i and j.

Motion of the i:th generator

$$\frac{dE_{k_i}}{dt} \approx 2E_{k_{i0}} \cdot \frac{\omega_i \cdot \dot{\omega}_i}{\omega_0^2} \approx \frac{2}{\omega_0} E_{k_{i0}} \dot{\omega}_i$$

where ω_i is set to $\omega_0 = 2\pi \cdot f_0$ rad/s. The nominal frequency is designated by f_0. According to Assumption 5 we get $\dot{\delta}_i \approx \dot{\theta}_i$. We define

$$H_i = \frac{E_{k_i}}{S_{r_i}}$$

i.e.,

$$\dot{E}_{k_i} = \frac{2H_i \cdot S_{r_i}}{\omega_0} \dot{\omega}_i$$

The differential equation of the motion in p.u. becomes

$$\frac{2H_i \cdot S_{r_i}}{\omega_0 S} \dot{\omega}_i + D_i\omega_i = P_{m_i} - P_{g_i} \tag{2.3}$$

From (2.3) and (2.1) we get

$$P_{g_i} = P_i + P_{L_i}$$

i.e., (2.3) becomes

$$m_{ii} \cdot \dot{\omega}_i + D_i\omega_i + P_i(\overline{V},\overline{\theta}) = P_{m_i} - P_{L_i}(\overline{V},\overline{\omega}) \tag{2.4}$$

where

$$\overline{V}^T = (V_1, V_2, \ldots, V_n), \qquad \overline{\theta}^T = (\theta_1, \theta_2, \ldots, \theta_n)$$
$$\overline{\omega}^T = (\dot{\theta}_1, \dot{\theta}_2, \ldots, \dot{\theta}_n), \qquad m_{ii} = \frac{2H_i \cdot S_{r_i}}{\omega_0 S}$$

For n generators the differential equation system can be written as

$$M\,\dot{\overline{\omega}} + DG\,\overline{\omega} + \overline{P}(\overline{V},\overline{\theta}) + \overline{P}_L(\overline{V},\overline{\omega}) = \overline{P}_m \tag{2.5}$$

$$M = \mathrm{diag}(m_{11}, \ldots, m_{nn})$$
$$DG = \mathrm{diag}(D_1, \ldots, D_n)$$

Equation (2.5) is called the General Swing Equation (GSE). The algebraic equation for the reactive power is, according to Eqs. (2.1) and (2.2), $Q_{g_i} = Q_i + Q_{L_i}$. For SDS analysis this equation is always considered to be fulfilled. The generator never reaches any limitations.

2.4 Linearized Structure Preserving Model

The General Swing Equation for Small Oscillations

Assuming that $\overline{P}_m$ is constant and small disturbances, the general swing equation becomes:

$$M\,\Delta\dot{\overline{\omega}} + \left[DG + \partial_\omega(\overline{P}_{L_0})\right]\Delta\overline{\omega} + \partial_\theta(\overline{P}_0)\Delta\overline{\theta} = -\partial_V(\overline{P}_0 + \overline{P}_{L_0})\Delta\overline{V} \tag{2.6}$$

$$D \triangleq DG + \partial_\omega(\overline{P}_{L_0})$$
$$B \triangleq -\partial_V(\overline{P}_0 + \overline{P}_{L_0})$$
$$K \triangleq \partial_\theta(\overline{P}_0) \qquad \text{synchronous stiffness matrix}$$
$$K_2 \triangleq -\partial_V(\overline{P}_0) \qquad \text{voltage stiffness matrix}$$

i.e.,

$$M\,\Delta\dot{\overline{\omega}} + D\,\Delta\overline{\omega} + K\,\Delta\overline{\theta} = B\,\Delta\overline{V}$$

Now we derive the Jacobian matrices

$$P_i = \sum_{j=1}^{n} \frac{V_i V_j}{x_{ij}} \sin(\theta_i - \theta_j)$$
$$\frac{\partial P_i}{\partial \theta_i} = \sum_{j\neq i} \frac{V_i V_j}{x_{ij}} \cos(\theta_i - \theta_j)$$
$$\frac{\partial P_i}{\partial \theta_k} = -\frac{V_i V_k}{x_{ik}} \cos(\theta_i - \theta_k); \quad i \neq k$$

i.e., the sum of the elements in each row of the K-matrix is zero and the matrix is symmetric, because $x_{ij} = x_{ji}$.

$$\frac{\partial P_i}{\partial V_i} = \frac{\partial}{\partial V_i}\left\{\sum_{j=1}^{n} \frac{V_i V_j}{x_{ij}} \sin(\theta_i - \theta_j)\right\} = \sum_{j\neq i}^{n} \frac{V_j}{x_{ij}} \sin(\theta_i - \theta_j)$$
$$\frac{\partial P_i}{\partial V_k} = \frac{\partial}{\partial V_k}\left\{\sum_{j=1}^{n} \frac{V_i V_j}{x_{ij}} \sin(\theta_i - \theta_j)\right\} = \frac{V_i}{x_{ik}} \sin(\theta_i - \theta_k); \quad i \neq k$$

$$\sum_{j\neq i} \frac{V_j}{x_{ji}} \sin(\theta_j - \theta_i) = -\sum_{j\neq i} \frac{V_j}{x_{ij}} \sin(\theta_i - \theta_j)$$

i.e., the sum of the elements in each column of the K_2-matrix is zero and it is skew-symmetric (off diagonal) if $V_k = V_i \quad \forall\ k$ and i.

Assumptions of load characteristics gives

$$P_{L_i} = P_{L_i}(V_i, \omega_i)$$

i.e.,

$$\frac{\partial \overline{P}_{L_0}}{\partial \overline{V}} = \operatorname{diag}\left(\frac{\partial P_{L1_0}}{\partial V_1}, \ldots, \frac{\partial P_{Ln_0}}{\partial V_n}\right)$$

$$\frac{\partial \overline{P}_{L_0}}{\partial \overline{\omega}} = \operatorname{diag}\left(\frac{\partial P_{L1_0}}{\partial \omega_1}, \ldots, \frac{\partial P_{Ln_0}}{\partial \omega_n}\right)$$

$$D = \operatorname{diag}\left(D_i + \frac{\partial P_{L_i}}{\partial \omega_i}\right); \quad 1 \leq i \leq n$$

$$B = -\left(\frac{\partial P_{i_0}}{\partial V_j}\right) - \operatorname{diag}\left(\frac{\partial P_{Li_0}}{\partial V_i}\right); \quad 1 \leq i \leq n, 1 \leq j \leq n$$

Summary

The equation of motion for small oscillations is

$$\begin{cases} M\,\Delta\ddot{\overline{\theta}} + D\,\Delta\dot{\overline{\theta}} + K\,\Delta\overline{\theta} = B\,\Delta\overline{V} \\ \Delta\dot{\overline{\theta}} = \Delta\overline{\omega} \end{cases} \tag{2.7}$$

where

$$\left.\begin{aligned} K &= \partial_\theta(\overline{P}_0) \\ B &= -\partial_V(\overline{P}_0) - \operatorname{diag}\left(\frac{\partial P_{L_i 0}}{\partial V_i}\right) \\ D &= \operatorname{diag}\left(D_i + \frac{\partial P_{L_i 0}}{\partial \omega_i}\right) \\ M &= \operatorname{diag}\left(2H_i \frac{S_{r_i}}{\omega_0 S}\right) \end{aligned}\right\} \tag{2.8}$$

The equilibrium condition is

$$\overline{P}_{m_0} - \overline{P}_0 - \overline{P}_{L_0} = 0$$

The designations K and K_2 is according to Heffron and Phillips (1952). In this paper, though, K is called K_1.

The assumptions made for simplified implementation are: Equation (2.7) can be obtained from Appendix A by setting $\overline{\delta} = \overline{\theta}$ and $|\overline{E}'| = |\overline{V}|$. We can also see that $N_1 = \operatorname{diag}\left(\frac{\partial P_{L_i 0}}{\partial V_i}\right)$, $P_{ge} = \partial_v(\overline{P}\overline{F}_o)$ and $-B = P_{ge} + N_1$.

2.5 The Model (KM)

We are interested in slow and poorly damped principle modes. Consider the homogeneous part of Eq. (2.7) and introduce the approximation $D = 0$. Then

$$\begin{cases} M\,\Delta\ddot{\overline{\theta}} + K\,\Delta\overline{\theta} = \overline{0} \\ \Delta\dot{\overline{\theta}} = \Delta\overline{\omega} \end{cases} \tag{2.9}$$

$D = 0$ is motivated by the knowledge of that slow modes have relative damping less than about 5% in a large power system. This is called the model (KM). M is a positive definite matrix and K is a positive semi-definite matrix for stable power systems i.e, $|\theta_i - \theta_j| \leq \frac{\pi}{2}$ (Appendix B).

By preserving the topological structure of the swing equation and by excluding the damping of load and asynchronous damping power of the generator we have got a model suitable for linear analysis. Especially we can use the method for calculating eigenvalues and eigenvectors of large power system. The components of the eigenvectors can physically be interpreted as an approximation of the angel deviations of the machines.

According to Assumption 5, data from a converged load flow can be used in order to update the matrices in the model (KM). This speeds up the analysis considerably. For the uncontrolled system the equations become:

$$\begin{aligned} \frac{d}{dt}\begin{pmatrix} \Delta\overline{\theta} \\ \Delta\dot{\overline{\theta}} \end{pmatrix} &= \begin{pmatrix} 0 & I \\ -M^{-1}K & 0 \end{pmatrix}\begin{pmatrix} \Delta\overline{\theta} \\ \Delta\dot{\overline{\theta}} \end{pmatrix} \\ A &= \begin{pmatrix} 0 & I \\ -M^{-1}K & 0 \end{pmatrix} \end{aligned} \tag{2.10}$$

Eigenvectors and eigenvalues of $A(2n \times 2n)$ are obtained from

$$\begin{aligned} & A\overline{u} = \lambda\overline{u} \\ & \Leftrightarrow \\ & (A - \lambda_i I)\overline{u}_i = \overline{0}; \quad \overline{u}_i = \begin{pmatrix} \overline{u}_{iu} \\ \overline{u}_{il} \end{pmatrix} \\ & \begin{pmatrix} -\lambda_i I & I \\ -M^{-1}K & -\lambda_i I \end{pmatrix}\begin{pmatrix} \overline{u}_{iu} \\ \overline{u}_{il} \end{pmatrix} = \overline{0} \\ & \Leftrightarrow \\ & \begin{cases} -\lambda_i\overline{u}_{iu} + \overline{u}_{il} = \overline{0} \\ -M^{-1}K\overline{u}_{iu} - \lambda_i\overline{u}_{il} = \overline{0} \end{cases} \\ & \Leftrightarrow \\ & \begin{cases} \overline{u}_{il} = \lambda_i\overline{u}_{iu} \\ M^{-1}K\overline{u}_{iu} + \lambda_i^2\overline{u}_{iu} = \overline{0} \end{cases} \end{aligned} \tag{2.11}$$

According to Appendix B we know that $\overline{u}_{iu}^T K\,\overline{u}_{iu} = K_{ii}\delta_{ij}$ and $\overline{u}_{iu}^T M\,\overline{u}_{iu} = M_{ii}\delta_{ij}$, i.e.

$$\lambda_i^2 = -\frac{\overline{u}_{iu}^T K\,\overline{u}_{iu}}{\overline{u}_{iu}^T M\,\overline{u}_{iu}} = -\frac{K_{ii}}{M_{ii}}; \quad 1 \le i \le n \tag{2.12}$$

Now we get

$$\lambda_i = \pm j \cdot \sqrt{\frac{K_{ii}}{M_{ii}}} \triangleq \pm j \cdot \alpha_i \tag{2.13}$$

Let the matrix U_u contain all the eigenvectors $\overline{u}_{iu}$. Now we can write

$$U_u^T M\,U_u = \mathrm{diag}(M_{ii}) \triangleq M_D \tag{2.14}$$

Order now the left eigenvectors in a matrix, V_u, of the model (KM) in the same sequence as for the right eigenvectors in U_u. We know that

$$V_u^T U_u = I \quad \text{i.e.} \quad V_u^T = U_u^{-1}$$

From Eq. (2.14) we get

$$V_u = \left(U_u^T\right)^{-1} = M \cdot U_u \cdot M_D^{-1} \tag{2.15}$$

A right eigenvector of the system (2.10) can be written according to Eq. (2.11) as

$$\overline{u}_i = \begin{pmatrix} \overline{u}_{iu} \\ j\alpha_i \cdot \overline{u}_{iu} \end{pmatrix}$$

and a left eigenvector can be written as

$$\overline{v}_i = \begin{pmatrix} -j \cdot \alpha_i \cdot M\overline{u}_{iu} \\ M \cdot \overline{u}_{iu} \end{pmatrix} \tag{2.16}$$

$\overline{v}_i$ belongs to the eigenvalue, λ_i^*. By calculating the vectors $\overline{u}_{iu}$, the eigenvectors for the expanded system and left eigenvectors are known. This insight is used throughout the thesis, especially during the sensitivity analysis.

An interesting similar transformation of the system equations Eq. (2.11) to do is:

$$x_{iu} = (\sqrt{M})u_{iu}$$

i.e., x_{iu} are the mass scaled eigenvector for mode i. The system equations become:

$$\begin{cases} x_{il} = \lambda_i x_{iu} \\ M^{-1}K(\sqrt{M})^{-1}x_{iu} + \lambda_i^2(\sqrt{M})^{-1}x_{iu} = 0 \end{cases}$$

Finally,

$$\begin{cases} x_{il} = \lambda_i x_{iu} \\ (\sqrt{M})^{-1} K (\sqrt{M})^{-1} x_{iu} + \lambda_i^2 x_{iu} = 0 \end{cases}$$

The matrix $(\sqrt{M})^{-1} K (\sqrt{M})^{-1} = \tilde{K}$ is symmetric and this implies that all the x_{iu} can be chosen orthogonal, i.e.

$$X_u^T (\sqrt{M})^{-1} K (\sqrt{M})^{-1} X_u = \tilde{K}_D$$

(diagonal matrix and positive semi-definite). The columns of X_u are x_{iu}. From the equations above it is clear that

$$\tilde{K}_D(i,i) = -\lambda_i^2 \quad \text{or} \quad \lambda_i = \pm j \sqrt{\tilde{K}_D(i,i)} = \pm j \cdot \alpha_i$$

The new system matrix is

$$\tilde{A} = \begin{pmatrix} 0 & I \\ \tilde{K} & 0 \end{pmatrix} \tag{2.17}$$

$\tilde{K} = (\sqrt{M})^{-1} \cdot K \cdot (\sqrt{M})^{-1} = \sum_{i=1}^{n-1} \tilde{K}_{D_i} \cdot x_i \cdot x_i^T$, i.e. $\tilde{K}$ can be written as a sum of orthogonal rang one matrices, if we order the eigenvalues so that the rigid body motion is represented by $K_{D_n} = 0$.

A right eigenvector of the system (2.17) can be written as:

$$\overline{x}_i = \begin{pmatrix} \overline{x}_{iu} \\ j\alpha_i \overline{x}_{iu} \end{pmatrix}$$

The left eigenvector $(\overline{y}_i)$ of $\tilde{A}$ for the eigenvalue, λ_i^*, is obtained by

$$\overline{y}_i = \begin{pmatrix} -j\alpha_i \overline{x}_{iu} \\ \overline{x}_{iu} \end{pmatrix}$$

2.6 Separation of Slow and System Wide and Slow Local Modes

The basic solution of Eq. (2.9) is of the form:

$$\Delta\overline{\theta}_i(t) = e^{\lambda_i t} \overline{u}_{iu}$$

From Eq. (2.9) we can obtain the energy for the principle mode i of the power system.

$$T_i = \frac{1}{2} (\Delta\dot{\overline{\theta}}_i)^* M \, \Delta\dot{\overline{\theta}}_i = \frac{\lambda_i^2}{2} \overline{u}_{iu}^T M \, \overline{u}_{iu} = \frac{\lambda_i^2}{2} M_{ii} \tag{2.18}$$

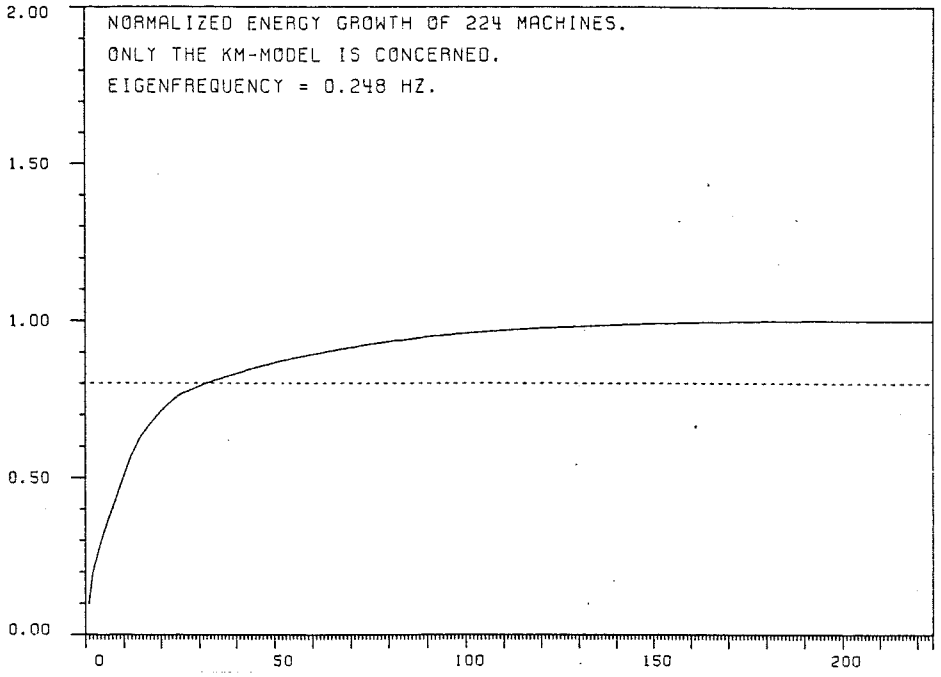

Figure 2.4 Energy growth for the slowest mode of Case 3.

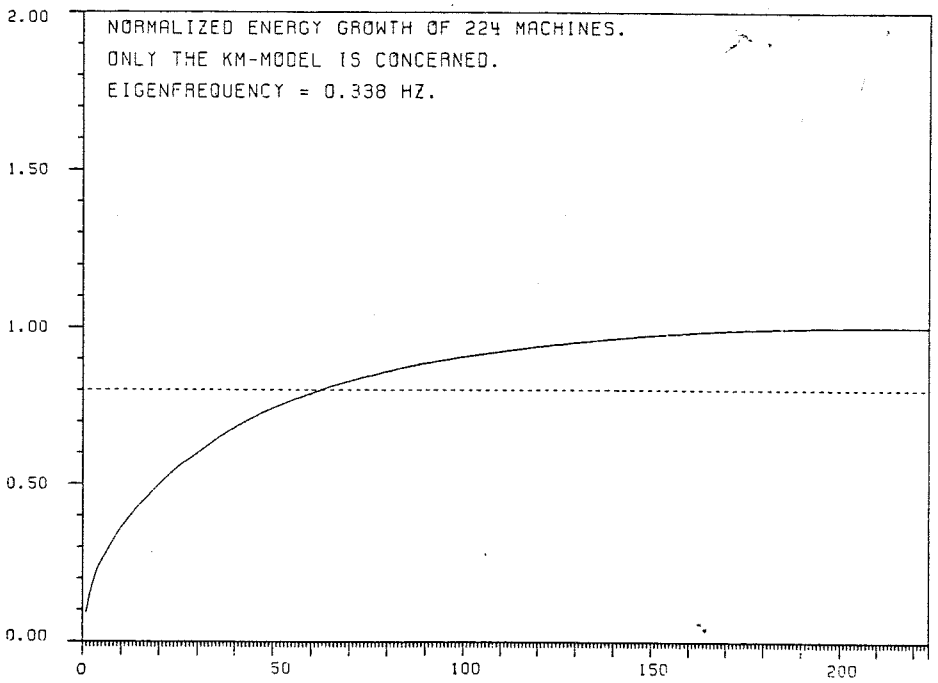

Figure 2.5 Energy growth for the second slowest mode of Case 3.

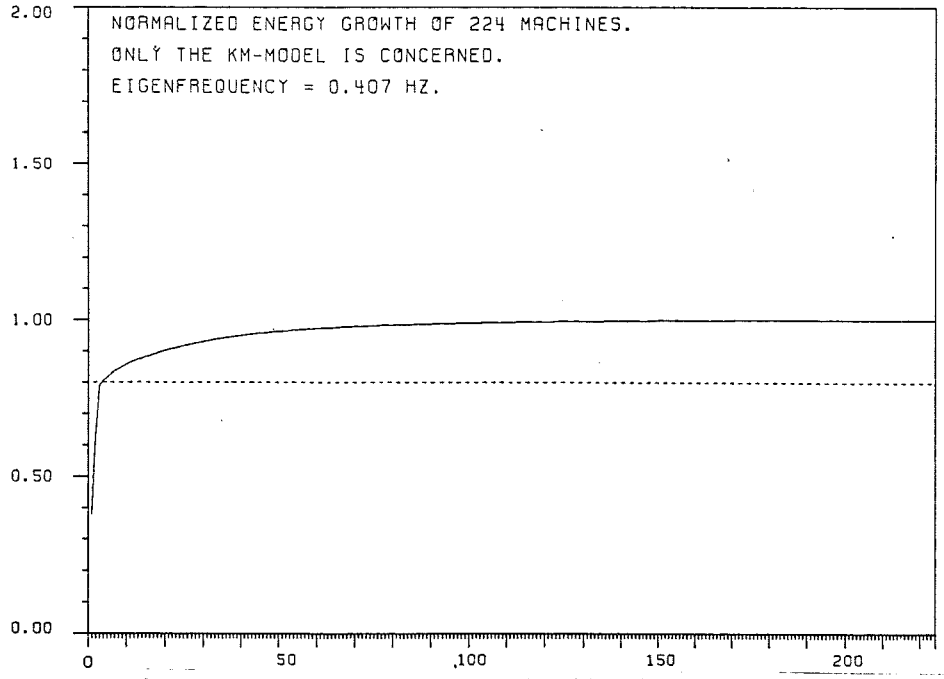

Figure 2.6 Energy growth for the third slowest mode of Case 3.

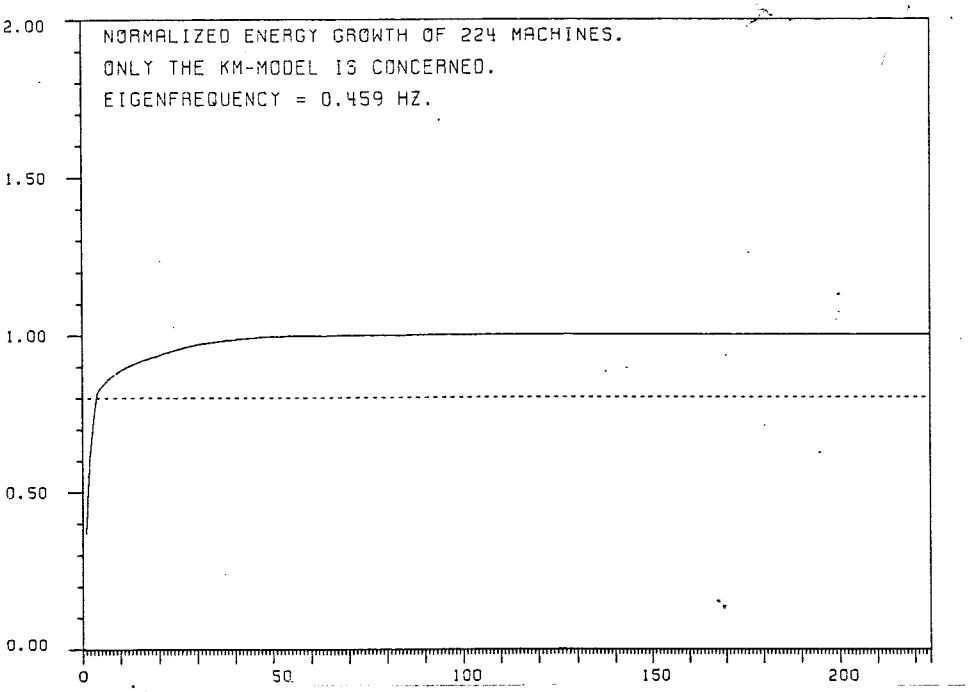

Figure 2.7 Energy growth of the fourth slowest mode of Case 3.

where

$$M_{ii} = \sum_{j=1}^{n} m_{jj}\, u_{iu_j}^2 \quad \text{(generalized mass)}$$

i.e., $\sqrt{M_{ii}}$ equal to the euclidian norm of the mass-scaled eigenvector. By using Eq. (2.18), it is possible to separate slow local modes and slow and system wide modes. The different contributions from each group (machine), are ordered in a decreasing sequence and the energy growth for each mode can be plotted.

The energy growth (T_i^k) for mode i is defined as:

$$T_i^k = T_i^{k-1} + m_{kk} u_{iu_k}^2 \quad k = 1, \ldots, n, \quad T_i^0 = 0$$

The ordering of $m_{kk}u_{iu_k}^2$ implies that

$$T_i^{K-1} + T_i^{K+1} \leq 2T_i^K$$

The ordering of the machines (eigenvector components) will vary, but we are only interested in the energy growth. The separation of system wide modes and local modes is empirically defined as:

> If more than 15% of the machines are needed for the energy growth to become greater than 80% of T_i^n, a system wide mode (i) is found. Otherwise a local mode is found.

Figures 2.4 to 2.7 show the energy growth for four different modes concerning Case 3. Figure 2.4 shows that 33 (15%) of the machines contribute with 80% of the normalized value. This mode (0.248 Hz) is considered to be a slow and system wide mode. Figure 2.5 shows that 53 (24%) of the machines contribute with 80% of the normalized value. This mode is also slow and system wide. Figures 2.6 and 2.7 show that 4 (2%) of the machines contribute with 80% of the normalized value. These modes are considered to be slow and local modes.

Only slow and system wide modes are of interest in this thesis. These are the troublesome modes to control and MIMO concept is needed. In the literature different kinds of modes are described, but no technique for finding different modes is described. For local modes a SISO concept can be used for design of proper damping equipment.

2.7 Validation of the Model with Respect to Slow Oscillations

The validation of the model (KM) is based on two basic questions:

1. How well are the machine angle deviations of a nonlinear model approximated by the model KM in the low frequency range?

2. How close is the sinusoidal steady-state swing pattern of the nonlinear model at resonance an eigenvector?

These questions are answered in the following procedure.

Only Case 2 is considered (44 machines). The model (KM) is validated by excitation of resonances of a much more complex model. The nonlinear model has 428 states of which 88 states corresponds to the swing equation. The states which describe the deviation of the machine angles, when a sinusoidal disturbance is introduced, are of great interest. The eigenvector components of the model (KM) is an approximation of the angle deviations of the nonlinear model. By comparing the mass scaled angle deviations (max value) at sinusoidal steady-state condition with the mass scaled eigenvector components for corresponding machines, the swing pattern of the two models can be studied. No PSSs were installed and the mechanical torque for each machine was constant during the simulation. Only the AVRs were installed and a full nonlinear model of each generator was simulated. This is an open system simulation. The nonlinear model contains, however, the natural damping introduced by the damper windings of the generators.

The simulation is done by using PTI's simulations package, PSS/E. The procedure for finding the resonances was executed in the following way: The dynamic model of 44 machines (Case 2) was disturbed by a sinusoidal signal with a frequency calculated by the model (KM). When the transient has settled (after roughly 50 seconds, real time), the machine angles of each machine are compared with corresponding eigenvector component of the model (KM). The disturbed machine is selected by checking which machine has the largest component in the mass scaled eigenvector. The AVR-reference of the selected machine was disturbed by this sinusoidal signal. The amplitude was selected in the range of (0.1–2)% p.u. The eigenfrequency was varied around the KM-value until the largest machine angle deviations were found in sinusoidal steady-state.

When the resonance had been found, it was of great interest to see how close the machine angle deviations of the nonlinear system were corresponding eigenvector components. The structure of the damping matrix of the nonlinear model is very important. This can be understood for a general second order system. The structure of the mass- and stiffness-matrix are the same as for the model (KM). If the KM-orthogonal eigenvectors also diagonalize the damping matrix, we have found an eigenvector. If the damping matrix can be written as a linear combination matrix can be written as linear combination of M and K we are through. Even when the original damping matrix is diagonal with positive elements, it is not necessarily diagonalized by the eigenvector matrix of the model (KM). With this background, it is hardly not believable that we have excited a true eigenvector for the nonlinear system.

In order to check if the eigenvector components of the machine angle deviations in the nonlinear model (482 states) had been excited, the sinusoidal signal was removed after an even number of periods when the transient has settled.

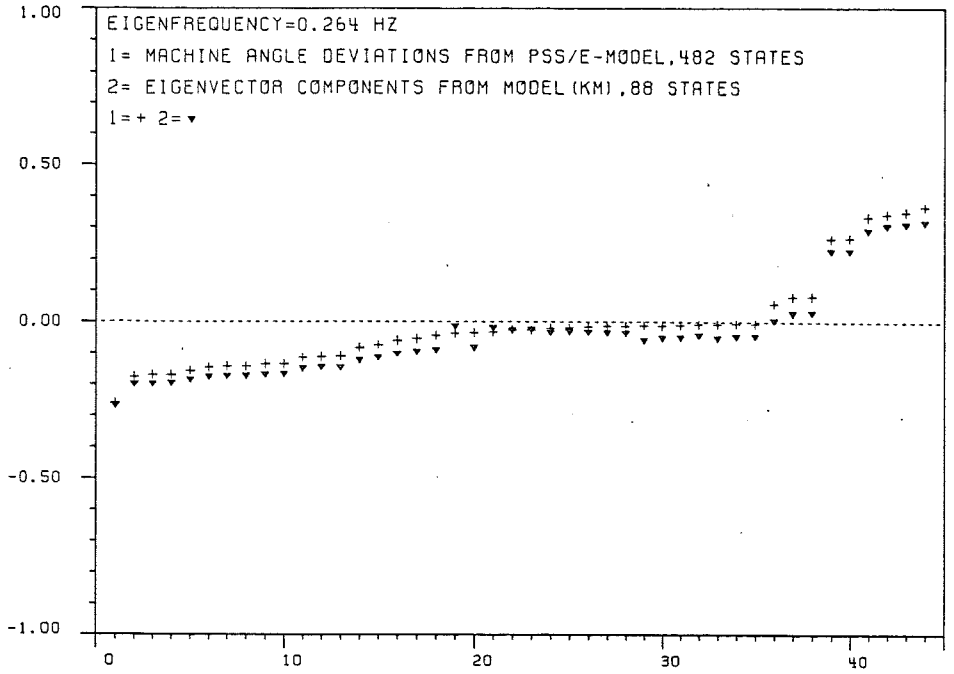

Figure 2.8 Comparison of the machine angles of the nonlinear model (482 states) and the eigenvector components of the model (KM) (88 states). Case 2, mode #1 according to Table 3.2.

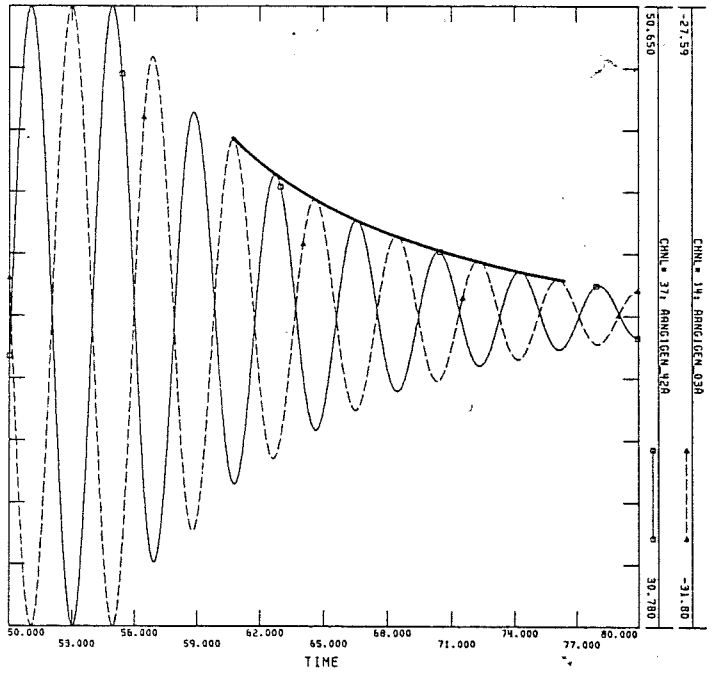

Figure 2.9 Comparison of the machine angles of two opposite swinging generators after the excitation signal is removed. Case 2, mode #1 according to Table 3.2.

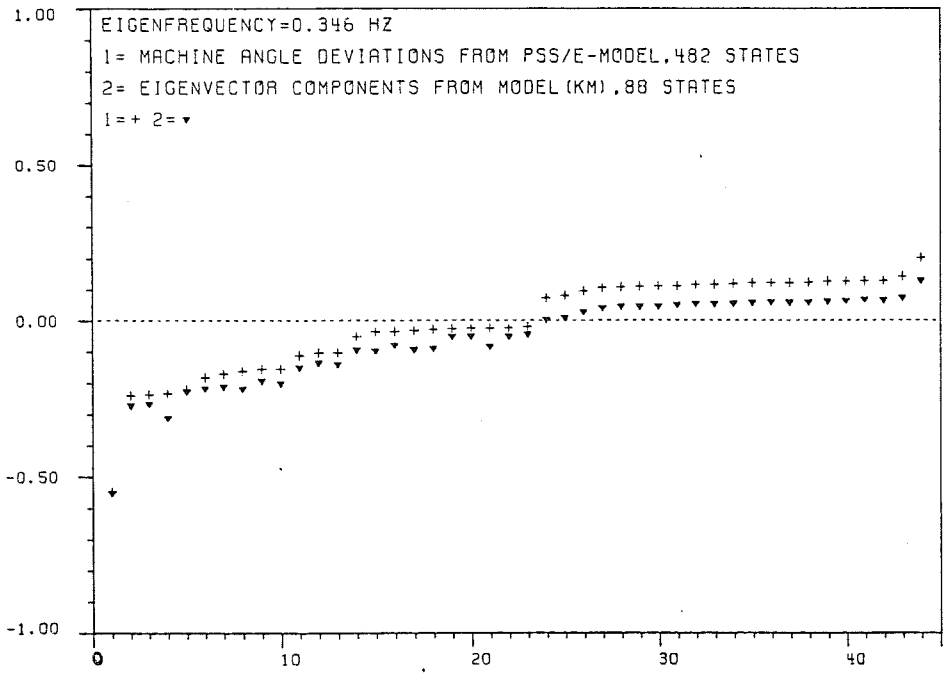

Figure 2.10 Comparison of an excited eigenvector of a nonlinear model (482 states) and the eigenvector components of the model (KM) (88 states). Case 2, mode #2 according to Table 3.2.

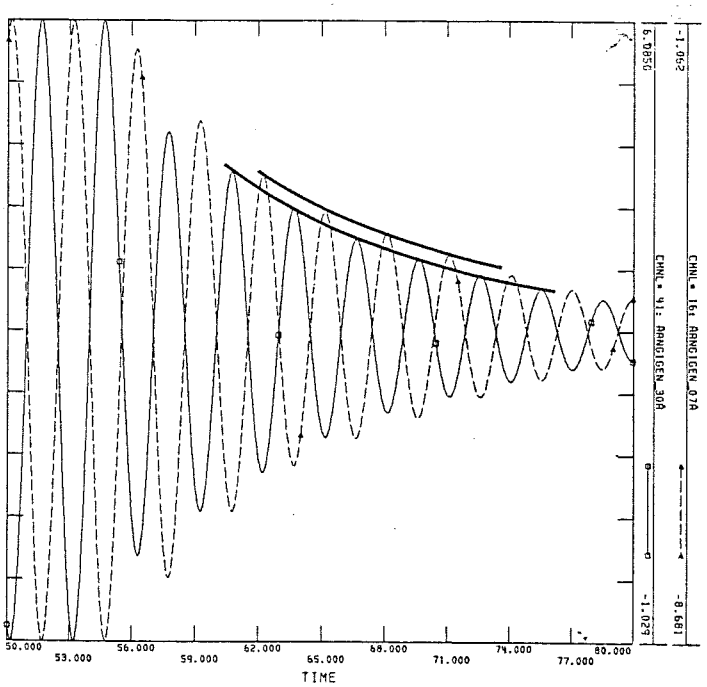

Figure 2.11 Comparison of the machine angles of two opposite swing generators after the excitation signal is removed. Case 2, mode #2 according to Table 3.2.

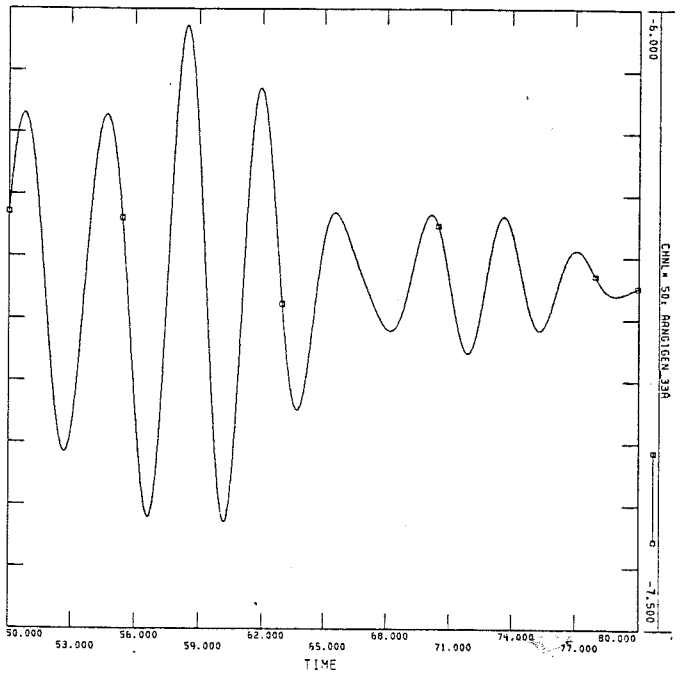

Figure 2.12 The machine angle for minor participating machine.

The result is shown in Figs. 2.8 to 2.12. Figure 2.8 shows the machine angle deviations for Case 2, marked with +, compared with the eigenvector components from model (KM), marked $\triangledown$. The mode shown has a KM-eigenfrequency of 0.264 Hz. The resonance frequency was found to be 0.256 Hz. The sinusoidal was removed and Fig. 2.9 shows the machine angles for two significant opposite swinging generators. The damping for these two machines can be calculated to be 0.1. The relative damping is less than 0.06. This implies that it is not unrealistic to work with a model with damping matrix equal to zero. The method used is the logarithmic decrement, i.e.

$$\Delta_i = \frac{1}{k} \ln \left(\frac{A_i}{A_{i+k}} \right)$$

$$T_d = \frac{T_{\text{period}}}{\Delta_{\text{average}}}$$

This is an experimental calculation for a damped sinus represented by

$$A \cdot e^{-t/T_d} \sin(\omega t + \phi)$$

where $T_{\text{period}} = 2\pi/\omega$. The amplitude of the sinusoidal disturbance was 0.005 p.u. Figures 2.10 and 2.11 show the most significant opposite swinging generators

for the next system wide mode (0.346 Hz). The experimental calculation of the resonance frequency was 0.329 Hz. The amplitude of the sinusoidal disturbance was 0.005 pu.

Figure 2.12 shows the machine angle of a minor participating machine for mode 0.264 Hz. The figure shows that a true eigenvector not is excited. But the author has checked a lot of machines and the most important machines behaves very well according to the eigenvector of the model (KM).

These figures show that the model (KM) describes the electro-mechanical slow oscillations of a large power system accurate enough for design purposes.

2.8 The Model (KM) for a General Network

In Section 2.3 we assumed generator/load buses only. We can quite easily rewrite Eq. (2.5) in a general way.

Order all machine/load buses and all pure load buses in a sequential order. The $\overline{P}(V,\theta)$ for the machine modes is designated by $\overline{P}_1(V_1,V_2,\theta_1,\theta_2)$. The vector V_1 contains the magnitude of the terminal voltage of the machine nodes. The vector V_2 contains the magnitude of the voltage of the load buses. The vector θ_1 contains the angle of the terminal voltage of the machine buses. The vector θ_2 contains the angle of the voltage at the load buses.

All matrices and vectors of the GSE-equation are split in this way. The GSE in the general case becomes:

$$\begin{pmatrix} M_{11} & 0 \\ 0 & 0 \end{pmatrix} \begin{pmatrix} \ddot{\theta}_1 \\ \ddot{\theta}_2 \end{pmatrix} + \begin{pmatrix} DG & 0 \\ 0 & 0 \end{pmatrix} \begin{pmatrix} \dot{\theta}_1 \\ \dot{\theta}_2 \end{pmatrix} + \begin{pmatrix} \overline{P}_1(V_1,V_2,\theta_1,\theta_2) \\ \overline{P}_2(V_1,V_2,\theta_1,\theta_2) \end{pmatrix} + \\ + \begin{pmatrix} \overline{P}_{L_1}(V_1,V_2,\omega_1,\omega_2) \\ \overline{P}_{L_2}(V_1,V_2,\omega_1,\omega_2) \end{pmatrix} = \begin{pmatrix} \overline{P}_{m_1} \\ \overline{0} \end{pmatrix}$$

Small disturbance stability is studied and from Assumption 1 we have

$$\begin{pmatrix} M_{11} & 0 \\ 0 & 0 \end{pmatrix} \begin{pmatrix} \Delta\ddot{\theta}_1 \\ \Delta\ddot{\theta}_2 \end{pmatrix} + \begin{pmatrix} DG & 0 \\ 0 & 0 \end{pmatrix} \begin{pmatrix} \Delta\dot{\theta}_1 \\ \Delta\dot{\theta}_2 \end{pmatrix} + \\ + \begin{pmatrix} \partial_{V_1}\overline{P}_1 & \partial_{V_2}\overline{P}_1 & \partial_{\theta_1}\overline{P}_1 & \partial_{\theta_2}\overline{P}_1 \\ \partial_{V_1}\overline{P}_2 & \partial_{V_2}\overline{P}_2 & \partial_{\theta_1}\overline{P}_2 & \partial_{\theta_2}\overline{P}_2 \end{pmatrix} \begin{pmatrix} \Delta\overline{V}_1 \\ \Delta\overline{V}_2 \\ \Delta\overline{\theta}_1 \\ \Delta\overline{\theta}_2 \end{pmatrix} + \\ + \begin{pmatrix} \partial_{V_1}\overline{P}_{L_1} & \partial_{V_2}\overline{P}_{L_1} & \partial_{\omega_1}\overline{P}_{L_1} & \partial_{\omega_2}\overline{P}_{L_1} \\ \partial_{V_1}\overline{P}_{L_2} & \partial_{V_2}\overline{P}_{L_2} & \partial_{\omega_1}\overline{P}_{L_2} & \partial_{\omega_2}\overline{P}_{L_2} \end{pmatrix} \begin{pmatrix} \Delta\overline{V}_1 \\ \Delta\overline{V}_2 \\ \Delta\dot{\theta}_1 \\ \Delta\dot{\theta}_2 \end{pmatrix} = \begin{pmatrix} \overline{0} \\ \overline{0} \end{pmatrix}$$

We also assume that $\partial_{V_2}\overline{P}_{L_1} = 0$, $\partial_{\omega_2}\overline{P}_{L_1} = 0$, $\partial_{V_1}\overline{P}_{L_2} = 0$ and $\partial_{\omega_1}\overline{P}_{L_2} = 0$, i.e. the loads only depend on local values of the voltage and the frequency. The linearized model becomes:

$$\begin{pmatrix} M_{11} & 0 \\ 0 & 0 \end{pmatrix} \begin{pmatrix} \Delta\ddot{\overline{\theta}}_1 \\ \Delta\ddot{\overline{\theta}}_2 \end{pmatrix} + \begin{pmatrix} (DG + \partial_{\omega_1}\overline{P}_{L_1}) & 0 \\ 0 & \partial_{\omega_2}\overline{P}_{L_2} \end{pmatrix} \begin{pmatrix} \Delta\dot{\overline{\theta}}_1 \\ \Delta\dot{\overline{\theta}}_2 \end{pmatrix} +$$
$$+ \begin{pmatrix} \partial_{\theta_1}\overline{P}_1 & \partial_{\theta_2}\overline{P}_1 \\ \partial_{\theta_1}\overline{P}_2 & \partial_{\theta_2}\overline{P}_2 \end{pmatrix} \begin{pmatrix} \Delta\overline{\theta}_1 \\ \Delta\overline{\theta}_2 \end{pmatrix} =$$
$$= - \begin{pmatrix} \partial_{V_1}(\overline{P}_1 + \overline{P}_{L_1}) & \partial_{V_2}\overline{P}_1 \\ \partial_{V_1}\overline{P}_2 & \partial_{V_2}(\overline{P}_2 + \partial_{V_2}\overline{P}_{L_2}) \end{pmatrix} \begin{pmatrix} \Delta\overline{V}_1 \\ \Delta\overline{V}_2 \end{pmatrix}$$

This is the correspondence of Eq. (2.6) for the general case.

The system equations above is now of the form:

$$\begin{pmatrix} M_{11} & 0 \\ 0 & 0 \end{pmatrix} \begin{pmatrix} \Delta\ddot{\overline{\theta}}_1 \\ \Delta\ddot{\overline{\theta}}_2 \end{pmatrix} + \begin{pmatrix} D_{11} & 0 \\ 0 & D_{22} \end{pmatrix} \begin{pmatrix} \Delta\dot{\overline{\theta}}_1 \\ \Delta\dot{\overline{\theta}}_2 \end{pmatrix} +$$
$$+ \begin{pmatrix} K_{11} & K_{12} \\ K_{12}^T & K_{22} \end{pmatrix} \begin{pmatrix} \Delta\overline{\theta}_1 \\ \Delta\overline{\theta}_2 \end{pmatrix} = \begin{pmatrix} B_{11} & B_{12} \\ B_{21} & B_{22} \end{pmatrix} \begin{pmatrix} \Delta\overline{V}_1 \\ \Delta\overline{V}_2 \end{pmatrix} \tag{2.19}$$

The quadratic stiffness matrix is again positive semi-definite. It is well known that the Schur complement of this matrix preserves the properties. It can be shown for a general stable power system that the submatrix K_{22} always is non-singular (Lemma B.3, Appendix B).

The equations can now be written as:

$$M_{11}\Delta\ddot{\overline{\theta}}_1 + D_{11}\Delta\dot{\overline{\theta}}_1 - K_{12}K_{22}^{-1}D_{22}\Delta\dot{\overline{\theta}}_2 + \left(K_{11} - K_{12}K_{22}^{-1}K_{12}^T\right)\Delta\overline{\theta}_1 =$$
$$= \left(B_{11} - K_{12}K_{22}^{-1}B_{21}\right)\Delta\overline{V}_1 + \left(B_{12} - K_{12}K_{22}^{-1}B_{22}\right)\Delta\overline{V}_2$$

The generalized model (KM) is

$$M_{11}\Delta\ddot{\overline{\theta}}_1 + \left(K_{11} - K_{12}K_{22}^{-1}K_{12}^T\right)\Delta\overline{\theta}_1 = 0$$

This equation has the same properties as for the model (KM) in Section 2.5. The eigenvalues and eigenvectors can now be calculated.

The sensitivity studies will be changed. If the weak coupling between angles and magnitudes of the voltage is set to zero, it is possible to show that $\Delta\overline{V}_2$ is a linear transformation of $\Delta\overline{V}_1$. To show this, the reactive power equation also must be used.

Further details is found in Appendix A. The general case is beyond this thesis and is not more discussed.

2.9 Computational Aspects

Most of the computational features of the model (KM) are summarized below.

System Assumptions

- No load damping
- No asynchronous damping of the generators

Features of the Model (KM)

- Calculating λ^2 instead of λ i.e., we gain roughly a factor of 8 with respect to computation time.
- The numerical accuracy of eigenvectors and eigenvalues can be checked by the quantity $\lambda_i^2 = K_{ii} \,/\, M_{ii}$.
- Validation of the model (KM) can be done by reasonable amount of work.
- If more than two eigenvalues are zero, the network is not completely connected.
- The coherency of generators can easily be applied to this model and can physically be interpreted.
- For the uncontrolled system only the half of the right eigenvectors need to be calculated for sensitivity analysis.

2.10 Conclusions

Modes faster than about 0.9 Hz are rather well damped due to the damper windings in generators and load characteristics.

It is a difficult task to master tuning of e.g., PSS-equipment for slow modes. The model (KM) is intended to provide a good base to continue with aggregated models of power systems and do siting and coordinated tuning studies for damping equipment in general. The nonlinear model includes governors, AVRs, 6 states generators, which shall be compared to 2 states for each machine in the model (KM).

The electro-mechanical properties of slow oscillations in a large power system are described well in the model (KM). Two states per generator are enough. Especially the mass scaled eigenvectors carry information of sites with significant impact on a certain mode. The sensitivity derivatives in the next chapter carry more information about important sites because the voltage dependence of the load is included.

3

Aggregation of Large Power Systems

3.1 Introduction

In general, large power systems demand a large amount of manpower for dynamic studies. In many cases, it is therefore a need to reduce the order of the system from different aspects. Many stability analyses concern only a local area of the power system. The surrounding area is then regarded as external. The external power system is then aggregated with different techniques. As long as the interacting effect of the external system on the study system can be faithfully represented, the behavior of the various machines within the external system is of secondary interest.

The control problem in this thesis can not regard any part of the system as external. Mainly two demands are the base for this new coherency technique:

1. Speed up the programming and testing of the developed methods in this thesis.
2. Give possibilities to reduce the number of the free parameters in coordinated tuning procedure (Chapter 5).

The second item is not used, because the tuning procedure can handle the introduced number of free parameters without any problem.

The slow and system wide modes of oscillation are quite tricky to stabilize adequately by means of the available damping equipment (e.g., PSS). There are also problems during the commissioning, especially to verify a suitable tuning of the PSS equipment. That is why we pay attention to slow system modes when we aggregate the generators.

A new technique is described for aggregation of generators in a (very) large power system. The technique of aggregation focuses on slow system oscillations to be used in siting studies and coordinated tuning of control parameters for different damping equipment, particularly PSSs (Power System Stabilizers), SVCs (Static Var Compensators) and HVDC (High Voltage Direct Current) links. The equivalent parameters for the turbine governors and synchronous machines are calculated as weighted mean values of the parameters of included governers and machines in the coherent group. Model parameters for voltage control, power system stabilizers etc., have the same control characteristics as the largest machine in the coherent group according to Edström (1985). The primary advantage of this procedure is that the definition of coherent machines within a certain frequency window can easily be interpreted physically and the definition is disturbance independent, i.e. no disturbances are applied to the power system for coherency analysis. Other definitions of coherency are shown in the references of papers concerning coherency, aggregation and reduction of power systems. The definition of coherency in these papers is mainly based on the quantity $|\Delta\delta_i(t) - \Delta\delta_j(t)|$ in different performance indices, where $\Delta\delta_i$ is the angle deviation of machine i.

Oshawa and Hayashi (1978) show another approach of defining coherency using Liapunov-functions. These definitions are used for large disturbance stability analysis (LDSA), as well as for small disturbance stability analysis (SDSA). The coherency of generators will depend on where the disturbance is or disturbances are applied in the power system and will also depend on the frequency spectrum of the disturbances. It is also difficult to inject enough energy in all modes of the power system, because different modes require different amount of energy to achieve comparable angular deviations. A modal-coherency technique for grouping of generators is used by Geeves (1988).

In Chapter 6 of Yu (1983) three different types of dynamic equivalencing techniques are described. The techniques are:

1. The modal approach
2. The coherency approach
3. The estimation approach (Kalman filter)

These aggregation techniques are based on a two system concept. One of the systems is the studied system and the rest of the power system is regarded as external. The external system is then aggregated to one or several equivalent machines.

In our case, we can't consider any part of the system to be external, because the generators interact in the slow system wide oscillations. That is why a new approach for aggregation is introduced.

The key features of the coherence analysis in this thesis are:

- The characteristics of slow system wide modes are preserved during the reductions.

- The aggregation of the generators is independent of the excitation.
- The slow and poorly damped system modes are considered only.
- Easy physical interpretation of coherency.
- Fast and reliable computational method.

3.2 Coherency and Aggregation Method

We know that the eigenvector components of the model (KM) are an approximation of the angle deviations of the generators. From linear theory we know that a general deviation of the machine angles are, to a large extent, described by a linear combination of the slow principle modes.

Now we are ready to formulate the definition of coherent groups of generators.

DEFINITION 3.1
The eigenvalues of the model (KM) and corresponding eigenvectors are ordered in decreasing order, i.e. $\lambda_1^2 \geq \lambda_2^2 \geq \ldots \geq \lambda_{n-1}^2 \geq \lambda_n^2 = 0$. Then cut out a certain λ-window, i.e. select a certain number of slow modes, and define the following set:

$$\begin{aligned} S &= \{\overline{S}_k \mid s_{ki} = \text{sign}(u_{ki}), k = 1, \ldots, n, \lambda_n < |\lambda_i| \leq \lambda_c\} \\ \lambda_c &= \text{upper limit (rad/sec)} \end{aligned} \tag{3.1}$$

$$\begin{aligned} u_{ki} &= \text{eigenvector component (angle deviation)} \\ &\quad \text{for generator } k \text{ and mode } i \in \lambda\text{-window} \\ n &= \text{number of generators} \end{aligned}$$

Let the number of modes within the λ-window be p.

Two machines (l, m) are said to be completely coherent if the scalar product of corresponding $\overline{S}_l \in S$ and $\overline{S}_m \in S$ has the following quality:

$$\overline{S}_l^T \cdot \overline{S}_m = p \tag{3.2}$$

□

The definition is independent of time and excitation signals according to Eqs. (3.1) and (3.2). The definition treats all the machines equal, even if a machine participates very little in a mode or the whole chosen spectrum. Naturally, it is possible to define a concept: nearly coherent machines. In this case we will get a "grey zone" of nearly non-participating machines. The aggregation will give less number of groups, but the aggregation should depend on the order of the generators. After a few tests, we find that the "harder" definition fulfilled our demands and experiences from simulations of the Nordel system. The definition above was finally adapted and the aggregation works well.

Table 3.1

Gen #	$\lvert\lambda_1\rvert$	$\lvert\lambda_2\rvert$	$\lvert\lambda_3\rvert$	$\lvert\lambda_4\rvert$	$\lambda_5 = 0$
1	−0.01	0.3	−0.4	0.3	1
2	−0.02	0.01	−0.1	−0.2	1
3	0.7	−0.02	−0.2	−0.4	1
4	−0.2	−0.03	0.3	0.1	1
5	0.01	−0.9	0.1	0.1	1

We will now use the definition of coherency in an example: Assume a power system consisting of five generators. Ten complex conjugated eigenvalues are calculated by the model (KM) of which two eigenvalues are zero (the rigid body motion). Let us also assume that two of the four principle modes are system wide. The eigenvectors are shown in Table 3.1. The ordering of the modes is done for decreasing imaginary value of the complex conjugated eigenvalues, i.e. $|\lambda_1| > |\lambda_2| > |\lambda_3| > |\lambda_4| > \lambda_5 = 0$. The assumptions above imply that the modes (λ_3, λ_4) are system wide.

In analogy with coherent light, we may say that we have five light sources with a spectrum of four different frequencies. The electromagnetic vectors (eigenvector components) of these frequencies have different directions. This insight leads us to say that for the two slowest modes (λ_3, λ_4) the following coherent groups can be defined:

Group 1 consists of Gen 1.
Group 2 consists of Gen 2 and Gen 3.
Group 3 consists of Gen 4 and Gen 5.

If we now include another mode (λ_2) the following coherent groups can be defined:

Group 1 consists of Gen 1.
Group 2 consists of Gen 2.
Group 3 consists of Gen 3.
Group 4 consists of Gen 4 and Gen 5.

If we only pick one mode (λ_4) we will get two coherent groups and so on.

The Aggregation Method Presented Step By Step

1. Given the necessary load flow data, i.e. bus data, generator data, branch data and transformer data, a simulation package as PSS/E from PTI or SIMPOW from ABB can be used for calculation of a converged load flow.
2. The necessary matrices for the model (KM) are calculated.

Table 3.2 Selected system modes.

Case 1 21 machines		Case 2 44 machines		Case 3 224 machines	
Mode #	Hz	Mode #	Hz	Mode #	Hz
1	0.289	1	0.264	1	0.248
2	0.371	2	0.346	2	0.338
3*	0.468	7	0.654	8	0.604
7	0.753	8	0.679	9	0.645
8	0.822	11*	0.848	13*	0.826
9	0.979	12*	0.866	14*	0.843
		13*	0.875	15	0.855
		14	0.901		

* Modes not accepted as system wide modes

3. The eigenvalues and eigenvectors are calculated for the matrix $M^{-1}K$ or $(\sqrt{M})^{-1}K(\sqrt{M})^{-1}$.
4. The coherent groups are calculated with chosen frequency window.
5. With given coherent groups and dynamic data for the power system, i.e. dynamic data of generators, AVRs, governors etc., a new reduced model of the power system can be calculated according to Edström (1985).
6. The outcome from above calculation is new reduced load flow data and dynamic data which are used for further reductions if necessary.

3.3 Application to the Nordel Power System

Reduction of Order of a Large Power System

Two dynamic aggregation levels are calculated. The method described in this chapter is applied to the initial system of 224 machines (Case 3). The coherence analysis gives 44 coherent groups (Case 2) with a frequency window of (0.1–1.0) Hz. Seventeen modes are included in this window.

Another coherence analysis is done for further reduction of the 44 machine system. The frequency window used was (0.1–0.67) Hz, which gives 21 coherent groups (Case 1). Seven modes of the 44-group system was used. The dynamic equivalent is calculated again of these 21 coherent groups.

At this stage it was considered not to do any further reductions. Only the slow and system wide modes are considered, i.e. a majority of the coherent groups (machines) participate with a non-neglectable contribution to the energy, Eq. (2.18), of the principle modes.

Aggregation Analysis of System Wide Modes

The chosen cases are organized according to Table 3.2. The modes are ordered from low frequencies to high frequencies for each case. Some of the slow and local modes are not presented in the table. The modes are marked with the ordered sequential number. The eigenvalue corresponding to the rigid body motion is excluded.

The model (KM) is used for calculation of the mass-scaled eigenvectors. Equation (2.18) shows that the components (deviation of machine angles) of the mass-scaled eigenvector represents the contribution of the energy corresponding to a certain mode.

The aggregation of the slowest mode will now be shown. The presentation is done in two different ways. The first method is based on a more strict comparison of the eigenvectors and the second method shows the geographical structure of the modes in the Nordel system. The second method gives only a visual feeling of the aggregation. Only the two slowest modes are shown. Further information is shown in Eliasson (1989a). Modes of concern are according to Table 3.2: Modes #1 and #2 for Case 1, Case 2 and Case 3.

Figure 3.1 shows the mass scaled eigenvector components of Case 3 and Case 2 for mode #1. To each eigenvector component, from the Model (KM) of Case 2, it corresponds a coherent group from Case 3. The eigenvector components of each coherent group of Case 3 are scattered around a solid line, representing the components of Case 2. Figure 3.2 describes how coherent groups of Case 2 are aggregated into equivalent machines of Case 1 for corresponding mode. These two figures show that the slowest system wide mode in each aggregation preserves its structure during the aggregation. This means that the slow dynamics are preserved.

Figures 3.3 (Case 1), 3.4 (Case 2) and 3.5 (Case 3) show the mass-scaled eigenvector components in a geographical form for mode #1. The larger arrow the larger is the amplitude of the corresponding machine angle deviation. The largest amplitudes in both directions are marked with a star and the sign $(+,-)$ of the arrows corresponds to the sign of the components of the mass-scaled eigenvector.

Figures 3.6 to 3.10 show the same sequence of figures for mode #2. The figures clearly show that the system wide modes in the low frequency range aggregate quite well, i.e. the physics is preserved during the reduction. The coherent groups are marked on maps describing the different cases in the Nordel power system in Appendix E.

3.4 Conclusions

The definition of coherency given in Section 3.2 can be applied to nonlinear representation of a large power system, e.g. Case 3. There exist numerical methods for

calculation of one eigenvalue and corresponding eigenvector at a time for large systems. By picking the components of an eigenvector representing the angle deviations of the generators for selected modes and store them in new vectors, the definition of coherency can immediately be used. In general the slow and system wide modes are poorly damped, i.e. the imaginary part of the eigenvector component is very small compared to the real part. The real part is used for the coherency analysis.

Many mechanical systems are poorly damped, e.g. the axis of the turbine and generator. For more complex and poorly damped mechanical construction the definition can be applied immediately to the states representing displacement.

The slow and system wide principal modes aggregates satisfactory, Case 1 describes Case 3 good in the low frequency range. In this frequency range it is of great importance that damping equipment acts well when needed.

It was of principle importance to know how the slow dynamics were aggregated, before using the equivalent dynamic models for further investigation of siting and coordinated tuning of damping equipment of large power systems.

The computation time is drastically reduced for the aggregated models compared to a full system model. Calculation of eigenvalues, eigenvectors, check of orthogonality (Eq. 2.12) and back check of the eigenvalues (Eq. 2.13) takes about 55 CPU-minutes on a VAX 11/750 for Case 3. For Case 2 corresponding time is a couple of minutes.

Finally, and maybe most important, the coherence analysis doesn't depend on any kind of disturbance (excitation) signal. This method will give us a firm base for SDSA analysis of (very) large power systems. The hierarchy of models enables preliminary studies on smaller models to establish general ideas of siting and coordinated tuning. The process can be then repeated with more insight on the large models.

The cases and system wide modes shown in Table 3.2 will be the basis for the siting and coordinated tuning analysis.

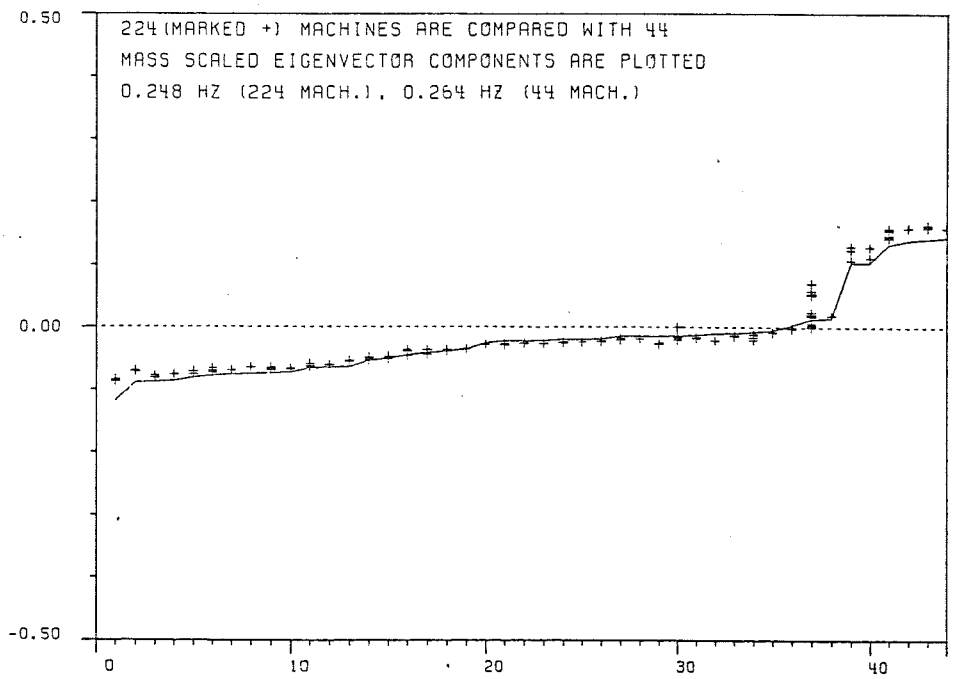

Figure 3.1 Eigenvector components of coherent groups of Case 3 (+) plotted together with eigenvector components of Case 2 (solid line). Mode #1.

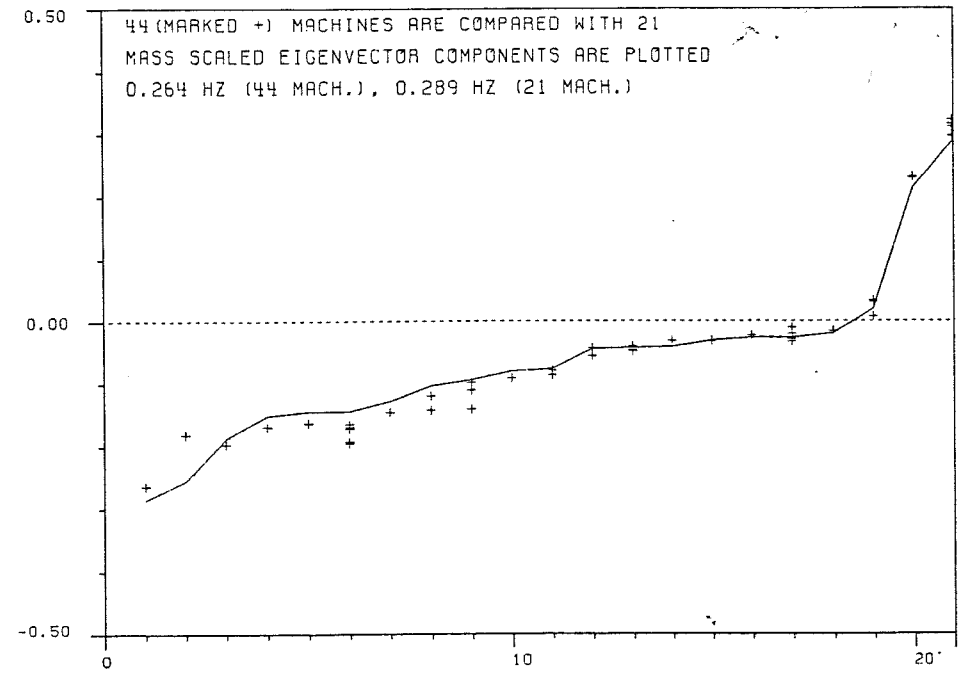

Figure 3.2 Eigenvector components of coherent groups of Case 2 (+) plotted together with eigenvector components of Case 1 (solid line). Mode #1.

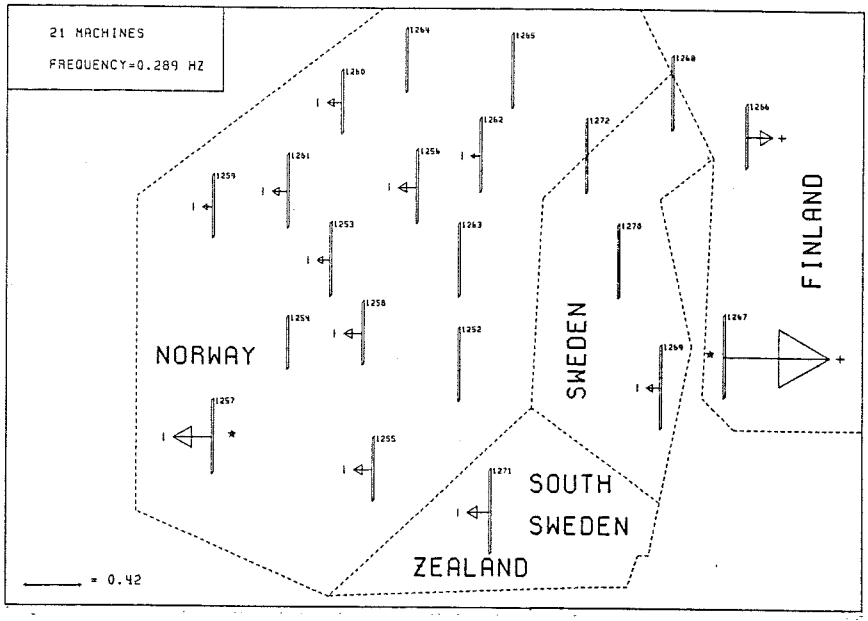

Figure 3.3 Mass-scaled eigenvector components of mode #1, Case 1. The largest components with opposite sign are marked with a star.

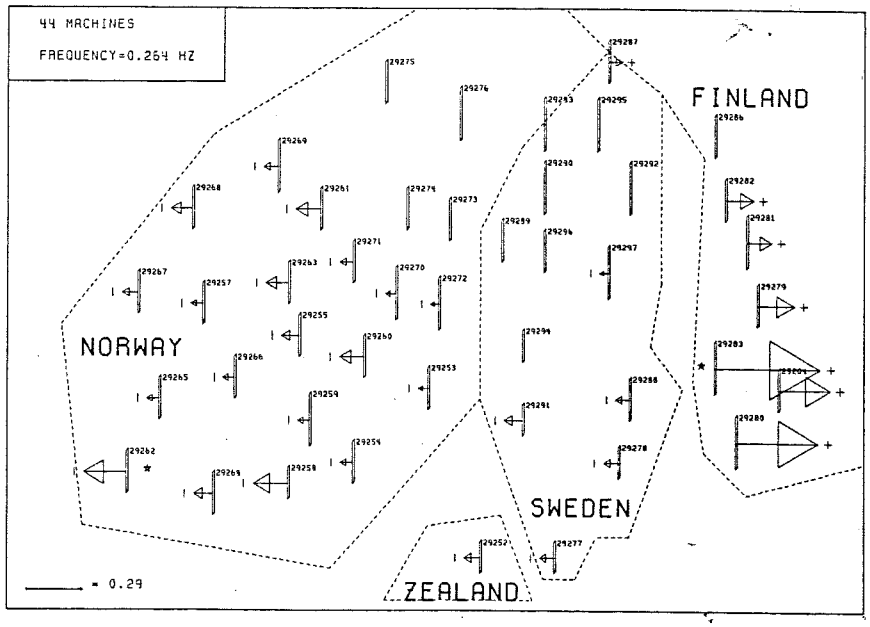

Figure 3.4 Mass-scaled eigenvector components of mode #1, Case 2. The largest components with opposite sign are marked with a star.

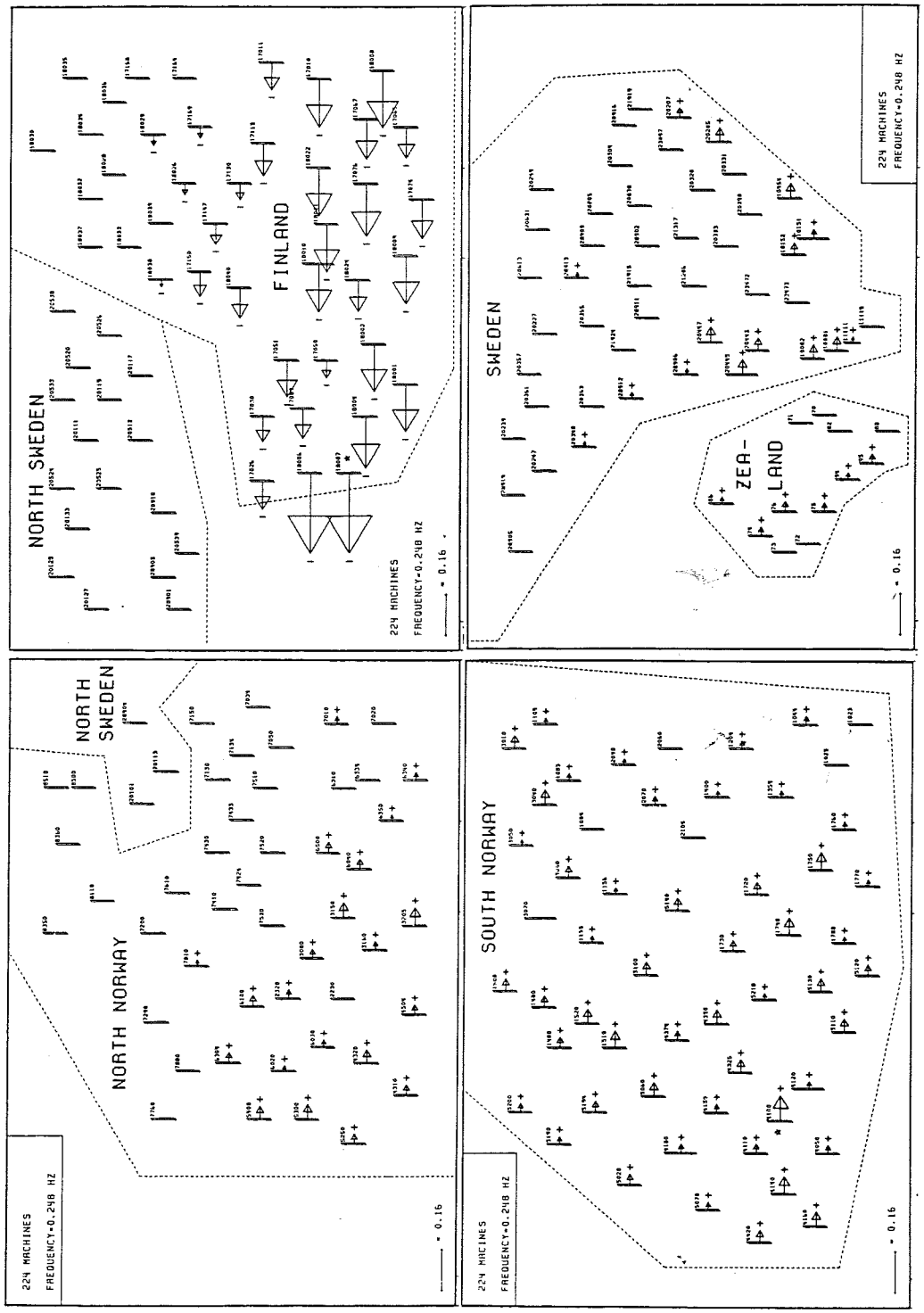

Figure 3.5 Mass-scaled eigenvector components of mode #1, Case 3. The largest components with opposite sign are marked with a star.

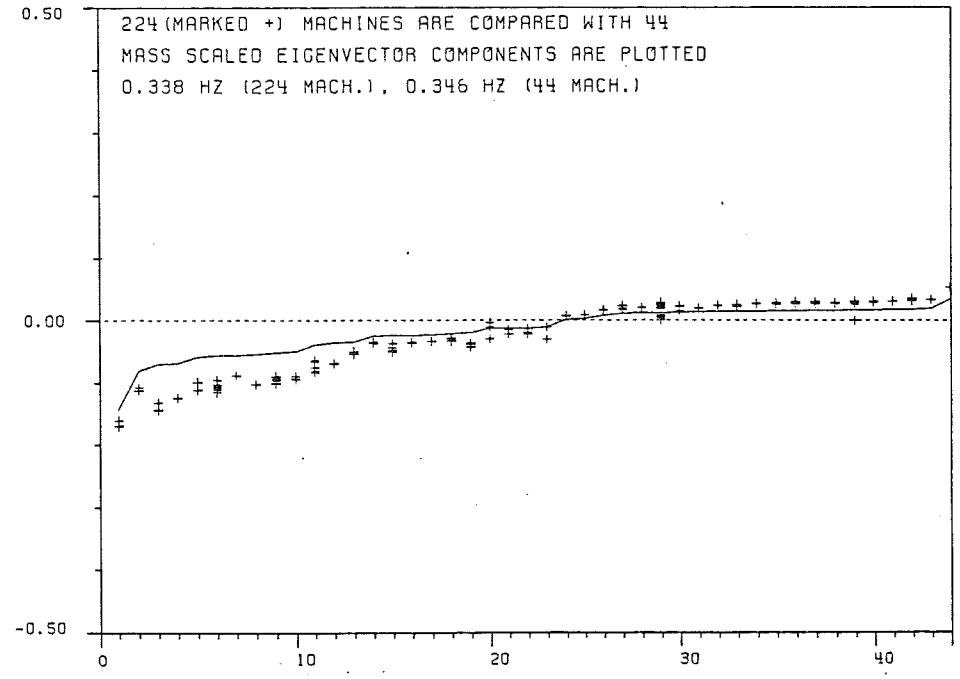

Figure 3.6 Eigenvector components of coherent groups of Case 3 (+) plotted together with eigenvector components of Case 2 (solid line). Mode #2.

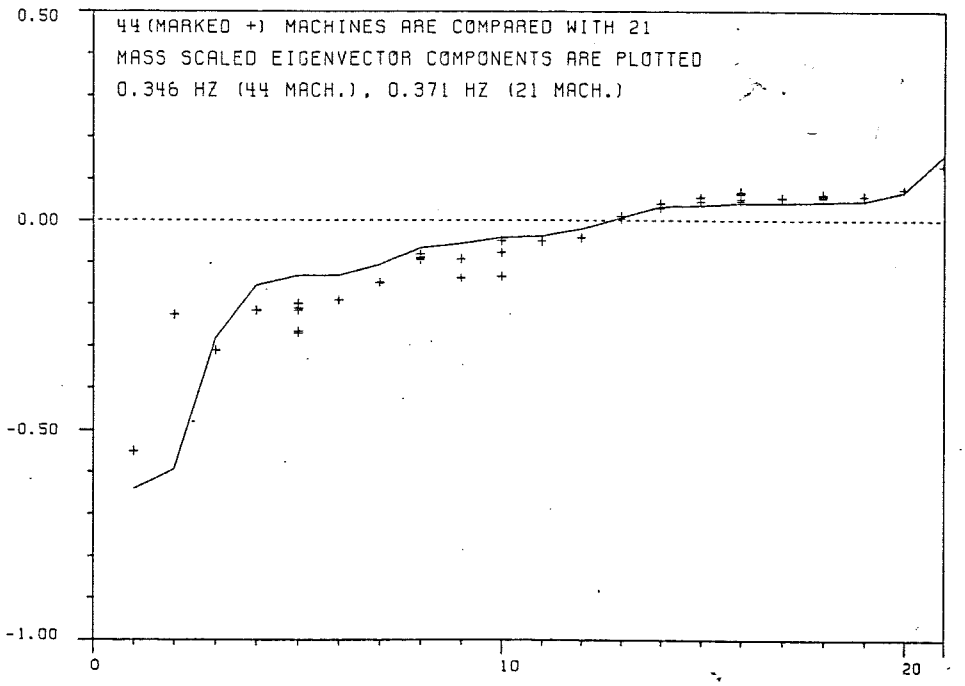

Figure 3.7 Eigenvector components of coherent groups of Case 2 (+) plotted together with eigenvector components of Case 1 (solid line). Mode #2.

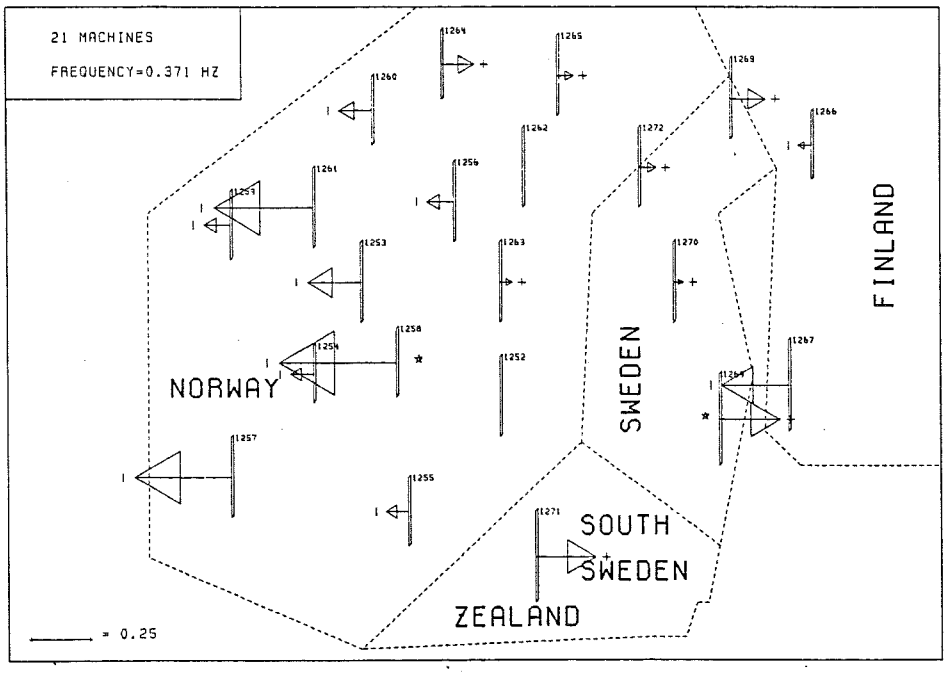

Figure 3.8 Mass-scaled eigenvector components of mode #2, Case 1. The largest components with opposite sign are marked with a star.

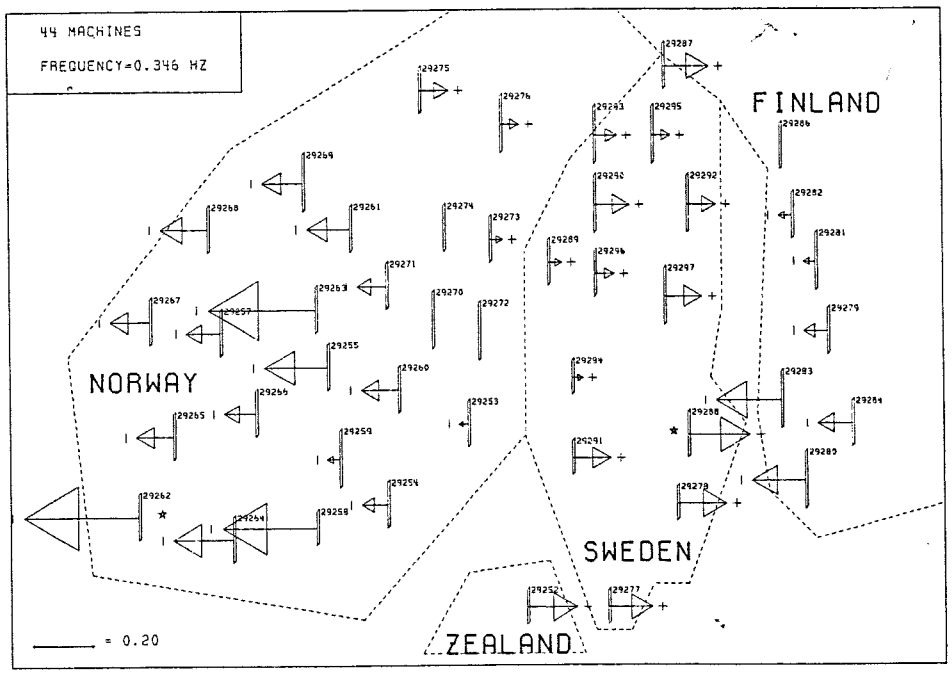

Figure 3.9 Mass-scaled eigenvector components of mode #2, Case 2. The largest components with opposite sign are marked with a star.

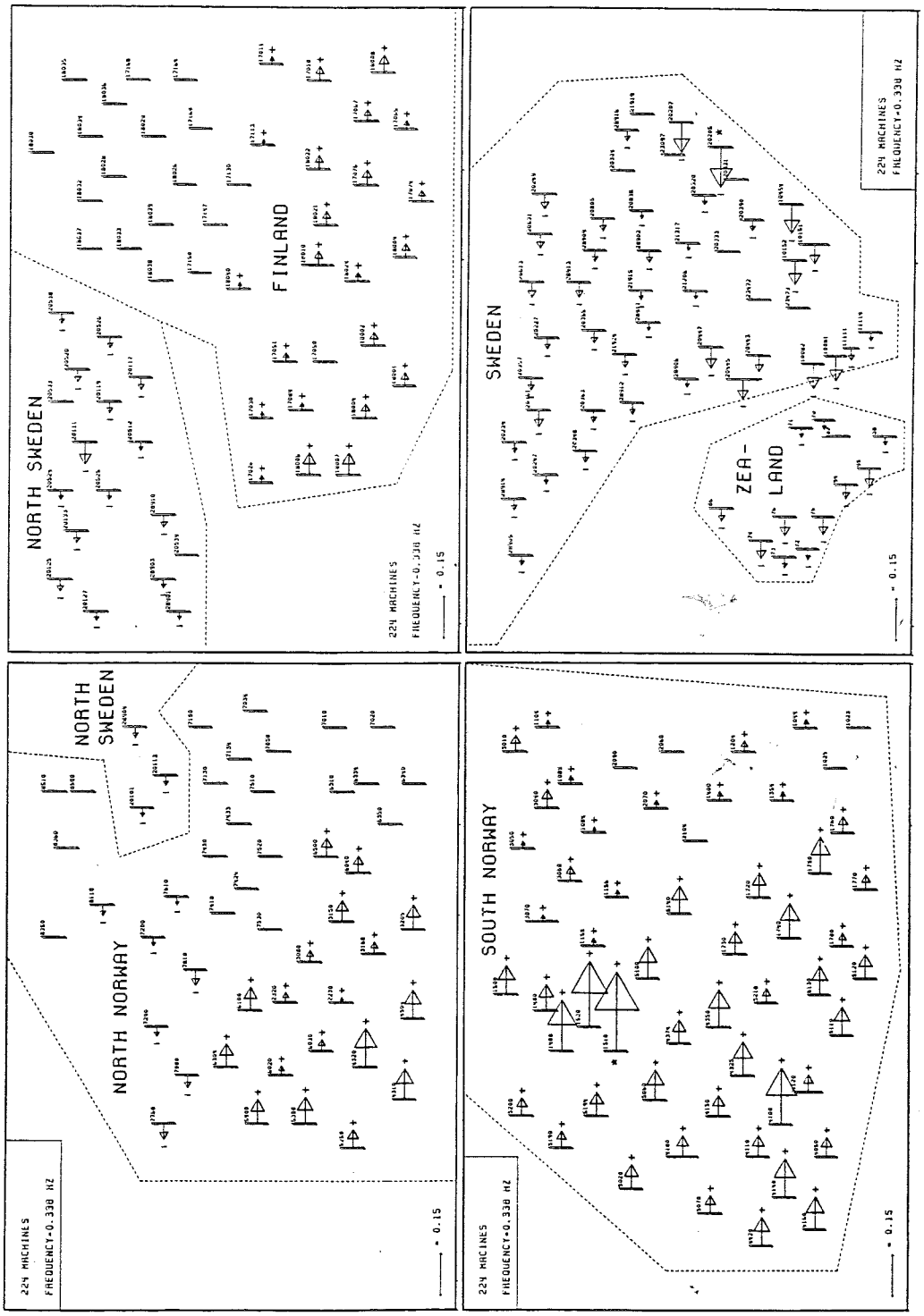

Figure 3.10 Mass-scaled eigenvector components of mode #3, Case 3. The largest components with opposite sign are marked with a star.

4

Siting Analysis of Damping Equipment

4.1 Introduction

An earlier report (Eliasson and Hill, 1989) gave a technique for studying of acceptable sites of damping equipment based on sensitivity studies of very large power systems. Damping equipment of concern for siting studies are PSSs (power systems stabilizer), SVCs (static var compensator) and HVDC (high voltage direct current) links.

The model (Chapter 2) used in this thesis is further simplified than the model given in Appendix A. This chapter will describe the robust siting technique used in this thesis. Some interesting analytical insights will also be presented.

The sensitivity technique is used for searching of robust sites of SVCs and PSSs within a chosen frequency window with respect to the voltage dependence of the load. For HVDC links the sensitivity technique is used for searching of best places of measurement providing overall good damping within a certain frequency window. Special emphasis is given to handle large power systems, voltage dependent loads and alternative measurement schemes. The techniques are applied to the Nordel power system. Three aggregated models are used (224, 44 and 21 machines). These models were obtained using the technique in Chapter 3.

The frequency and voltage dependence of the load is in general not known. By measurements the load characteristics can be found. The loads seen from the high voltage system is composed of different loads, from constant active and

reactive power loads to impedance loads. A typical industrial load can have the following composition:

Induction motors, 60%
Synchronous motors, 20%
Other "ingredients", 20%

Such a load would have the following approximate parameters:

$\partial_V P \approx 1.0$ p.u./p.u.
$\partial_V Q \approx 1.3$ p.u./p.u.
$\partial_f P \approx 1.0$ p.u./p.u.
$\partial_f Q$ is of less importance.

The voltage dependence of the loads will play an important role for siting of PSSs and SVCs. These equipments affect the voltage (magnitude) at the siting buses. If the control is done in a proper way with known voltage dependence of the load, it is possible to damp EMOs. The loads increase in general with increasing voltage.

Due to the reason that the voltage dependence of the load is not exactly known, a robust siting technique must be used. The sites for PSSs and SVCs must be good for different load characteristics. The technique presented in this thesis is robust against the voltage dependence of the loads.

The frequency dependence of the loads will influence the impact on the damping of EMOs by HVDC links. The control concept applied to the HVDC link will act as a frequency dependent active load. The damping submatrix from HVDC links will be symmetric and positive semidefinite. It is a well known property that the symmetric part of a damping matrix will introduce positive dissipative forces.

The frequency dependence of composite loads is in general positive, i.e. with increasing frequency the load will increase. If the frequency dependence from loads is added to the contribution from the HVDC links, it will always give additional positive damping. In this thesis the links are not sited in the same manner as for the PSSs and SVCs. Only alternative points of measurement of the frequency deviations are calculated. At the points of injection for the link are the frequency dependence of the load equal for all alternative points of measurement. That is why the positive damping from the link only is considered.

To analyze the stability problem of a large power system, it is necessary that the used method allows:

- Presence of PSSs and SVCs
- Presence of HVDC links
- Different load characteristics
- Possibility of alternative signals
- Graphical presentation of results

Existing techniques (deMello *et al.* (1980), Lysfjord *et al.* (1982), Larsen and Swann (1981) and Padiyar *et al.* (1981)) do not cater for above features integrated.

In Eliasson and Hill (1989) a simplified model for eigenvalue sensitivity analysis, which allows inclusion of these features, is presented. Realizing that we may need to consider power systems of order of several hundreds of generators, the basic models of components must be simplified in order to reduce computer time as much as possible but not violate the properties of the slow dynamics.

Some new procedures will be introduced, such as:

- Method for siting of PSSs and SVCs with respect to slow and system wide modes and different load characteristics with respect to voltage.
- Method for best points of measurement for given site of HVDC links with respect to damping within a certain frequency window and loss of communication.

Some of the most interesting general findings are:

- The role of load modeling in siting turns out to be very important.
- Graphical presentation makes it very easy to study large systems.
- The new Fenno-Skan link (HVDC) has excellent impact on damping with correct site of measurement of frequency deviation. Also the effect of lost communication is considered.
- Robust siting of PSSs with respect to load characteristics and within selected slow and system wide modes are presented.
- Robust siting of SVCs with respect to load characteristics and within selected slow and system wide modes are presented.

4.2 Simplified PSS Control Structure

The model of the power system is basically described in Chapter 2. The control is assumed to have the structure:

$$\begin{aligned} \Delta \overline{V}_{\mathrm{PSS}} &= K_{se}\Delta\dot{\bar{\theta}} + K_{sed}\Delta\ddot{\bar{\theta}} \\ K_{se} &= \mathrm{diag}\,(K_{se_i}) \quad \text{(speed error)} \\ K_{sed} &= \mathrm{diag}\,(K_{sed_i}) \quad \text{(speed error derivative)} \end{aligned} \tag{4.1}$$

If a PSS is placed at bus i, $K_{se_i} \neq 0$ and/or $K_{sed_i} \neq 0$, otherwise $K_{se_i} = K_{sed_i} = 0$. K_{se_i} represents a feedback from angle velocity. K_{sed_i} represents a feedback from acceleration. This choice is motivated because the most common input signals to the PSSs are angle frequency and angle acceleration. For the

second order concept presented in this thesis, it is of minor interest to include K_{sed}. From now on we consider $K_{sed} = 0$. The K_{se}-matrix is diagonal. This is a consequence of that only local measurements are considered, i.e. no transmission of signals between the PSSs is included. For a PSS installed at generator i the control is:

$$\Delta V_i = K_{se_i} \cdot \Delta\dot{\theta}_i \tag{4.2}$$

4.3 Simplified SVC Control Structure

Alternative points of measurement of SVC- and HVDC-equipment are investigated below. The approach is believed to be new. Consider a SVC equipment placed at bus i and remote speed transducer at bus $l(+)$ and at bus $k(-)$. The control law becomes:

$$\Delta V_i = K_{\mathrm{SVC}_i}(\Delta\dot{\theta}_l - \Delta\dot{\theta}_k) \tag{4.3}$$

The control law for a given number of SVCs can be written in matrix form:

$$\Delta\overline{V}_{\mathrm{SVC}} = T_s^{\mathrm{SVC}} \cdot K_{\mathrm{SVC}} \cdot (T_m^{\mathrm{SVC}})^T \Delta\dot{\theta} \tag{4.4}$$

T_s^{SVC} is the siting incident matrix with dimension number of buses times number of SVCs.

T_m^{SVC} is the measurement incident matrix with the same dimension as T_s^{SVC}.

K_{SVC} is the gain matrix (diagonal) with the dimension number of SVCs times number of SVCs.

Each column in T_s^{SVC} and T_m^{SVC} takes care of one SVC, e.g. if the SVC number j is installed at bus i, it will cause $T_s^{\mathrm{SVC}}(i,j) = 1$ and if measurement takes place at bus $k(+)$ and bus $l(-)$ will cause $T_m^{\mathrm{SVC}}(k,j) = 1$ and $T_m^{\mathrm{SVC}}(l,j) = -1$. $K_{\mathrm{SVC}}(j,j)$ contains the gain for SVC number j.

T_m^{SVC} contains only ± 1 or 0 in each column. T_s^{SVC} contains only $+1$ or 0 in each column.

4.4 Simplified HVDC Control Structure

An HVDC link introduces a frequency dependent active load. Consider a link installed with the rectifier at bus i and inverter at bus j. The measurements are taken at bus $l(+)$ and bus $k(-)$. The control law becomes according to Eq. (2.5):

$$\Delta P_{L_i}^{\mathrm{DC}} = K_{\mathrm{DC}_i}(\Delta\dot{\theta}_l - \Delta\dot{\theta}_k) \tag{4.5}$$

We also assume that control is executed by the rectifier and within the current margin for the link, which will give

$$\Delta P_{L_j}^{\mathrm{DC}} = -\Delta P_{L_i}^{\mathrm{DC}} = K_{\mathrm{DC}_i}(\Delta\dot{\theta}_k - \Delta\dot{\theta}_l)$$

The control law for a given number of HVDC links can be written in matrix form:

$$D_{\mathrm{DC}}\Delta\dot{\bar{\theta}} = T_s^{\mathrm{DC}} \cdot K_{\mathrm{DC}} \cdot (T_m^{\mathrm{DC}})^T \cdot \Delta\dot{\bar{\theta}} \tag{4.6}$$

The only difference from the SVC concerning the incidence matrices, is that T_s^{DC} contains both ± 1 and 0 in each column, e.g. if link number k has its rectifier at bus i and inverter at bus j, it gives $T_s^{\mathrm{DC}}(i,k) = +1$ and $T_s^{\mathrm{DC}}(j,k) = -1$. Otherwise everything corresponds with the SVC case.

4.5 Introduced Damping Structure

It is a well known problem that the inherent damping of the generators and high AVR gain can give negative damping during heavy load conditions. This problem is not included in the model used in this thesis, because the second order concept/generator wants to be investigated.

It is assumed, conservatively, that the damping from damper windings of the generators can be neglected and the load doesn't vary with the frequency, i.e.

$$\begin{aligned} D_g &= 0 \\ \partial_\omega \overline{P}_L &= D_{\mathrm{DC}} \end{aligned} \tag{4.7}$$

The voltage deviation obtained for the PSSs and the SVCs is

$$\Delta\overline{V} = \Delta\overline{V}_{\mathrm{PSS}} + \Delta\overline{V}_{\mathrm{SVC}}$$

System equations:

$$\begin{cases} M \cdot \Delta\ddot{\bar{\theta}} + D_{\mathrm{DC}} \cdot \Delta\dot{\bar{\theta}} + K \cdot \Delta\bar{\theta} = B\left(\Delta\overline{V}_{\mathrm{PSS}} + \Delta\overline{V}_{\mathrm{SVC}}\right) \\ \Delta\dot{\bar{\theta}} = \Delta\bar{\omega} \end{cases} \tag{4.8}$$

$$\begin{aligned} \Delta\overline{V}_{\mathrm{PSS}} &= K_{se} \cdot \Delta\dot{\bar{\theta}} \\ \Delta\overline{V}_{\mathrm{SVC}} &= T_s^{\mathrm{SVC}} \cdot K_{\mathrm{SVC}} \cdot (T_m^{\mathrm{SVC}})^T \cdot \Delta\dot{\bar{\theta}} \\ D_{\mathrm{DC}} &= T_s^{\mathrm{DC}} \cdot K_{\mathrm{DC}} \cdot (T_m^{\mathrm{DC}})^T \end{aligned}$$

i.e.

$$\begin{cases} M \cdot \Delta\ddot{\bar{\theta}} + \tilde{D} \cdot \Delta\dot{\bar{\theta}} + K \cdot \Delta\bar{\theta} = \bar{0} \\ \Delta\dot{\bar{\theta}} = \Delta\bar{\omega} \end{cases}$$

where

$$\tilde{D} = D_{\text{DC}} - B \cdot K_{se} - B \cdot T_s^{\text{SVC}} K_{\text{SVC}} (T_m^{\text{SVC}})^T \triangleq D_{\text{DC}} + D_{PSS} + D_{\text{SVC}}$$
$$K = \partial_\theta(\overline{P}_0)$$

In matrix form

$$\frac{d}{dt}\begin{pmatrix} \Delta\bar{\theta} \\ \Delta\dot{\bar{\theta}} \end{pmatrix} = \begin{pmatrix} 0 & I \\ -M^{-1}K & -M^{-1}\tilde{D} \end{pmatrix}\begin{pmatrix} \Delta\bar{\theta} \\ \Delta\dot{\bar{\theta}} \end{pmatrix} \tag{4.9}$$

With

$$\begin{pmatrix} \Delta\bar{\theta} \\ \Delta\dot{\bar{\theta}} \end{pmatrix} = \bar{x} \quad \text{and} \quad A = \begin{pmatrix} 0 & I \\ -M^{-1}K & -M^{-1}\tilde{D} \end{pmatrix}$$

the system equation becomes

$$\dot{\bar{x}} = A\bar{x}$$

From Eq. (2.17) we saw that the system matrix A can be transformed to a new system, matrix $\tilde{A}$. The similar transformation (S) is given by

$$S = \begin{pmatrix} (\sqrt{M})^{-1} & 0 \\ 0 & (\sqrt{M})^{-1} \end{pmatrix}$$

and

$$\tilde{A} = \begin{pmatrix} 0 & I \\ -(\sqrt{M})^{-1}K(\sqrt{M})^{-1} & -(\sqrt{M})^{-1}\tilde{D}(\sqrt{M})^{-1} \end{pmatrix}$$

The eigenvectors for the two systems are different, but have the same property for the uncontrolled system, Eq. (2.11).

4.6 Siting Analysis for Damping Equipment

According to Fadeev and Fadeeva (1963) and Wilkinson (1965) the differential of an eigenvalue λ_i of a square matrix A can be written as:

$$\partial\lambda_i = \frac{\overline{v}_i^* \, \partial A \, \overline{u}_i}{\overline{v}_i^* \, \overline{u}_i} \tag{4.10}$$

where

$\overline{u}_i$ is the right eigenvector of A associated with λ_i

$\overline{v}_i$ is the right eigenvector of A^T associated with λ_i^*

An interesting special case to examine is the derivatives when the feedback gains are zero, i.e. the uncontrolled system. This corresponds to the initial direction of movement of the selected eigenvalues when the controller is introduced. This is used by deMello *et al.* (1980) too. To calculate the derivatives for zero gains is motivated by the following: The PSSs and SVCs are restricted to a maximum change of the bus voltage to 5% and during normal operation the HVDC links are restricted to change the active load to roughly 5–10% for damping purposes. These restrictions will give sufficient damping but not increase the relative damping for the slowest modes with more than approximately 0.1 for a single equipment. For such small changes of the eigenvalues the eigenvectors do not, in general, change much either. The analysis of the sensitivity derivatives with the gains equal to zero will therefore give a good information of where to site equipment before tuning. Also by varying important system parameters it is possible to get robust sites. The derivatives above are calculated for each type of damping equipment and for selected system wide modes.

In order to find robust sites for PSSs and SVCs, the voltage dependence of the load is varied between two limits. Only the active power of the load is considered. We assume that the load is proportional to $|V|^{\alpha}$, where $|V|$ is the magnitude of the voltage at the load bus. The upper limit was chosen to 1.5 and the lower limit was chosen to 0. The upper limit corresponds to 50% constant current and 50% constant impedance load. The lower limit corresponds to constant active load. For the HVDC links the sites of the rectifier and the inverter are considered to be known. Only alternative points of measurement of the frequency deviations are investigated. The expression of Eq. (4.10) is now calculated for each type of equipment.

The sensitivity derivatives of each equipment are given in two ways. The first presented expression is valid for a general system. The second expression is valid only when the feedback matrices are equal to zero. In the last expression we know the left eigenvectors when the right eigenvectors are known. The mass-scaled coordinates are also used for the "zero" case.

Sensitivity with Respect to K_{se}

For the system matrix as in Eq. (4.9) we get

$$\begin{aligned}
\partial^{K_{se}} A &= \begin{pmatrix} 0 & 0 \\ 0 & -\partial^{K_{se}} \left(M^{-1} \tilde{D} \right) \end{pmatrix} \\
\partial^{K_{se}} \left(M^{-1} \tilde{D} \right) &= M^{-1} \left(\partial^{K_{se}} \tilde{D} \right) \\
\tilde{D} &= D_{\mathrm{DC}} + D_{K_{se}} + D_{\mathrm{SVC}} \\
\partial^{K_{se}} \tilde{D} &= \partial^{K_{se}} D_{K_{se}} = \partial^{K_{se}} \left(-B K_{se} \right) \\
&= -B I_{K_{se}}
\end{aligned}$$

$I_{K_{se}}$ is a diagonal matrix with a 1 in position l if a PSS is installed at bus l, otherwise zero. Off-diagonal elements are zero.

Summary:

$$\partial^{K_{se}}\lambda_i = \frac{\overline{v}_i^* \begin{pmatrix} 0 & 0 \\ 0 & M^{-1}BI_{K_{se}} \end{pmatrix} \overline{u}_i}{\overline{v}_i^* \, \overline{u}_i}$$

For the feedback matrices equal to zero we get

$$\partial^{K_{se}}\lambda_i = \frac{x_{iu}^T(\sqrt{M})^{-1} \cdot B \cdot I_{K_{se}} \cdot (\sqrt{M})^{-1} \cdot x_{iu}}{2} \tag{4.11}$$

Sensitivity with Respect to K_{SVC}

$$\partial^{K_{\mathrm{SVC}}} A = \begin{pmatrix} 0 & 0 \\ 0 & -\partial^{K_{\mathrm{SVC}}}\left(M^{-1}\tilde{D}\right) \end{pmatrix}$$

$$\partial^{K_{\mathrm{SVC}}}\left(M^{-1}\tilde{D}\right) = M^{-1}\left(\partial^{K_{\mathrm{SVC}}}\tilde{D}\right)$$

$$\begin{aligned} \partial^{K_{\mathrm{SVC}}}\tilde{D} &= \partial^{K_{\mathrm{SVC}}} D_{\mathrm{SVC}} \\ &= -BT_S^{\mathrm{SVC}} I_{\mathrm{SVC}} (T_M^{\mathrm{SVC}})^T \end{aligned}$$

The matrix I_{SVC} is is equal to the unit matrix with the dimension equal to number of installed SVCs.

Summary:

$$\partial^{K_{\mathrm{SVC}}}\lambda_i = \frac{\overline{v}_i^* \begin{pmatrix} 0 & 0 \\ 0 & M^{-1}BT_s^{\mathrm{SVC}} I_{\mathrm{SVC}} (T_m^{\mathrm{SVC}})^T \end{pmatrix} \overline{u}_i}{\overline{v}_i^* \, \overline{u}_i}$$

For the feedback matrices equal to zero we get

$$\partial^{K_{\mathrm{SVC}}}\lambda_i = \frac{x_{iu}^T(\sqrt{M})^{-1} \cdot B \cdot T_s^{\mathrm{SVC}} \cdot I_{\mathrm{SVC}} \cdot (T_m^{\mathrm{SVC}})^T \cdot (\sqrt{M})^{-1} \cdot x_{iu}}{2} \tag{4.12}$$

Sensitivity with Respect to K_{DC}

$$\partial^{K_{\mathrm{DC}}} A = \begin{pmatrix} 0 & 0 \\ 0 & -\partial^{K_{\mathrm{DC}}}\left(M^{-1}\tilde{D}\right) \end{pmatrix}$$

$$\partial^{K_{\mathrm{DC}}}\left(M^{-1}\tilde{D}\right) = M^{-1}\left(\partial^{K_{\mathrm{DC}}}\tilde{D}\right)$$

$$\begin{aligned} \partial^{K_{\mathrm{DC}}}\tilde{D} &= \partial^{K_{\mathrm{DC}}} D_{\mathrm{DC}} = \partial^{K_{\mathrm{DC}}}\left(T_s^{\mathrm{DC}} K_{\mathrm{DC}} (T_m^{\mathrm{DC}})^T\right) \\ &= T_s^{\mathrm{DC}} I_{\mathrm{DC}} (T_m^{\mathrm{DC}})^T \end{aligned}$$

The matrix I_{DC} is equal to the unit matrix with the dimension equal to number of installed HVDC links.

Summary:

$$\partial^{K_{\mathrm{DC}}}\lambda_i = -\frac{\overline{v}_i^* \begin{pmatrix} 0 & 0 \\ 0 & M^{-1}T_s^{\mathrm{DC}} I_{\mathrm{DC}} (T_m^{\mathrm{DC}})^T \end{pmatrix} \overline{u}_i}{\overline{v}_i^* \overline{u}_i}$$

For the feedback matrices equal to zero we get

$$\partial^{K_{\mathrm{DC}}}\lambda_i = -\frac{x_{iu}^T (\sqrt{M})^{-1} T_s^{\mathrm{DC}} \cdot I_{\mathrm{DC}} \cdot (T_m^{\mathrm{DC}})^T \cdot (\sqrt{M})^{-1} \cdot x_{iu}}{2} \tag{4.13}$$

4.7 Necessary Siting Condition for Positive Damping

The eigenvalues of A are either real or complex conjugated, i.e. the trace of A, $\mathrm{tr}\, A$, is equal to the sum of the real parts of the eigenvalues. This implies that the trace must decrease when a PSS or any other damping equipment is properly installed. A necessary condition for positive damping is that the component of the gradient of $\mathrm{tr}\, M^{-1}\tilde{D}$ is negative for all load characteristics (robust site).

We now want to make a physical interpretation of this condition.

PSS-equipment: The necessary positive damping condition gives for a PSS installed at bus i:

$$\frac{\partial\, \mathrm{tr}(A)}{\partial K_{se_i}} = \frac{B(i,i)}{m_{ii}} < 0$$

Since $m_{ii} > 0 \;\forall\; i = 1, \ldots, n$, we get the condition:

$$B(i,i) = \sum_{j \neq i}^{n} \sin(\theta_j - \theta_i) \frac{V_j}{X_{ij}} - \frac{\partial P_{L_i}}{\partial V_i} < 0$$

$$\Rightarrow \sum_{j \neq i}^{n} \sin(\theta_j - \theta_i) \frac{V_j}{X_{ij}} < \frac{\partial P_{L_i}}{\partial V_i}$$

$$\Rightarrow \sum_{j \neq i}^{n} P_{ij} > -V_i \frac{\partial P_{L_i}}{\partial V_i} \quad \text{because} \quad P_{ij} = \frac{V_i V_j}{X_{ij}} \sin(\theta_i - \theta_j)$$

Assume that

$$P_{L_i} = C V_i^{\alpha} \Rightarrow V_i \frac{\partial P_{L_i}}{\partial V_i} = \alpha P_{L_i} \tag{4.14}$$

To fulfill the necessary positive damping condition we must require that

$$\sum_{j \neq i} P_{ij} > -\alpha P_{L_i} \tag{4.15}$$

For $\alpha = 0$ it gives that

$$\sum_{j \neq i} P_{ij} > 0 \tag{4.16}$$

A rule of thumb may now be stated. If it is attempted to install a PSS-equipment in a coherent group of generators, the group should have a net surplus of power for all load conditions. The site will then be robust against load characteristics and different load conditions. If this is not the case, the sign of the K_{se}-parameter may ought to be changed or the PSS-controller should be turned off.

We are now going to extend this analysis for a chosen mode with the eigenvalue λ_s. Assume that we install a PSS at bus j and evaluate the sensitivity derivative for λ_s at $K_{se_j} = 0$ according to Eq. (4.11). We get

$$\begin{aligned}\frac{\partial \lambda_s}{\partial K_{se_j}} &= x_{su}^T \begin{pmatrix} \frac{B(1,j)}{\sqrt{m_1}} \\ \vdots \\ \frac{B(n,j)}{\sqrt{m_n}} \end{pmatrix} \frac{x_{su_j}}{2\sqrt{m_j}} \\ &= \frac{x_{su_j}}{2\sqrt{m_j}} \left\{ x_{su_1} \frac{B(1,j)}{\sqrt{m_1}} + \cdots + x_{su_j} \frac{B(j,j)}{\sqrt{m_j}} + \cdots + x_{su_n} \frac{B(n,j)}{\sqrt{m_n}} \right\}\end{aligned} \tag{4.17}$$

The damping matrix is

$$\tilde{D} = (\sqrt{M})^{-1} D (\sqrt{M})^{-1}, \quad D = -B \cdot K_{se}$$

where $K_{se} = \text{diag}(0 \ldots 0, K_{se_j}, 0 \ldots 0)$. From Eq. (2.8) we know that

$$B(j,j) = \sum_{i \neq j} -B(i,j) - \frac{\partial P_{Lj}}{\partial V_j}$$

Now the derivative becomes

$$\frac{\partial \lambda_s}{\partial K_{se_j}} = \sum_{l \neq j}^{n} \left(\left(\frac{x_{su_j} \cdot x_{su_l}}{2\sqrt{m_j}\sqrt{m_l}} - \frac{x_{su_j}^2}{2m_j} \right) B(l,j) \right) - \frac{x_{su_j}^2}{2m_j} \frac{\partial P_{Lj}}{\partial V_j} \tag{4.18}$$

Since the feedback matrices are zero, it follows that this expression is real. According to Eq. (4.14) we know that $\partial P_{L_j} / \partial V_j > 0$. This implies that the voltage dependence of the load always has a good influence on the real part of λ_s. Naturally, we always demand that $\partial \lambda_s / \partial K_{se_j} < 0$.

If the voltage dependence of the load is zero, Eq. (4.18) becomes:

$$\frac{\partial \lambda_s}{\partial K_{se_j}} = \sum_{l \neq j}^{n} \left(\left(\frac{x_{su_j} \cdot x_{su_l}}{2\sqrt{m_j}\sqrt{m_l}} - \frac{x_{su_j}^2}{2m_j} \right) B(l,j) \right)$$

This implies for negative sensitivity derivative that

$$\frac{x_{su_j}}{2\sqrt{m_j}}\left(\sum_{l\neq j}^{n}\frac{x_{su_l}}{\sqrt{m_l}}B(l,j)\right)-\frac{x_{su_j}^2}{2m_j}\sum_{l\neq j}^{n}B(l,j)<0$$

The site assumes to fulfill the necessary condition for $\alpha = 0$, which indicates that a site can have negative sensitivity derivative for

$$\sum_{l\neq j}^{n}\frac{x_{su_l}}{\sqrt{m_l}}B(l,j)>0 \tag{4.19}$$

This is not good from damping point of view and especially when we are going to use the trace of the system matrix during the optimization. We come back to this problem, but first we look at the quadratic form of the damping matrix.

The equation (4.17) above can also be obtained by

$$\frac{\partial\lambda_s}{\partial K_{se_j}}=-\frac{X_{su}^T\cdot\tilde{D}\cdot X_{su}}{2\,K_{se_j}} \tag{4.20}$$

For $\partial\lambda_s/\partial K_{se_j}<0$ it implies that $X_{su}^T\tilde{D}X_{su}>0$, because K_{se_j} is considered to be greater than zero.

The following can now be stated. For all chosen system modes (λ_s) and all acceptable sites of PSSs, it is equivalent to say that the quadratic form of corresponding $\tilde{D}$:s and upper half of the eigenvectors is positive.

In the thesis we only consider slow and system wide modes. For these modes, the statement above also implies that the introduced dissipative forces stabilize the system for slow and system wide oscillations. For other frequencies we can not say anything.

Finally, we will analyze the relationship between the sensitivity of the trace and the eigenvalues with respect to the same parameter, K_{se_j}. Equation (4.17) gives:

$$\frac{\partial\lambda_s}{\partial K_{se_j}}=\frac{x_{su_j}}{2\sqrt{m_j}}\left(\sum_{l\neq j}^{n}\frac{x_{su_l}B(l,j)}{\sqrt{m_l}}\right)+\frac{x_{su_j}^2}{2m_j}B(j,j)$$

We know that

$$\frac{\partial}{\partial K_{se_j}}(\mathrm{tr}\,A)=\frac{B(j,j)}{m_j}$$

Now we get

$$\frac{\partial\lambda_s}{\partial K_{se_j}}=\frac{x_{su_j}}{2\sqrt{m_j}}\sum_{l\neq j}^{n}\frac{x_{su_l}B(l,j)}{\sqrt{m_l}}+\frac{x_{su_j}^2}{2}\frac{\partial}{\partial K_{se_j}}(\mathrm{tr}\,A) \tag{4.21}$$

Equation (4.21) indicates that if

$$\sum_{l \neq j}^{n} x_{su_l} \frac{B(l,j)}{\sqrt{m_l}}$$

is close to zero, it is a minor difference of the sensitivity with respect to λ_s and $\operatorname{tr} A$. The site (j) is selected according to the value of x_{su_j}. From Eq. (2.8) we know that the sites with large, but less than one, mass-scaled eigenvector components has a major impact on the energy of the mode. It is even better to demand that the sum is less equal zero, i.e.

$$\sum_{l \neq j}^{n} \frac{x_{su_j}}{\sqrt{m_l}} B(l,j) = \sum_{l \neq j}^{n} \frac{x_{su_j}}{V_i \sqrt{m_l}} P_{jl} \leq 0 \tag{4.22}$$

where P_{jl} is the power going from bus j to bus l. This is a consequence of that it is always possible to choose $x_{su_j} > 0$ and $x_{su_j} < 1$.

Equation (4.22) will give a positive contribution to $x_{su}^T \tilde{D}\, x_{su}$ and the dissipative energy will increase. The expression (4.22) can be used as a search criterion for selected modes in order to find even better sites than the derivatives point out according to the expression (4.19). For sites where Eq. (4.22) is equal to zero, the derivatives of the trace are approximately the same as for the eigenvalues.

SVC-equipment: The positive damping conditions gives

$$\frac{\partial \operatorname{tr}(A)}{\partial K_{\mathrm{SVC}_i}} = \frac{B(l,i)}{m_{ll}} - \frac{B(k,i)}{m_{kk}} < 0$$

EXAMPLE 4.1
If $i \neq l$ and $i \neq k$, i.e. the measurements are outside the siting of the SVC,

$$B(l,i) = -\sin(\theta_l - \theta_i) \frac{V_l}{X_{il}}$$

The relation above becomes

$$-\frac{\sin(\theta_l - \theta_i) V_l}{m_{ll} X_{il}} < -\frac{\sin(\theta_k - \theta_i) V_k}{m_{kk} X_{ik}} \Leftrightarrow \frac{P_{il}}{m_{ll}} < \frac{P_{ik}}{m_{kk}}$$

The control law is $\Delta V_i = K_{\mathrm{SVC}_i}(\Delta\dot{\theta}_l - \Delta\dot{\theta}_k)$. This relation is not dependent on the voltage dependence of the load. □

EXAMPLE 4.2

Assume now the measurement at bus l moves to bus i, i.e.

$$\left.\begin{aligned} &\frac{B(i,i)}{m_{ii}} < \frac{B(k,i)}{m_{kk}} \\ &B(k,i) = -\sin(\theta_k - \theta_i)\frac{V_k}{X_{ik}} \\ &B(i,i) = \sum_{j\neq i}\sin(\theta_j - \theta_i)\frac{V_j}{X_{ij}} - \frac{\partial P_{L_i}}{\partial V_i} \end{aligned}\right\} \Rightarrow$$

$$\frac{1}{m_{ii}}\left(\sum_{j\neq i}\sin(\theta_j - \theta_i)\frac{V_j}{X_{ij}} - \frac{\partial P_{L_i}}{\partial V_i}\right) < -\frac{\sin(\theta_k - \theta_i)V_k}{m_{kk}X_{ik}}$$

$$\Rightarrow \quad \frac{1}{m_{ii}}\sum_{j\neq i}P_{ij} + \frac{V_i}{m_{ii}}\cdot\frac{\partial P_{L_i}}{\partial V_i} > -\frac{P_{ik}}{m_{kk}}$$

Assume

$$P_{L_i} = CV_i^{\alpha} \Rightarrow V_i\frac{\partial P_{L_i}}{\partial V_i} = \alpha P_{L_i}$$

This gives

$$\sum_{j\neq i}P_{ij} + \alpha P_{L_i} > P_{ki}\frac{m_{ii}}{m_{kk}} \Rightarrow \sum_{j\neq i}P_{ij} > -\alpha P_{L_i} + P_{ki}\frac{m_{ii}}{m_{kk}}$$

$$\Rightarrow \sum_{\substack{j\neq i\\ j\neq k}}P_{ij} > -\alpha P_{L_i} + P_{ki}\left(1 + \frac{m_{ii}}{m_{kk}}\right)$$

□

In this case it is not easy to formulate a rule of thumb, but some statements can be made:

1. If only one line is connected to the SVC-site, i.e.,

$$\sum_{\substack{j\neq i\\ j\neq k}}P_{ij} = 0 \Rightarrow \alpha P_{L_i} > P_{ki}\left(1 + \frac{m_{ii}}{m_{kk}}\right)$$

Assume $\alpha = 0 \Rightarrow P_{ki} < 0 \Leftrightarrow P_{ik} > 0$. This means that the SVC-site should be in the sending end of power.

2. If $P_{ki} < 0 \Leftrightarrow P_{ik} > 0$. This means that the area can have a net import of power and still have an impact on positive damping regardless of α.
3. If $P_{ki} > 0 \Leftrightarrow P_{ik} < 0$, then the area can either need to have surplus of power or import power depending on the relation between $-\alpha P_{L_i}$ and $P_{ki}\frac{m_{ii}}{m_{kk}}$ for positive damping.

HVDC-equipment: For the r:th link the positive damping condition gives

$$\frac{\partial \operatorname{tr}(A)}{\partial K_{\mathrm{DC}_r}} = -\left(m_{il}^{-1} + m_{ik}^{-1}\right) < 0 \Leftrightarrow m_{il}^{-1} + m_{jk}^{-1} > 0$$

i.e., the best impact on the damping is obtained when the measurements are taken at the stations. In that case the contribution to the damping is $m_{ii}^{-1} + m_{jj}^{-1}$. Then rectifier is at bus i and the inverter at bus j. This might be somewhat surprising, but the link introduces damping between two machines or groups of machines, mainly. The measurement of the frequency of the oscillation must therefore be related to at least one of the machines.

4.8 Siting Procedure

The calculations are performed according to Section 4.6. For each type of equipment a certain frequency window is chosen. For the PSSs and SVCs the voltage dependence of the loads are varied. The loads are varied from constant P (active power) and Q (reactive power) to a load with 50% constant current and 50% constant impedance load. The different load characteristics are called CLC and BLC, respectively. This type of load can be approximated by a load described by $P_L = P_0 \cdot V^{\alpha}$, where $\alpha = 0$ represents the CLC-case and $\alpha = 1.5$ represents the BLC-case.

For the PSSs and SVCs equipment a basic assumption must be fulfilled: The derivatives are calculated only for the two load characteristics BLC and CLC, which demands that the sensitivity derivatives with respect to K_i^{SVC} and K_j^{PSS} are monotonic functions of α, where $P_{L_i} = \sim V_i^{\alpha}$, $0 \leq \alpha \leq 2$. P_{L_i} is the voltage dependent load at bus i.

If $\partial_{V_i} P_{L_i}$ is a monotonic function of α, then the sensitivity derivatives, (4.11) and (4.12), are monotonic functions of α, because the B-matrix contains $\partial_{V_i} P_{L_i}$ as an item of the diagonal elements.

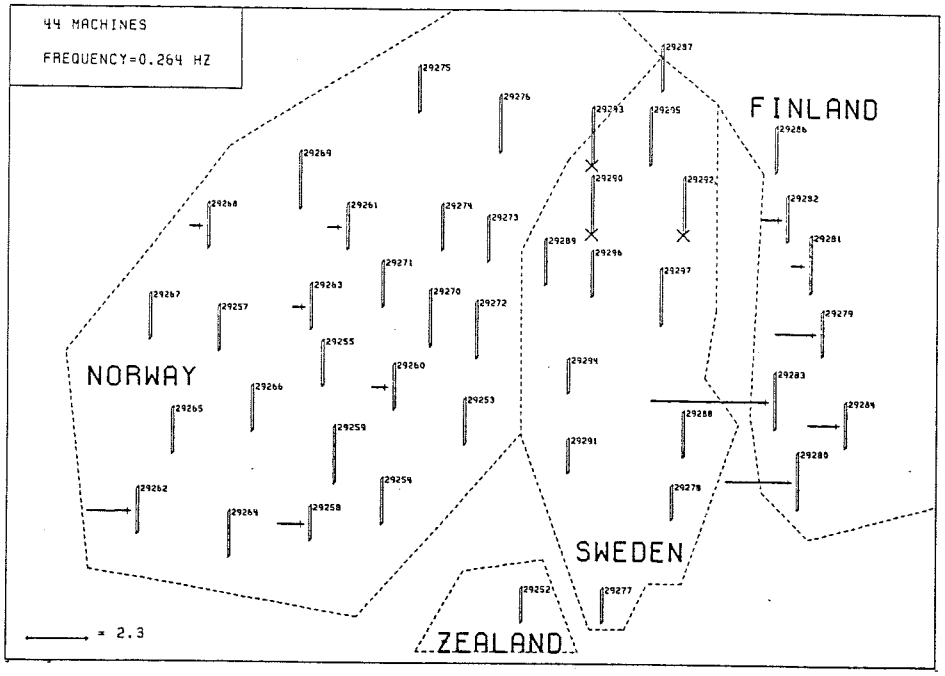

Figure 4.1 Sensitivity derivatives evaluated for $K_{se} = 0$ for the BLC-case. Mode #1, Case 2.

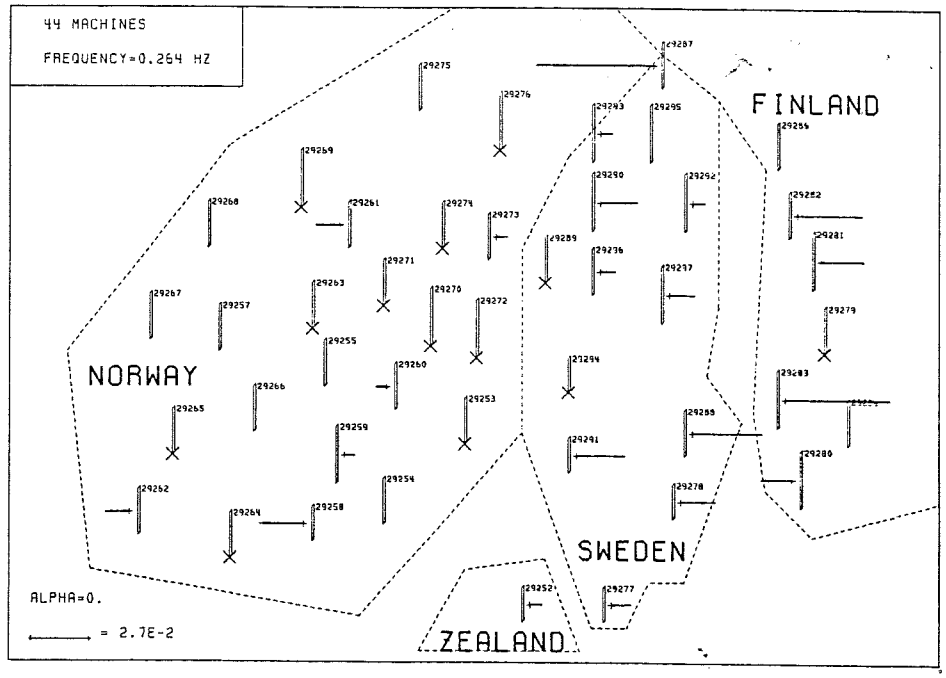

Figure 4.2 Sensitivity derivatives evaluated for $K_{se} = 0$ for the CLC-case. Mode #1, Case 2.

Statement: $\partial_{V_i} P_{L_i}$ is a monotonic function of α if $(1 + \alpha \ln |V_i|) > 0 \ \forall \ \alpha$; $0 \leq \alpha \leq 2$.

$$
\begin{aligned}
P_{L_i} &= P_{0_i} |V_i|^{\alpha} \ ; \quad P_{L_i} \geq 0 \\
\frac{\partial P_{L_i}}{\partial V_i} &= \frac{\alpha}{|V_i|} P_{L_i} \\
\frac{\partial^2 P_{L_i}}{\partial \alpha \partial V_i} &= P_{0_i} |V_i|^{\alpha - 1} + \alpha P_{0_i} \frac{\partial |V_i|^{\alpha - 1}}{\partial \alpha} \\
&= P_{0_i} |V_i|^{\alpha - 1} + \alpha P_{0_i} |V_i|^{\alpha - 1} \ln |V_i| \\
&= \frac{P_{L_i}}{|V_i|} (1 + \alpha \ln |V_i|)
\end{aligned}
$$

This implies that $(1 + \alpha \ln |V_i|)$ must fulfill the condition $(1 + \alpha \ln |V_i|) > 0 \ \forall \ \alpha$; $0 \leq \alpha \leq 2$. □

For $\alpha = 2 \Rightarrow |V_i| \leq 0.61$ p.u. for change of sign. This value of $|V_i|$ is unrealistic, because $|V_i| = (1.0 \pm 0.05)$ p.u. for acceptable load flows and other limitations. For reasonable load flows we can thus assume that the sensitivity derivative also is a monotonic function of α. Therefore it is enough to calculate the derivatives at the two extreme values of α.

A site is considered to be robust if the real parts of the sensitivity derivatives are less than zero for this two-load characteristics.

The HVDC links are not sited according to the values of the derivatives. An HVDC link can hardly be installed for damping only. The best points of measurement are of interest to find for a given site of the rectifier and the inverter. It might also be of interest to look at what happens when a measurement is lost for different configurations of measurement.

Robust Siting Procedure for PSSs

The procedure checks all machine sites in the whole power system in order to find robust and acceptable sites for PSSs. A site is considered to robust and acceptable, if the sensitivity derivatives are less than zero for the two load cases BLC and CLC.

The procedure:

1. The slow and system wide modes of interest are selected using the procedure in Section 2.6.
2. The derivatives are calculated for the BLC- and CLC-case for all possible sites according to Eq. (4.11). This is repeated for all selected modes.
3. A site is determined to be an acceptable PSS-site if $\partial_{K_{s_e}} \lambda_i < 0$ for all selected modes and the load cases BLC and CLC.

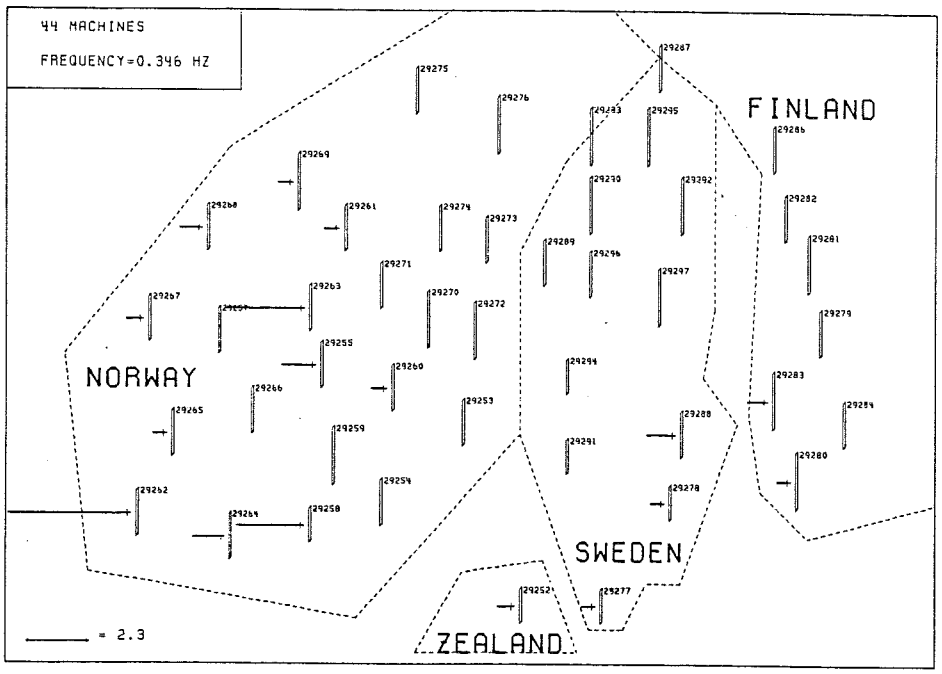

Figure 4.3 Sensitivity derivatives evaluated for $K_{se} = 0$ for the BLC-case. Mode #2, Case 2.

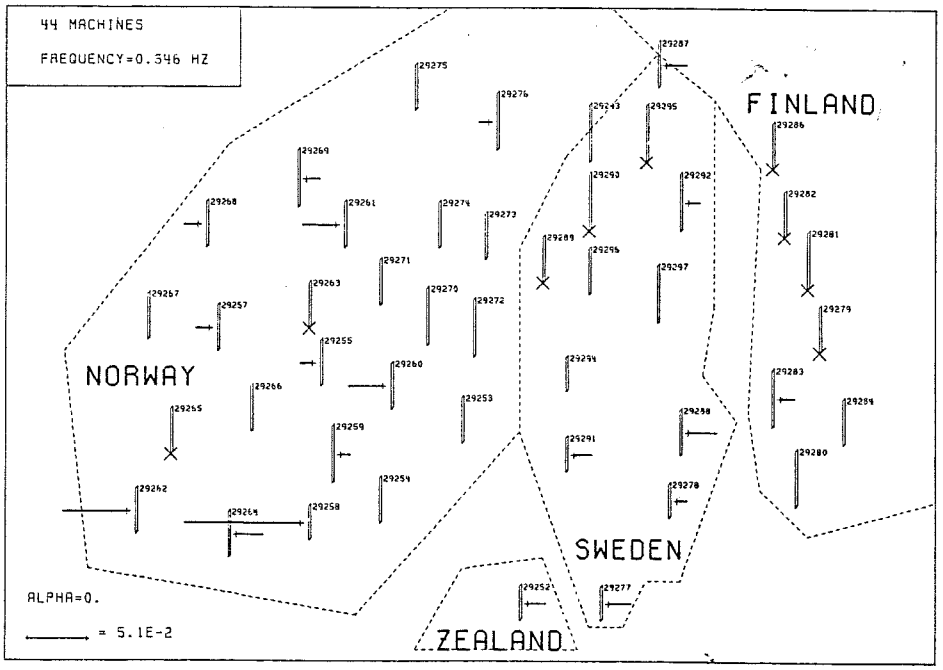

Figure 4.4 Sensitivity derivatives evaluated for $K_{se} = 0$ for the CLC-case. Mode #2, Case 2.

4. The PSS-sites which have a negligible impact (small negative values of the derivatives) on the damping of the selected modes are not equipped with any PSS.

Robust Siting Procedure for SVCs

The siting procedure is more complicated for the SVCs than for the PSSs. The freedom to choose points of measurement and the actual site of the SVC causes this complication. The proposed technique assumes it is possible to transmit measured frequency deviations freely throughout the entire system.

In Chapter 2 we show that the mass-scaled eigenvector carries information about the energy distribution of a mode, Eq. (2.18). Let us designate the largest negative and largest positive components of the mass-scaled eigenvector for I_- and I_+, respectively. To these components it corresponds a generator at a certain bus. Lets call these buses for SI_- and SI_+, respectively. These sites are important for the measurement of the frequency deviations. The amplitudes of the frequency deviations are large at these sites.

The SI-marked buses are used for siting of the SVCs. The procedure regards that the frequency deviation of these SI-marked buses can be transmitted to any other node in the system. The SI-marked buses varies from mode to mode. For instance, for five selected system wide modes, ten signals need to be transmitted at the most.

The procedure:

1. The slow and system wide modes are selected using the procedure in Section 2.6.
2. The SI-marked buses are determined.
3. For each mode and associated points of measurement, the derivatives are calculated for each site and for the two load cases BLC and CLC.
4. The information from item 3 is then used to determine all approved sites for each mode. The sites are approved if the derivatives are less than zero for the BLC and CLC cases. The approved sites per mode are then checked if they are valid for all modes. By this procedure it is possible to calculate a maximum number of modes for which the sites are valid. This number of modes is less than or equal to the selected ones.
5. The number of accepted sites are presented and the number of modes. If the number of accepted sites are too few, it is possible to reduce the number of modes, and recalculate the number of accepted sites.
6. When the number of acceptable sites have been determined, it is possible to present the derivatives for the BLC case or for the CLC case for accepted sites.
7. In order to be able to simulate the selected sites for SVCs, the best point of remote measurement is determined. This procedure is adopted, because all

SVCs of today can only measure the power on lines connected to the SVC bus. The remote bus, which gives the least real part of the derivative less than zero, is chosen as best remote point of measurement. The topological distance from the SVC site is chosen to be one.

8. The Tie-line based control laws for PSS equipment (Eliasson and Hill, 1989, page 11) are treated according to the SVC concept.
9. The implemented procedure do not use item 7. The SI-marked buses and selected modes are used for the robust siting analysis for SVCs

Siting Procedure for the Best Points of Measurement for HVDC Links

The sites for the rectifier and the inverter is not determined according to any siting procedure. This technique assumes that the rectifier and inverter for a HVDC link is determined on other basis than pure damping purposes.

The best points of measurements of the frequency deviations, though, are of great interest to examine. A realistic assumption is to limit the freedom of topological distance for the points of measurements. In our case we have the limitation of topological distance of one. The conventional way of measurements are to take the information from the inverter and rectifier sites.

The procedure:

1. The sites of the rectifiers and inverters are given.
2. The slow and system wide modes of interest are selected.
3. For each possible point of measurement within the topological distance of one for the rectifier, the derivatives are calculated for all possible points of measurement on the inverter side within the topological distance of one.
4. The procedure in item 3 is repeated for all points of measurement on the rectifier side and for all chosen modes.
5. Then the best combination of points of measurement at the rectifier and the inverter are determined for all modes or the largest possible number of modes within the selected ones.
6. The items 2 to 5 are then repeated for all links.
7. It is also possible to block transfer of measurements between the rectifier and inverter, in order to simulate a transducer fault or a communication fault.

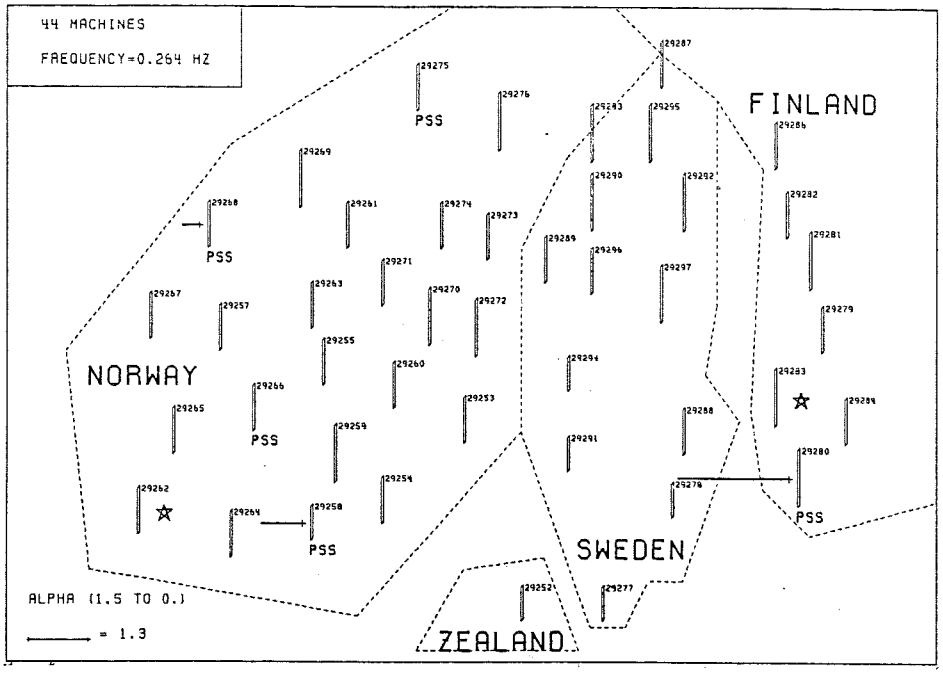

Figure 4.5 Robust PSSs sites for five system wide modes and α varied from 1.5 to 0, Case 2.

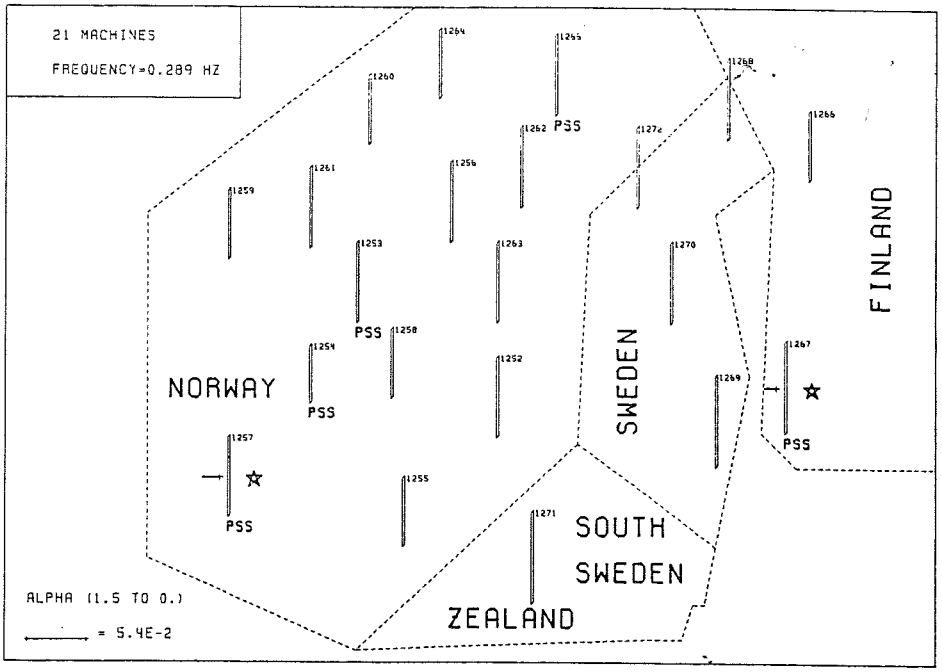

Figure 4.6 Robust PSSs sites for five system wide modes and α varied from 1.5 to 0, Case 1.

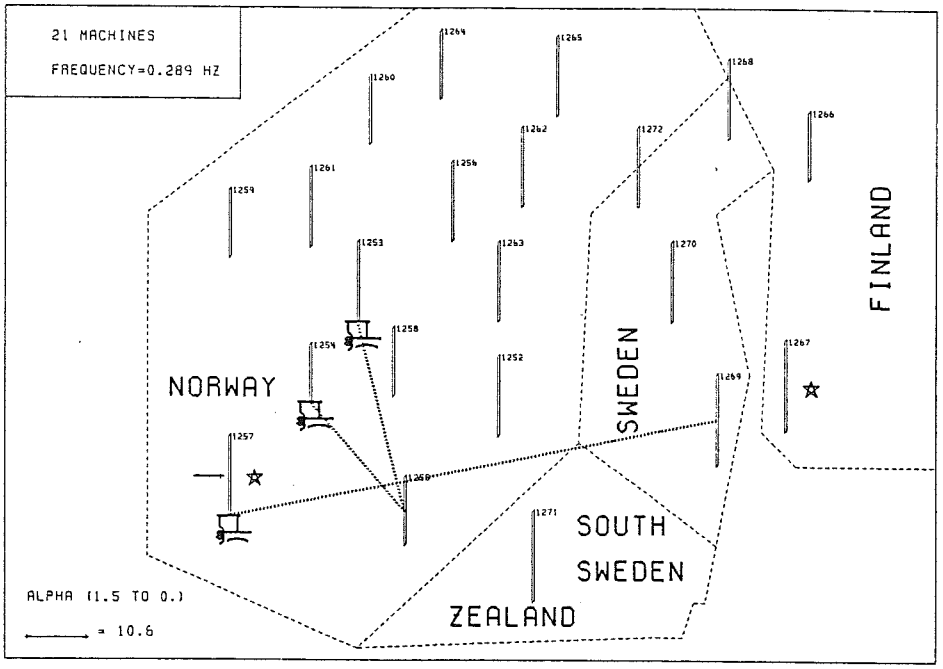

Figure 4.7 Robust SVCs sites for three system wide modes and α varied from 1.5 to 0, Case 1.

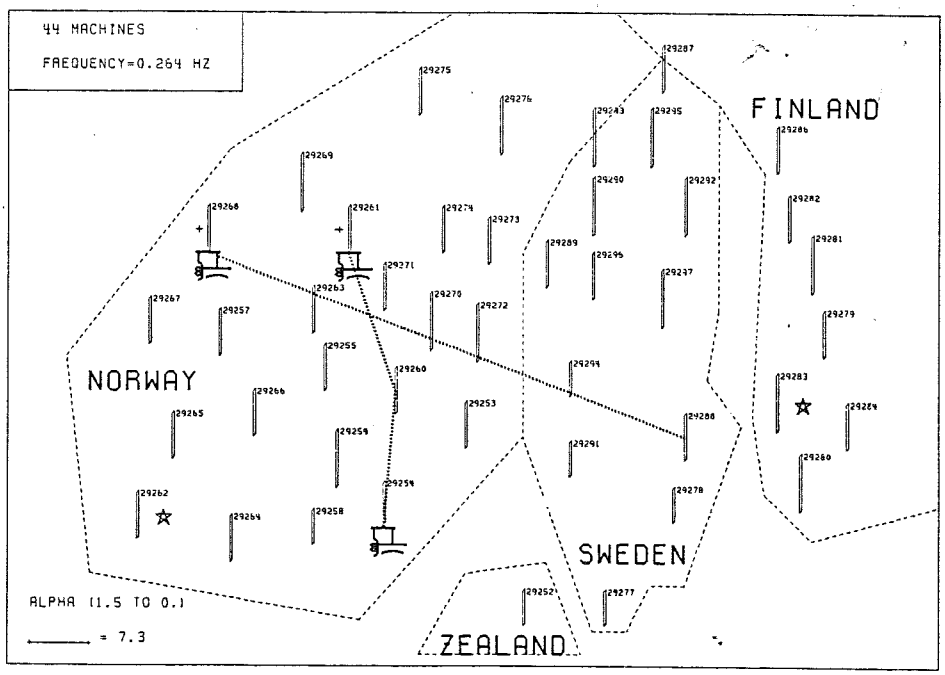

Figure 4.8 Siting analysis evaluated for K_{SVC} with variation of α from 1.5 to 0. Mode #1, Case 2.

4.9 Application to the Nordel Power System

In this section results from the previous described siting procedures are shown, mostly in a graphical form. All cases and numbers of the modes are according to Table 3.2. The results are organized in the following sequence:

- Presentation of sensitivity derivatives with respect to the parameters K_{se} and variation of load characteristics for Case 2 (44 machines) and Case 1 (21 machines).
- Presentation of acceptable sites of SVC equipment with given best two points of measurement for each chosen system wide mode (Case 2 and Case 1).
- Presentation of best points of measurement with respect to overall positive damping for given site of HVDC links for Case 3 (224 machines).
- Analysis of PSS installed at non acceptable site for Case 2.
- Damping properties of the Fenno-Skan link with alternative measurement for Case 3.

Robust PSSs Sites

Figures 4.1 to 4.5 show the result from the sensitivity (siting) analysis with respect to the K_{se}-parameter. Figure 4.5 summarizes the robust sites for five system wide modes according to Table 3.2, Case 2. Five robust sites are found for Case 2. A site is considered to be robust if the sensitivity derivatives is less than zero for the two load cases, BLC and CLC. Figure 4.6 shows the robust sites for five system wide modes for Case 1. Five robust sites are found for Case 1. The star-marked buses correspond to SI_- and SI_+ buses defined in the siting procedure of the SVCs.

The derivatives are marked near the buses (generators), Fig. 4.1. The cross at middle of the bus is the origin of the associated complex plane. If the real part of the derivatives are not greater than zero, the derivatives are shown on the left side of the bus, otherwise on the right side, Fig. 4.2. Too small derivatives are not shown, but if the real part of derivatives is greater than zero, the bus is marked with a cross at the bottom end of the bus. This indicates that the concerned eigenvalues may be moved in wrong direction, if an PSS is installed at this bus (generator). The figures 4.3 and 4.4 show the second chosen system wide mode for Case 2. The result is that the load characteristic is very important for siting of PPSs. When the derivatives with respect to K_{se} change sign according to BLC and CLC, it indicates that the value of the diagonal element of $\partial_V(\overline{P}_0)$-matrix change sign when the $\partial_V(\overline{P}_L)$-matrix is added (Eq. 2.8). Similar results can be shown for Case 1 and Case 3 (Eliasson (1989a)).

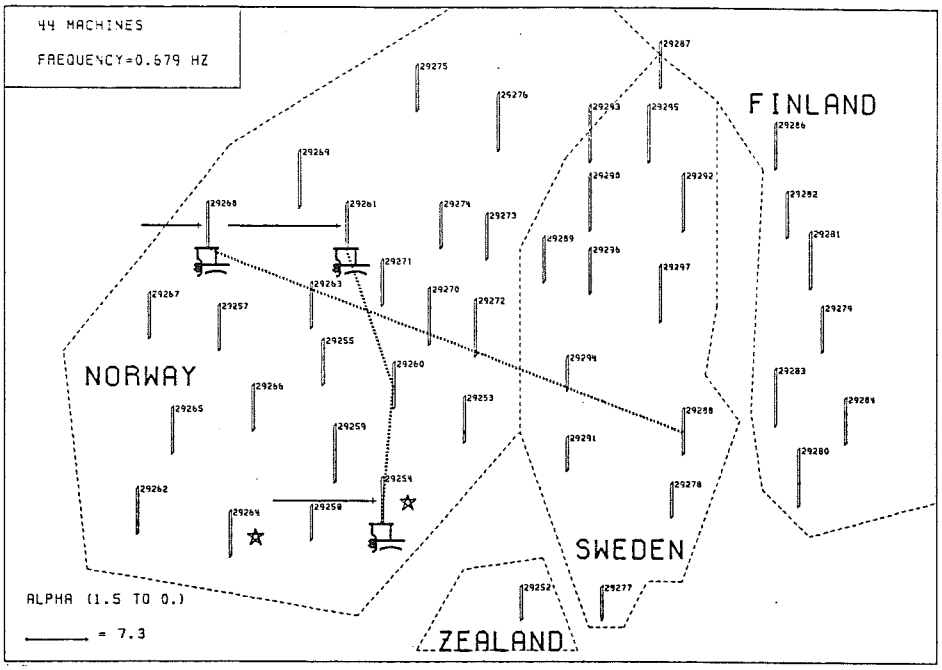

Figure 4.9 Siting analysis evaluated for K_{SVC} with variation of α from 1.5 to 0. Mode #8, Case 2.

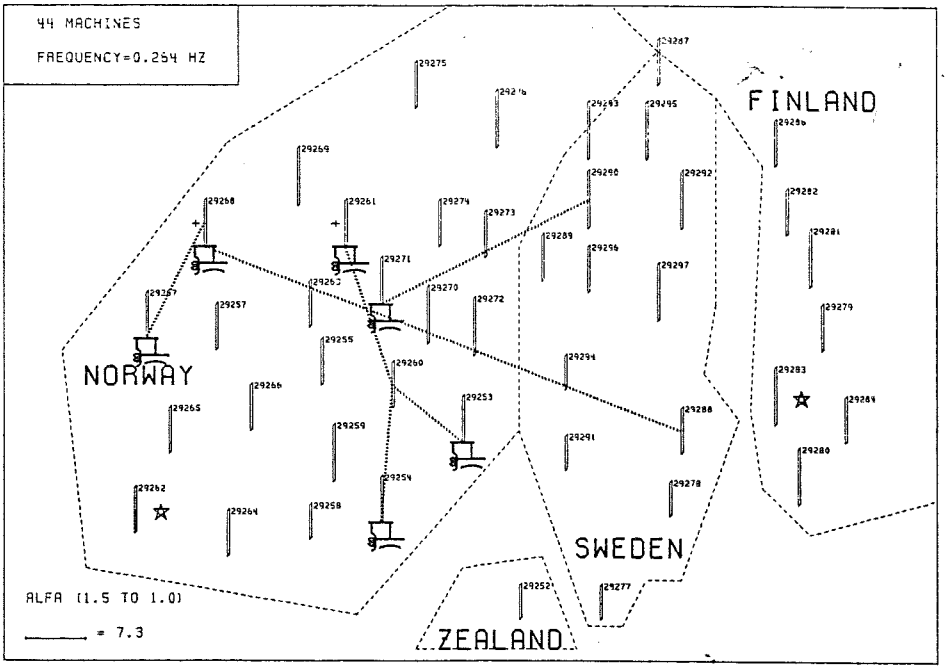

Figure 4.10 Siting analysis evaluated for K_{SVC} with variation of α from 1.5 to 1.0. Mode #1, Case 2.

Robust SVCs Sites

Figure 4.7 shows approved sites for SVCs in Case 1 when α is varied from 1.5 to 0. The dotted line between an accepted SVC site and a remote bus is the line used for real time simulation, according to item 7 of the robust siting procedure in the previous section. The star-marked buses correspond to the SI-marked buses. Three sites are approved.

The figures 4.8 to 4.11 show the results from the sensitivity (siting) analysis with respect to the K_{SVC}-parameter (Case 2). Figures 4.8 and 4.9 show the sensitivity derivatives with respect to K_{SVC}. The voltage dependence of the load is varied from 1.5 to 0. Figure 4.8 represents mode #1 and Fig. 4.9 represents mode #8. Figures 4.10 and 4.11 show what happens when the voltage dependence of the load is varied from 1.5 to 1.0. The demand of robustness is decreased. That is why number of possible sites increase.

For Case 1 only 3 modes out of chosen 5 modes fulfilled the criterion of acceptable sites.

For Case 2 five modes fulfill the criterion, but only one site is acceptable for this choice of depth of modes. In the program it is possible to choose the depth of modes and with a choice of 4 modes, three sites are acceptable for α varied from 1.5 to 0. Six sites are acceptable for α varied from 1.5 to 1.0.

For Case 3 the depth of modes is 5, i.e. equal to the demanded number of system wide modes. The number of acceptable SVC sites are 18. All derivatives are less than zero according to the described procedure.

This technique to use the sensitivity derivatives for siting of SVC equipment is believed to be new.

Analysis of the PSS Control Law at Non-acceptable Site

A PSS is installed at bus #29283 (western Finland) according to the load condition presented in Fig. 4.2. The site is not acceptable from the robust siting analysis. The K_{se} was chosen to 0.1 p.u./(rad/s). A PSS at this site with constant active and reactive power load will destabilize the system according to Table 4.1. Five slow and system wide modes will have positive real parts of the eigenvalues.

Best Points of Measurement from Damping Point of View at the Rectifier and Inverter End Based on Sensitivity Analysis

The result is shown in Fig. 4.12. Only one configuration of an HVDC link is considered. The link between Forsmark and Olkiluoto, the new Fenno-Skan link.

It is clearly shown in Table 4.2 that if the measurement ($\Delta\omega$) at the rectifier side is taken at bus 17074 and at Forsmark for the inverter side, the derivatives are more negative than for the conventional measurement. The improvement is not significant but still an improvement.

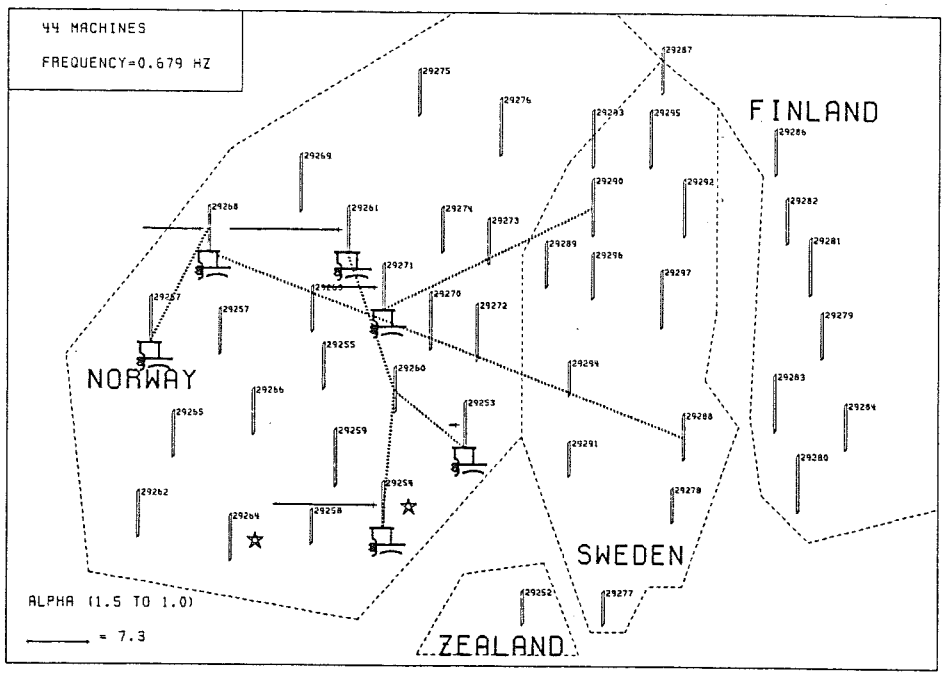

Figure 4.11 Siting analysis evaluated for K_{SVC} with variation of α from 1.5 to 1.0. Mode #8, Case 2.

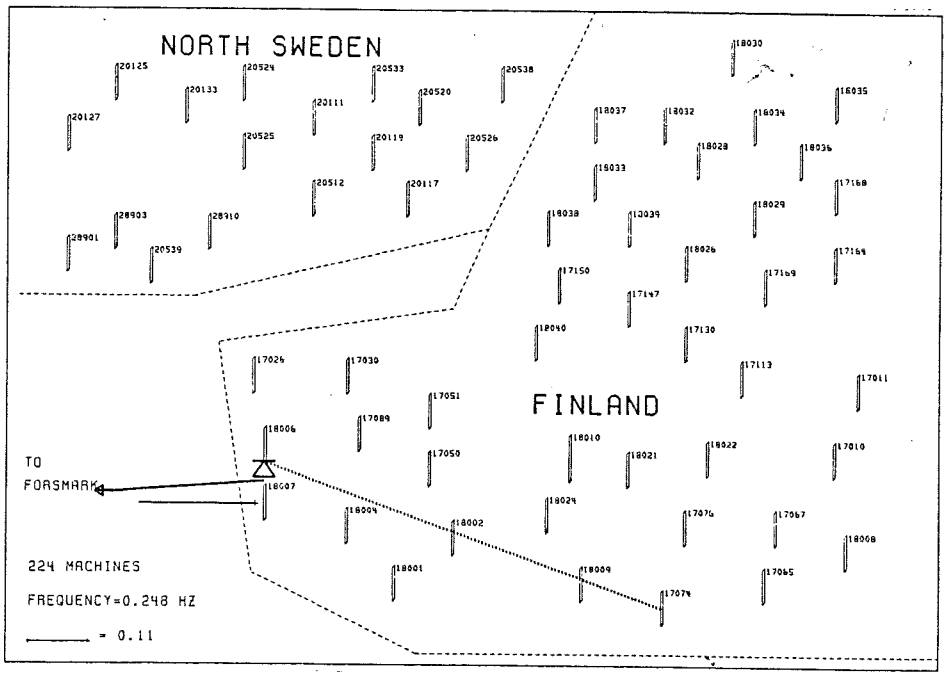

Figure 4.12 Alternative points of measurement for the Fenno-Skan link by use of sensitivity derivatives, Case 3.

Table 4.1 Eigenvalues when a PSS is installed at a non-acceptable site, Case 2.

Mode #	Eigenvalue
1	$4.9 \cdot 10^{-3} \pm j\ 0.264$
2	$1.2 \cdot 10^{-3} \pm j\ 0.346$
8	$5.7 \cdot 10^{-4} \pm j\ 0.654$
9	$2.9 \cdot 10^{-5} \pm j\ 0.679$
15	$5.3 \cdot 10^{-5} \pm j\ 0.901$

The Fenno-Skan Link with Loss of Measurement at the Rectifier Site or the Inverter Site

What happens when the measurement at Forsmark is lossed, due to malfunctioning transducer? The result is shown in Table 4.3.

If the conventional way of measurement is used, it will destabilize the system because the last mode (#15) becomes unstable. This means that the link has to be blocked when the measurement not is available at Forsmark or cut out a certain low frequency window. By using the alternative scheme, the link is stable for all chosen system wide modes.

Both cases are stable when the measurement is lossed at the Olkiluoto side. The alternative measurement has at the most a topological distance of one from the converter stations.

The Fenno-Skan Link with $K_{\mathrm{DC}} > 0$

The eigenvalues for $K_{Skan}^{Fenno} = 0.45$ p.u./(rad/s), base $\hat{=}$ 100 MW, are shown below. The sequential number according to Table 3.2.

$$\begin{aligned}
\lambda_1 &= (-0.097, \pm j\ 0.248) \\
\lambda_2 &= (-0.023, \pm j\ 0.337) \\
\lambda_8 &= (-0.014, \pm j\ 0.604) \\
\lambda_9 &= (-0.000039, \pm j\ 0.645) \\
\lambda_{15} &= (-0.011, \pm j\ 0.855)
\end{aligned}$$

The eigenvalues are moved nearly straight into the left half plane.

With this configuration the Fenno-Skan link has a good damping capability, at least for the two slowest modes, for the whole chosen frequency range of the Nordel power system.

Table 4.2 Sensitivity derivatives with respect to K_{DC} of the Fenno-Skan link.

Mode #	Conventional measurement	New alternative measurement
	Derivatives (K_{DC})	Derivatives (K_{DC})
1	$-1.6 \cdot 10^{-2}$	$-1.7 \cdot 10^{-2}$
2	$-1.1 \cdot 10^{-2}$	$-1.2 \cdot 10^{-2}$
8	$-7.1 \cdot 10^{-3}$	$-9.3 \cdot 10^{-3}$
9	$-3.1 \cdot 10^{-5}$	$-3.3 \cdot 10^{-5}$
15	$-8.3 \cdot 10^{-3}$	$-2.8 \cdot 10^{-2}$

Table 4.3 Sensitivity derivatives for loss of measurement at Forsmark.

Mode #	Conventional measurement	New alternative measurement
	Derivatives (K_{DC})	Derivatives (K_{DC})
1	$-1.4 \cdot 10^{-2}$	$-1.6 \cdot 10^{-2}$
2	$-5.3 \cdot 10^{-3}$	$-6.2 \cdot 10^{-3}$
8	$-1.8 \cdot 10^{-3}$	$-3.9 \cdot 10^{-3}$
9	$-7.5 \cdot 10^{-7}$	$-2.4 \cdot 10^{-6}$
15	$+1.4 \cdot 10^{-2}$	$-5.8 \cdot 10^{-3}$

4.10 Conclusions

The sensitivity study gives an indication where to place PSS and SVC equipment in order to damp slow and system wide modes when different load characteristics are considered. An acceptable PSS site is a site where the derivatives are negative real and do not change sign when the voltage dependence of load is varied.

The robust siting technique concerning the SVC equipment is new and gives stabilizing sites. The siting condition for positive damping gives nice analytical results concerning the chosen damping equipment, especially for the PSS equipment, Eqs. (4.15) and (4.16).

For HVDC links this technique can be used for searching of best points of measurement of frequency deviation for the rectifier and the inverter.

This technique, i.e. sensitivity derivatives with respect to slow and system wide modes and different load characteristics, can be applied to very large power systems. In this thesis it is applied to a power system of 224 machines. When the eigenvectors for the uncontrolled system are used, i.e. the control parameters are zero, the left eigenvectors are known when the right eigenvectors are known. For this special case a very fast analysis of robust sites can be performed.

5

Coordinated Tuning of Control Parameters

5.1 Introduction

Chapter 4 gives the basis for the coordinated tuning and the verification study (Chapter 6). The considered damping equipments are PSSs, SVCs and HVDC links. In this chapter special emphasis is given to handle large power systems from an optimization point of view. Techniques in the literature do not cover tuning of damping equipment in large power systems for slow and system wide modes.

The ultimate aim of this chapter is to show how the coordinated tuning can be performed in large power systems. The verification part also includes suggestion of a new PSS design for slow and system wide modes in large power systems.

The coordinated tuning put special emphasis on
- Formulation of the optimization problem.
- Importance of load modeling.
- Graphical presentation of results.

Previous techniques do not cover different types of damping equipment, influence of load modeling and proper siting in large power systems. The coordinated and optimized tuning of parameters have, in many cases, constraints on the real part of the eigenvalues, which can hardly lead to a successful optimization in large power systems. See, e.g., Vournes and Papadias (1987), Lefebvre (1983), Sivakumar *et al.* (1984) and Dahlquist (1987).

Generally it can be stated that models used for generators, AVRs etc. contains too many states for modeling of slow power oscillation. This will naturally limit the size of the system from an optimization point of view. Important aspects, such as characteristics of load, different load cases and change of topology, are not discussed in the papers mentioned above.

A SISO (Single Input Single Output) concept for tuning stabilizers aimed for slow and system wide modes can hardly lead to a successful design, which is the weak part in the papers Larsen and Swann (1981), and deMello *et al.* (1980). The design has to use a MIMO (Multi Input Multi Output) concept (Kailath, 1980; Brockett, 1970; Friedland, 1986). The author think that the most critical part is to formulate a suitable optimization criterion for a MIMO-system of the size of a power system. In this chapter a special constraint will be formulated with respect to large systems. The formulated optimization problem with the constraints fulfills the damping demands of slow and system wide modes.

5.2 The System Equation

We neglect the damping from damper windings of the generators, which is a conservative assumption. Equation (4.7) gives the system equations:

$$\begin{cases} M \cdot \Delta\ddot{\bar{\theta}} + \tilde{D} \cdot \Delta\dot{\bar{\theta}} + K \cdot \Delta\bar{\theta} = \bar{0} \\ \Delta\dot{\bar{\theta}} = \Delta\bar{\omega} \end{cases}$$

where

$$\tilde{D} = T_s^{\mathrm{DC}} K_{\mathrm{DC}} (T_m^{\mathrm{DC}})^T - BK_{se} - BT_s^{\mathrm{SVC}} K_{\mathrm{SVC}} (T_m^{\mathrm{SVC}})^T \triangleq D_{\mathrm{DC}} + D_{\mathrm{PSS}} + D_{\mathrm{SVC}}$$
$$K = \partial_\theta(\overline{P}_0)$$

The system equations in matrix form are

$$\frac{d}{dt}\begin{pmatrix} \Delta\bar{\theta} \\ \Delta\dot{\bar{\theta}} \end{pmatrix} = \begin{pmatrix} 0 & I \\ -M^{-1}K & -M^{-1}\tilde{D} \end{pmatrix} \begin{pmatrix} \Delta\bar{\theta} \\ \Delta\dot{\bar{\theta}} \end{pmatrix} \tag{5.1}$$

5.3 General Demands on the Optimization Procedure

All damping equipments (PSSs, SVCs and HVDC links) are operating with limitations based on different reasons. The generators are specified according to IEC 34, which means that the terminal voltage of the generator is not allowed

to vary more than ±5% during normal operation. The generators equipped with a PSS must operate under the same conditions.

The SVCs with thyristor control are allowed to change the bus voltage, at the most ±5%. The HVDC links can operate in different modes. We exclude all emergency modes (SDSA analysis) and consider only small modulations of the active power. The short circuit condition at the terminals is such that no modeling of reactive power flow is necessary. The limitation of small power modulations are normally set to about 8% of rated power of the link. The control actions for damping purposes are then within the current margin, i.e. no delays are needed to be modeled for slow EMOs.

These limitations of the operative actions must naturally be included in the optimization procedure. Furthermore, the parameters (K_{se}, K_{SVC}, K_{DC}) are not allowed to be negative, i.e. only positive values of the parameters are allowed regardless of the load characteristics and the load flow conditions.

Different load characteristics may affect the values of the parameters. Especially the voltage dependence of the load affects the values of K_{se}:s and K_{SVC}:s. This is also pointed out in the thesis. In the thesis we determine the parameters during high load conditions. For other load cases the parameters may change.

The imaginary parts of the poles of the uncontrolled system should not be decreased, if possible, in the low frequency range. If a reduction of the slow modes is inevitable in order to fulfill the damping demands, the reduction should not be more than 10%. This demand is based on the fact that the inherent damping capacity of the generators decrease when the frequency decreases.

The damping ratio of slow EMOs must not be less than 0.1, i.e. the amplitude of an oscillation of 0.1 Hz is reduced by 50% within 10 seconds.

From the specification above we can now estimate reasonable limits of the parameters.

Estimation of Limits of the Parameters

PSS equipment: The maximum frequency deviation for small disturbance stability analysis is not greater than 0.1 Hz. The control law of a PSS is (see Eq. (4.2)):

$$\Delta V_i = K_{se_i} \Delta f \cdot 2\pi$$

This gives the limit

$$K_{se_i}^{\lim} = \frac{\Delta V_i}{\Delta f \cdot 2\pi} = \frac{0.1}{0.1 \cdot 2\pi} = 0.16 \text{ p.u./(rad/s)}$$

SVC equipment: The control law of a SVC is $\Delta V_i = K_{\mathrm{SVC}_i}(\Delta\dot{\theta}_l - \Delta\dot{\theta}_k)$ (see Eq. (4.3)). This gives the limit

$$K^{\lim}_{\mathrm{SVC}_i} = \frac{\Delta V_i}{2 \cdot \Delta f \cdot 2\pi} = 0.08 \text{ p.u./(rad/s)}$$

HVDC equipment: A current margin of 10% means that 10% of rated power (P_r) of the link can be used for damping purposes. The rated power of the link is given in per unit value of the system base.

From the control law Eq. 4.5 we get

$$K^{\lim}_{\mathrm{DC}_i} = \frac{0.1 \cdot P_r}{2 \cdot 0.1 \cdot 2\pi} = 0.08 \cdot P_r \quad \text{p.u./(rad/s)}$$

5.4 Qualitative Aspects of the Proposed Optimization Procedure

As mentioned earlier, optimization based on linear quadratic theory or pole placement technique is not feasible for large power systems due to the computation time needed. Also methods, which put constraints on the eigenvalues, can hardly lead to a successful design, because the Jacobian matrix must in general be numerically updated. To put too hard constraints on the maximum step length, destroys the performance of efficient optimization techniques.

To find analytical expressions for the eigenvalues as a function of control parameters will limit the number of machines to less than 10, even if a program for symbolic manipulation, e.g., Macsyma is used.

The intention of this section is to qualitatively explain the final formulation in Section 5.6. The intention is to apply an existing fast method to the problem for a large power system. Motivated by Eq.(4.21) we are going to use the trace during the optimization. The aim is obvious, the calculation of the trace is fast in comparison with the calculation of the eigenvalues. In this thesis we will minimize the trace of the system matrix subject to a special choice of constraint function instead of putting constraints on the eigenvalues. We come back to the choice of the constraint function.

We are now going to see what happens, if we try to minimize the trace of the system matrix, A. According to equation (5.1), the A-matrix is real. The spectrum of the matrix, A, will therefore consist of complex conjugated and/or real eigenvalues.

The sum of the eigenvalues will be a real number. This number is equal to the trace of A, designated tr A. These words can be formulated as

$$\mathrm{tr}\, A(\Theta) = \sum_{i=1}^{2n} \lambda_i(\Theta) = 2 \sum_{i=1}^{n} \mathrm{Real}\ \left(\lambda_i(\Theta)\right) \in R \quad \forall\ \Theta \in R$$

Table 5.1 The poles of the uncontrolled and controlled system ($\alpha = 1.5$, Case 1 (21 machines)).

	Mode #1	Mode #2
Uncontrolled	$\pm j \cdot 1.82$	$\pm j \cdot 2.33$
Controlled	$-0.97 \pm j \cdot 1.30$	$-1.97 \pm j \cdot 0.97$
$\Delta\omega$ (%)	-29	-58

where

$$\Theta = \left(\Theta_1^{K_{se}}, \ldots, \Theta_{m_1}^{K_{se}},\ \Theta_1^{\text{SVC}}, \ldots, \Theta_{m_2}^{\text{SVC}},\ \Theta_1^{\text{DC}}, \ldots, \Theta_{m_3}^{\text{DC}}\right)$$

$$m_1 + m_2 + m_3 = m \text{ (number of parameters)}$$

$$n = \text{number of generators}$$

For the uncontrolled system, i.e. $\Theta = 0 \Rightarrow \text{tr } A(0) = 0$.

The siting analysis (Chapter 4) points out the most powerful sites for the equipment with respect to load characteristics and selected system modes. These sites are hopefully such that no mode moves into the right half plane when tuning is performed. A qualitatively discussion in Section 4.7 has motivated this statement. The eigenvalues of the closed loop system are calculated when the tuning is finished. The result of the tuning is accepted only if the poles are in the left half plane.

The siting procedure points out robust sites where the $\overline{\nabla}_\Theta\left(\text{tr } A(\Theta)\right)$ has only negative components and especially the sites, which decrease the real part of λ_i for system wide modes. Therefore, formulation of the problem as:

$$\underset{\Theta \in R^m}{\text{Minimize}}\ \text{tr } A(\Theta)$$

$$\text{Subject to } 0 < \Theta_i \leq u_i;\ \ i = 1, \ldots, m$$

will lead to a solution of $\Theta_i = u_i\ \forall i$. The solution is motivated in the following example.

EXAMPLE 5.1

In this qualitative discussion we only consider PSSs sited according to Fig. 4.6, Case 1. The control law for each PSS is given in Eq. (4.2).

What has happened to the poles of the closed loop system? We are only interested in the slowest modes in this discussion. The two slowest modes for the closed loop system and the uncontrolled system are shown in Table 5.1 (see also Table 3.2, Case 1). The eigenvalues of the controlled system show that no unstable mode occurs. Some of the eigenvalues, though, are still on the imaginary axes.

The trajectory of the slowest eigenvalue shows that the eigenvalue in the beginning has a direction into the left half plane. When the values of the parameters increase, the trajectory of the slowest eigenvalue has an opposite direction. The values of the parameters are about in the middle of range when the direction changes. For these small values of the limits of the parameters, though, the eigenvalues are not moved into any unstable condition. Other eigenvalues with larger imaginary values seem to move with a direction into the left half plane.

The trace decreases for increasing values of the parameters, which motivates the above solution.

As discussed in Section 5.3, the changes of the imaginary values of the poles are too large. Also the damping ratio is unrealistic for a power system. The example illustrates that it is possible to introduce considerable damping, but the swing of the control signals demands unrealistic reactive power swings of the generators. Also the inherent damping of the generators is poor for such low oscillations. □

In order not to affect the imaginary parts of the eigenvalues as much as in Table 5.1, we have to find a constraint function, so we can move the eigenvalues more straight into the left half plane. For large power systems we need numerically stable methods and constraint functions, which are fast to update.

We are now going to study the trace of A^TA, which is equal to the sum of squares of the singular values of A. Any matrix, especially A, can be written as

$$A = U \cdot \Sigma \cdot V^T \tag{5.2}$$

where U and V are unitary matrices and Σ contains the ordered singular values of A.

From Eq. (5.1) we get

$$A^T(\Theta)A(\Theta) = \begin{pmatrix} KM^{-2}K & KM^{-2}\tilde{D}(\Theta) \\ \tilde{D}^T(\Theta)M^{-2}K & I + \tilde{D}^T(\Theta)M^{-2}\tilde{D}^T(\Theta) \end{pmatrix}$$

The trace of A^TA is

$$\operatorname{tr} A^T(\Theta)A(\Theta) = \operatorname{tr} KM^{-2}K + \operatorname{tr} \tilde{D}^T(\Theta)M^{-2}\tilde{D}(\Theta) + n \tag{5.3}$$

For the feedback gains equal to zero we get

$$\operatorname{tr} A^T(0)A(0) = \operatorname{tr} KM^{-2}K + n$$

It might be of interest to present the figures of $\operatorname{tr} KM^{-2}K$ for Case 1, Case 2 and Case 3:

$$\text{Case1}: \quad \operatorname{tr} KM^{-2}K \approx 84 \cdot 10^3$$

$$\text{Case2}: \quad \operatorname{tr} KM^{-2}K \approx 31 \cdot 10^4$$

$$\text{Case3}: \quad \operatorname{tr} KM^{-2}K \approx 15 \cdot 10^9$$

It is quite easy to show that

$$\operatorname{tr} KM^{-2}K = \sum_{i=1}^{n} |\lambda_i|^4 \quad \text{if} \quad (\sqrt{M})^{-1}X_u = X_u(\sqrt{M})^{-1}$$

This is, however, not valid in our case. X_u is defined in Section 2.5 and M is the mass matrix of the system. In our case, we can only estimate the norm of $KM^{-2}K$, e.g. the 2-norm.

$$\frac{M_{\min}}{M_{\max}} |\lambda_{\max}|^4 \leq \|KM^{-2}K\|_2 \leq |\lambda_{\max}|^4 \frac{M_{\max}}{M_{\min}}$$

$M_{\min}$ is the smallest mass of the generators, $M_{\max}$ is the largest mass of the generators. From Eq. (5.3) we get with PSSs only

$$\Delta\big(\operatorname{tr} A^T(\Theta)A(\Theta)\big) = \operatorname{tr}(B\,K_{se})^T M^{-2}(B\,K_{se})$$

Only a few sites out of the total number of sites are occupied by PSSs. If we extract all PSS parameters for approved sites and store them in a vector Θ, we can reformulate the above equation as:

$$\Delta\big(\operatorname{tr} A^T(\Theta)A(\Theta)\big) = \Theta^T Q(\alpha)\Theta$$

The parameter α is the voltage dependence of the load. The matrix Q has the dimension number of PSS times number of PSSs. Since the structure of $Q(\alpha)$ is $Q(\alpha) = \operatorname{diag}\big(B_i^T(\alpha) \cdot B_i(\alpha)\big)$, the quadratic form of the Q-matrix is positive definite. The diagonal elements of the Q-matrix consist of an inner product where

$$B_i^T(\alpha) = \left(\frac{B(1,i)}{m_1}, \ldots \frac{B(i,i)(\alpha)}{m_i}, \ldots, \frac{B(n,i)}{m_n}\right); \quad i = 1, \ldots, \#\text{PSSs}$$

The system structure and the property of the load imply that $\Delta\big(\operatorname{tr} A^T(\Theta)A(\Theta)\big)$ will increase for increasing Θ:s. We also know that

$$\Delta\big(\operatorname{tr} A^T(\Theta)A(\Theta)\big) = \Delta\left(\sum_{i=1}^{2n} \sigma_i^2\right)$$

where the σ_i^2:s are the singular values of A. The changes of the σ_i^2:s are caused by the real part of the eigenvalues for small values of the Θ:s according to the siting procedure.

We are now going to use $\Delta\big(\operatorname{tr} A^T(\Theta)A(\Theta)\big)$ in the optimization procedure. We know that

$$B(i,i) = -\left(\sum_{j\neq i}^{n} B(j,i) + \frac{\partial P_{L_i}}{\partial V_i}\right) = -\left(\sum_{j\neq i}^{n} \frac{P_{ij}}{V_i} + \frac{\partial P_{L_i}}{\partial V_i}\right)$$

Table 5.2 The poles of the uncontrolled and controlled system ($\alpha = 1.5$, Case 1 (21 machines)).

	Mode #1	Mode #2
Uncontrolled	$\pm j \cdot 1.82$	$\pm j \cdot 2.33$
Controlled	$-0.77 \pm j \cdot 1.57$	$-0.41 \pm j \cdot 2.46$
$\Delta\omega$ (%)	-14	$+6$

The necessary siting condition in Section 4.7 implies that $\sum_{j\neq i}^{n} P_{ij} > 0$. We assume that $P_{L_i} = C\,V_i^{\alpha}$, where V_i is the magnitude of the voltage at mode i. For normal composite loads we know that $\frac{\partial P_{L_i}}{\partial V_i} > 0$. When we add the voltage dependence, we increase the diagonal elements of $Q(\alpha)$. The worst case for damping with PSSs occurs for $\alpha = 0$, i.e.

$$B(i,i) = -\sum_{j\neq i}^{n} \frac{P_{ij}}{V_i}$$

When $\alpha = 0$ we need to use the largest control signals, i.e. $\Theta_i^{\max} = 0.16$ according to Section 5.2. We can now calculate $\Delta\big(\mathrm{tr}\, A^T(\Theta)A(\Theta)\big)$ for all Θ_i equal to 0.16. This will give an upper limit (u) of $\Delta\big(\mathrm{tr}\, A^T(\Theta)A(\Theta)\big)$.

Now we go back to a more realistic load characteristic, i.e. $\alpha > 0$ for all loads. The upper limit, u, of $\Delta\big(\mathrm{tr}\, A^T(\Theta)A(\Theta)\big)$ is now used for all other values of $\alpha > 0$. Let us formulate the optimization problem as

$$\begin{aligned} &\text{Minimize } \mathrm{tr}\, A(\Theta) \\ &\text{Subject to } 0 \leq \Theta_i \leq u_i;\ \ i = 1, \ldots, m \\ &\qquad \Delta\big(\mathrm{tr}\, A^T(\Theta)A(\Theta)\big) = u \end{aligned} \tag{5.4}$$

The reformulation of the optimization problem will now be shown in an example based on Example 5.1 for $\alpha = 1.5$.

EXAMPLE 5.2
From Example 5.1 we get the numerical value of $\Delta\big(\mathrm{tr}\, A^T(\Theta)A(\Theta)\big)$ to about 36 for $\alpha = 0$. All the PSSs have reached their upper limits when $\alpha = 0$. The eigenvalues of the two slowest modes of the controlled system with all Θ:s equal to 0.16 p.u./(rad/s) and $\alpha = 0$ are not moved at all from the imaginary axes. The values of the two slowest modes for the uncontrolled system are shown in Table 5.1.

We do the optimization according to Eq. (5.4) for $\alpha = 1.5$ and $u = 36$. The parameters will now be less than 0.16 because the $\Delta\big(\mathrm{tr}\, A(\Theta)A(\Theta)\big)$ grows when the voltage dependence of the load increases. The result is shown in Table 5.2. The parameters are (0.045, 0.045, 0.050, 0.090, 0.061). According to the specifications in Section 5.3 we have got a much better tuning.

The relative damping of the two shown modes in Table 5.2 is

$$\zeta_1 = 0.44 \qquad \zeta_2 = 0.16$$

These values are considered to be very good for power systems. □

These two examples and the qualitative discussion in this section serve as an introduction to a theoretical analysis in next section.

5.5 Theoretical Analysis of the Optimization Problem

Motivated by the discussion in Section 5.4 we formulate the optimization problem as:

$$\begin{aligned} &\underset{\Theta \in R^m}{\text{Minimize}} \ \operatorname{tr} A(\Theta) \\ &\text{Subject to } 0 \leq \Theta_i \leq u_i; \ \ i = 1, \ldots, m \\ &\qquad\qquad 0 < \Delta\big(\operatorname{tr} A^T(\Theta) A(\Theta)\big) \leq u \end{aligned}$$

For the analysis we assume that only PSSs are installed. We also assume that no Θ_i:s reaches any limits and that $\Delta\big(\operatorname{tr} A^T(\Theta)A(\Theta)\big)$ reaches the limit u. Later we will see that the adopted optimization procedure will confirm these assumptions. According to Luenberger (1984, Chapter 10, page 301) we can write

$$l(\Theta, \lambda) = \operatorname{tr} A(\Theta) + \lambda \left(\Delta\big(\operatorname{tr} A^T(\Theta)A(\Theta)\big) - u\right)$$

where λ is the Lagrange multiplier. The necessary condition for optimality is of the form

$$\begin{cases} \nabla_\Theta l(\Theta, \lambda) = 0 \\ \nabla_\lambda l(\Theta, \lambda) = 0 \end{cases}$$

From Eq. (4.9) we get (only PSSs):

$$\operatorname{tr} A(\Theta) = \operatorname{tr}\big(M^{-1} B \cdot K_{se}\big)$$

Introduce now a new sequence of numbers $n_1, \ldots, n_k$ representing the index of the diagonal elements, where a PSS is installed. Instead of K_{se_i} we use Θ_{n_i}. Now we get the trace of A:

$$\operatorname{tr} A(\Theta) = \sum_{n_i=1}^{k} \frac{B(n_i, n_i)\Theta_{n_i}}{M_{n_i}} \triangleq \Theta^T \cdot b$$

$$\Delta\big(\operatorname{tr} A^T(\Theta)A(\Theta)\big) = \sum_{i=1}^{k} \Theta_{n_i}^2 B_{n_i}^T B_{n_i} \triangleq \Theta^T \cdot \Gamma \cdot \Theta$$

where

$$B_{n_i}^T = \left(\frac{B(1,n_i)}{m_1}, \ldots, \frac{B(n,n_i)}{m_n} \right)$$

$$\Gamma = \text{diag}\left(B_{n_i}^T \cdot B_{n_i}\right)$$

n = number of generators

k = number of installed PSSs

We know from Chapter 4 that

$$B(n_i,n_i) = -\left(\sum_{j \neq n_i}^{n} B(j,n_i) + \frac{\partial P_{L_{n_i}}}{\partial V_{n_i}} \right)$$

and

$$B(j,n_i) = -\sin\left(\theta_j - \theta_{n_i}\right) \frac{V_j}{X_{j_{n_i}}} = \frac{P_{n_{ij}}}{V_{n_i}}$$

The optimization problem can now be formulated as

$$\begin{array}{ll} \text{Minimize} & \Theta^T b \\ \text{Subject to} & 0 \leq \Theta_{n_i} < u_{n_i}; \quad n_i = 1, \ldots, k \\ & \Theta^T \cdot \Gamma \cdot \Theta - u = 0 \end{array}$$

We have assumed that Θ_{n_i} never reach the upper limits for normal loads. The necessary conditions become

$$\begin{cases} b + 2\lambda \cdot \Gamma \cdot \Theta = 0 \\ \Theta^T \cdot \Gamma \cdot \Theta - u = 0 \end{cases}$$

The parameter vector from the first equation is substituted into the second and we get λ:

$$\left(\frac{\Gamma^{-1}b}{2\lambda}\right)^T \Gamma \left(\frac{\Gamma^{-1}b}{2\lambda}\right) - u = 0$$

$$2\lambda = \frac{\left(b^T\Gamma^{-1}b\right)^{1/2}}{\sqrt{u}}$$

Finally we get Θ:

$$\Theta = -\frac{(\Gamma^{-1}b)}{(b^T\Gamma^{-1}b)^{1/2}}\sqrt{u} = -\frac{\Gamma^{-1}b}{2} g_{K,\epsilon}(\alpha) \cdot \sqrt{u} \tag{5.5}$$

where

$$g_{K_{se}}(\alpha) = \frac{2}{(b^T\Gamma^{-1}b)^{1/2}}$$

It is possible to show that $(b^T\Gamma^{-1}b)^{1/2}$ has a value in the range

$$0 < \left(b^T\Gamma^{-1}b\right)^{1/2} < (k)^{1/2}$$

The value k is reached when no power is injected to any connecting lines for all the PSS sites. All the power is delivered to the local loads. The value zero is reached for constant P and Q load connected to all sites and the net export of power is zero for all PSS sites.

The expression $-\Gamma^{-1}b/2$ is the optimal solution of the quadratic problem

$$\text{Minimize} \quad \text{tr}\, A(\Theta) + \text{tr}\, A^T(\Theta)A(\Theta)$$

For a PSS installed at bus i we get for the quadratic problem

$$\left(-\frac{\Gamma^{-1}b}{2}\right)_i = -\frac{B(i,i)m_{ii}^{-1}}{2\sum_{j=1}^{n}\frac{B^2(j,i)}{m_{jj}^2}} \tag{5.6}$$

This implies that PSS-sites, where $B(i,i) > 0$ must be excluded. If these sites are chosen, the optimization will come up with $\theta_i = 0$. Similar discussion for the SVCs will impose restrictions on the SVC-sites.

In many cases it is seen from load flow data that the dominant item in the $B(i,i)$ expression comes from the partial derivation of the load (P_{L_i}) with respect to the voltage (V_i).

$$B(i,i) = \sum_{j\neq i}\sin(\theta_j - \theta_i)\frac{V_j}{X_{ij}} - \frac{\partial P_{L_i}}{\partial V_i} \approx -\frac{\partial P_{L_i}}{\partial V_i}$$

$$\sum_{j=1}^{n}\frac{B^2(j,i)}{m_{jj}^2} = \frac{B^2(1,i)}{m_{11}^2} + \cdots + \frac{B^2(i,i)}{m_{ii}^2} + \cdots + \frac{B^2(n,i)}{m_{nn}^2} \geq \frac{\left(\frac{\partial P_{L_i}}{\partial V_i}\right)^2}{m_{ii}^2}$$

$$\Rightarrow \quad \left(-\frac{\Gamma^{-1}b}{2}\right)_i \approx \frac{\frac{\partial P_{L_i}}{\partial V_i}m_{ii}^{-1}}{2\left(\frac{\partial P_{L_i}}{\partial V_i}\right)^2 m_{ii}^{-2}} = \frac{m_{ii}}{2\cdot\frac{\partial P_{L_i}}{\partial V_i}} = \frac{m_{ii}V_i}{2\alpha P_{L_i}} \tag{5.7}$$

if we assume $P_{L_i} = CV_i^{\alpha}$. On the other hand, if the load is assumed to be constant P and Q, i.e.

$$\frac{\partial P_{L_i}}{\partial V_i} = 0$$

the value of $\left(-\frac{\Gamma^{-1}b}{2}\right)_i$ becomes:

$$\left(-\frac{\Gamma^{-1}b}{2}\right)_i = -\frac{B(i,i)m_{ii}^{-1}}{2\sum_{j=1}^{n} B^2(j,i)m_{jj}^{-2}}$$

where

$$B(i,i) = \sum_{j\neq i} \sin(\theta_j - \theta_i)\frac{V_i}{X_{ij}} = -V_i^{-1}\sum_{j\neq i} P_{ij}$$

P_{ij} is the power from node i to node j.

$$\begin{aligned}\left(-\frac{\Gamma^{-1}b}{2}\right)_i &= \frac{\left(\sum_{j\neq i} P_{ij}\right)(m_{ii}V_i)^{-1}}{2V_i^{-2}\left(\sum_{j\neq i} P_{ij}^2 m_{jj}^{-2} + m_{ii}^{-2}\left(\sum_{j\neq i} P_{ij}\right)^2\right)} \\ &\leq \frac{(m_{ii}V_i)^{-1}}{2(m_{ii}V_i)^{-2}\sum_{j\neq i} P_{ij}} = \frac{m_{ii}V_i}{2\sum_{j\neq i} P_{ij}}\end{aligned} \tag{5.8}$$

$\sum_{j\neq i} P_{ij}$ is positive according to the assumption, i.e., a net exporting site of power. Equation (5.6) makes sense according to Larsen and Swann (1981), Part II page 3026, which states:

> "The plant has the highest gain and the least phase lag under conditions of full load on the unit with a moderate to weak ac systems when bus frequency is used as input for the stabilizer."

This statement indicates that the PSS-parameter must be reduced, which also occurs in Eq. (5.6). This strengthen the basic idea behind the formulation of the optimization problem.

The general expression for the PSS-parameter can be written in terms of power. The items in Eq. (5.6) becomes:

$$B(i,i) = \sum_{j\neq i} \sin(\theta_j - \theta_i)\frac{V_j}{X_{ij}} - \frac{\partial P_{L_i}}{\partial V_i} = V_i^{-1}\left(\sum_{j\neq i}(-P_{ij}) - V_i\frac{\partial P_{L_i}}{\partial V_i}\right)$$

Assume

$$P_{L_i} = CV_i^{\alpha} \Rightarrow V_i\frac{\partial P_{L_i}}{\partial V_i} = \alpha P_{L_i}$$

Substituting αP_{L_i} into the expression above gives

$$B(i,i) = V_i^{-1}\left(\sum_{j\neq i}(-P_{ij}) - \alpha P_{L_i}\right)$$

$$\sum_{j=i}^{n}\frac{B^2(j,i)}{m_{jj}^2} = \frac{\sin^2(\theta_1-\theta_i)V_1^2}{m_{11}^2X_{i1}^2} + \cdots + \frac{B^2(i,i)}{m_{ii}^2} + \cdots + \frac{\sin^2(\theta_n-\theta_i)V_n^2}{m_{nn}^2X_{in}^2}$$

$$= V_i^{-2}\left(P_{i1}^2m_{11}^{-2} + \cdots + m_{ii}^{-2}\left(\sum_{j\neq i}P_{ij} + \alpha P_{L_i}\right)^2 + \cdots + P_{in}^2m_{nn}^{-2}\right)$$

Now we define

$$\tilde{P}_i^T \triangleq \left(P_{i1},\ldots,\left(\sum_{j\neq i}P_{ij} + \alpha P_{L_i}\right),\ldots,P_{in}\right)$$

Now Eq. (5.5) becomes in the general case:

$$\Theta_i = \left(-\frac{\Gamma^{-1}b}{2}\right)_i g_{K_{se}}(\alpha)\sqrt{u} = \frac{V_i\left(\sum_{j\neq i}P_{ij} + \alpha P_{L_i}\right)m_{ii}^{-1}}{2\tilde{P}_i^TM^{-2}\tilde{P}_i}\cdot g_{K_{se}}(\alpha)\sqrt{u} \qquad (5.9)$$

Similar expressions can be calculated for the SVC concept. Using this expression, it would be possible to tune the Θ_i-parameter continuously by measurement of power on lines connected to the site and knowing the equivalent α-parameter for the site and the masses of the incident generators.

Remark. Only power lines connected to the site are included in the $\tilde{P}_i$-vector. Power lines with no incident on site, i, is represented by zero. □

Equation (5.9) explains to some extent the trade-off between the mass of the machine and the load flow and the voltage dependence of load. This relationship is natural to include in the optimization problem.

If the optimization problem is formulated as a quadratic problem with scaling, it will give the same solution as for the introduced constraint function for a proper choice of the scaling factor.

The quadratic optimization with scaling is

$$\text{Minimize}\quad \operatorname{tr}A(\Theta) + \beta\Delta\left(\operatorname{tr}A^T(\Theta)A(\Theta)\right)$$

The solution is equal to the solution of Eq. (5.5) with

$$\Theta = -\frac{\Gamma^{-1}b}{2\beta}$$

where β is:

$$\beta = \frac{\left(b^T \Gamma^{-1} b\right)^{1/2}}{2\sqrt{u}}$$

Similar expressions can be evaluated for SVCs and HVDC links. For the quadratic optimization problem with $\beta = 1$ we get:

$$K_{\mathrm{SVC}_i} = -\frac{\left(B(l,i)m_{ll}^{-1} - B(k,i)m_{kk}^{-1}\right)}{4\sum_{j=1}^{n} \frac{B^2(j,i)}{m_{jj}^2}} \tag{5.10}$$

If one of the measurements takes place at nod i for the SVC,

$$K_{\mathrm{SVC}_i} = -\frac{\left(B(i,i)m_{ii}^{-1} - B(k,i)m_{kk}^{-1}\right)}{4\sum_{j=1}^{n} \frac{B^2(j,i)}{m_{jj}^2}}$$

$$K_{\mathrm{DC}_r} = \frac{m_{il}^{-1} + m_{jk}^{-1}}{4\left(m_{ii}^{-2} + m_{jj}^{-2}\right)} \tag{5.11}$$

If both measurements for the HVDC takes place at the station,

$$K_{\mathrm{DC}_r} = \frac{m_{ii}^{-1} + m_{jj}^{-1}}{4\left(m_{ii}^{-2} + m_{jj}^{-2}\right)} = \frac{m_{ii}m_{jj}}{4} \cdot \frac{(m_{ii} + m_{jj})}{m_{ii}^2 + m_{jj}^2} \tag{5.12}$$

Summary

The theoretical analysis is now summarized. Generally it can be stated:

1. The siting procedure points out robust places. The system properties together with normal load characteristics will cause the $\Delta(\mathrm{tr}\, A^T A)$ to increase when the parameters increase.
2. The procedure for finding the limit of $\mathrm{tr}\, A^T A$ or the scale factor β is based on system properties.
3. The theoretical analysis of the optimal values of the PSS parameters indicates that the powerflow and the voltage dependence of the load (process gain) is introduced in a natural way. It is also confirmed by discussion in Larsen and Swann (1981).
4. The siting analysis points out robust sites for damping equipment (SVCs and PSSs) with good damping properties for selected system wide modes. It can not be proved that the optimization procedure favor these modes in terms of damping. The setup and initial values of the sensitivity derivatives are, however, such that good damping can be achieved for selected slow modes.

5. The examples and the theoretical analysis make the formulation of the optimization problem reasonable for a large power system. Next chapter will show that the values of the optimized parameters introduce augmented damping very well. A strict proof that the suggested method give better damping according to the specifications is, however, not given.

5.6 Formulation of the Optimization Problem and Numerical Methods

The optimization problem can now be stated in the following form:

$$\left.\begin{aligned} &\underset{\Theta \in R^m}{\text{Minimize}} \ \operatorname{tr} A(\Theta) \\ &\text{Subject to } 0 \le \Theta_i \le u_i; \ \ i = 1, \ldots, m \\ &\qquad\qquad 0 < \Delta\left(\operatorname{tr} A^T(\Theta) A(\Theta)\right) \le u \end{aligned}\right\} \tag{5.13}$$

$$\Theta = \left(\Theta_1^{K_{se}}, \ldots, \Theta_{m_1}^{K_{se}}, \Theta_1^{\text{SVC}}, \ldots, \Theta_{m_2}^{\text{SVC}}, \Theta_1^{\text{DC}}, \ldots, \Theta_{m_3}^{\text{DC}}\right)$$

$$m_1 + m_2 + m_3 = m \ \text{(number of parameters)}$$

$\operatorname{tr} A^T(\Theta) A(\Theta)$ is the nonlinear constraint function and $\operatorname{tr} A(\Theta)$ is a linear objective function. A reliable method for solving this problem is the augmented Lagrangian method (NAG, EO4UCF).

Remark. For the quadratic problem, with or without scaling efficient methods are available. See NAG, EO4JAF, Conjugated Direction methods and Quasi-Newton methods. (See NAG, EO4NAF.) □

The EO4UCF-routine was used most of the time in order to maintain the possibility to use a nonlinear objective function and/or a nonlinear constraint function later in the project.

All necessary information about mentioned methods can be read in NAG (1988). The mathematics and numerics about the methods are described in Luenberger (1984), Dennis and More (1977), Dennis and Schnabel (1981, 1983), Gill, Murray and Wright (1981, 1986), Powell (1974), and Fletcher (1981).

A lot of optimization procedures were tested before the optimization problem was formulated as in (5.13). We know from Section 5.5 that an analytical solution exists for this formulation. In this perspective it was convenient to use the routine EO4UCF most of the time.

Estimation of the Limits of the Constraints Function

In order to get a robust operational swing of the parameters due to variation of the voltage dependence of load the following procedure is followed:

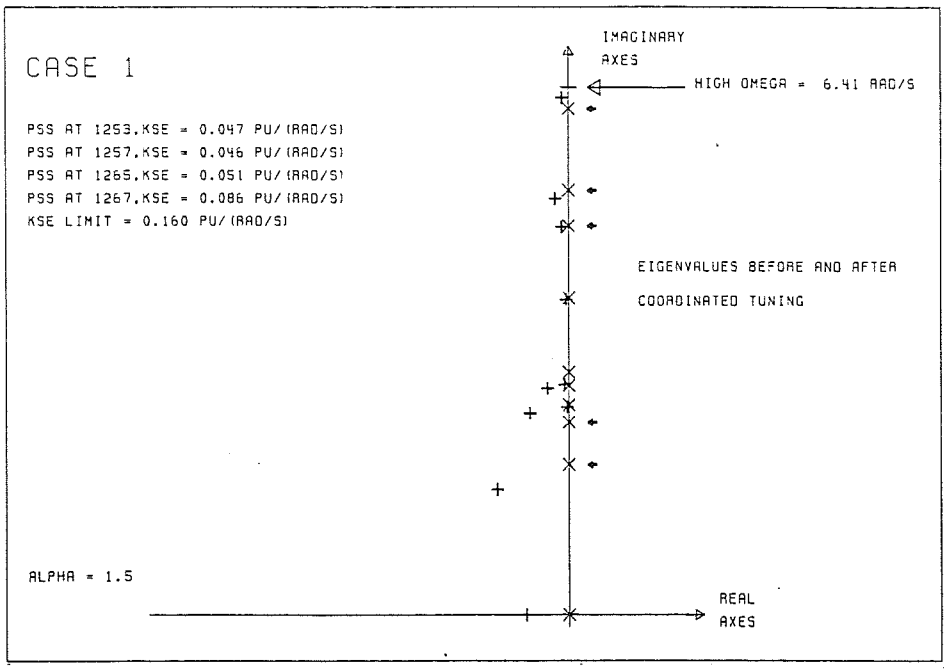

Figure 5.1 Eigenvalues for the slowest modes before (×) and after (+) the tuning. The arrows points on the chosen system wide modes, Case 1.

1. The voltage dependence of the load is set equal to zero, i.e. constant P and Q load is considered.
2. Only approved sites from the siting are considered for PSSs and SVCs. During normal operational conditions the HVDC links have no destabilizing affect.
3. The limit, u, of $\Delta\big(\mathrm{tr}\, A^T(\Theta)A(\Theta)\big)$ is then varied until almost all the parameters have reached their limits by the opimization procedure. The PSS parameters use to reach their limits first. This limit of $\Delta(\mathrm{tr}\, A^T A)$ is then used for the actual configuration of the damping equipment.
4. The characteristics of the loads are set to actual values, e.g. $\alpha = 1.5$.
5. The optimization can now be performed.

5.7 Application to the Nordel Power System

The optimization procedure is now applied to the Nordel power system. The augmented damping introduced by the optimization procedure will be presented. Only results from 21- and 224-machines are shown to limit the number of figures. Detailed information can be found in the report Eliasson (1989b). These configurations of PSSs are later used in Chapter 6 during the verification of augmented damping.

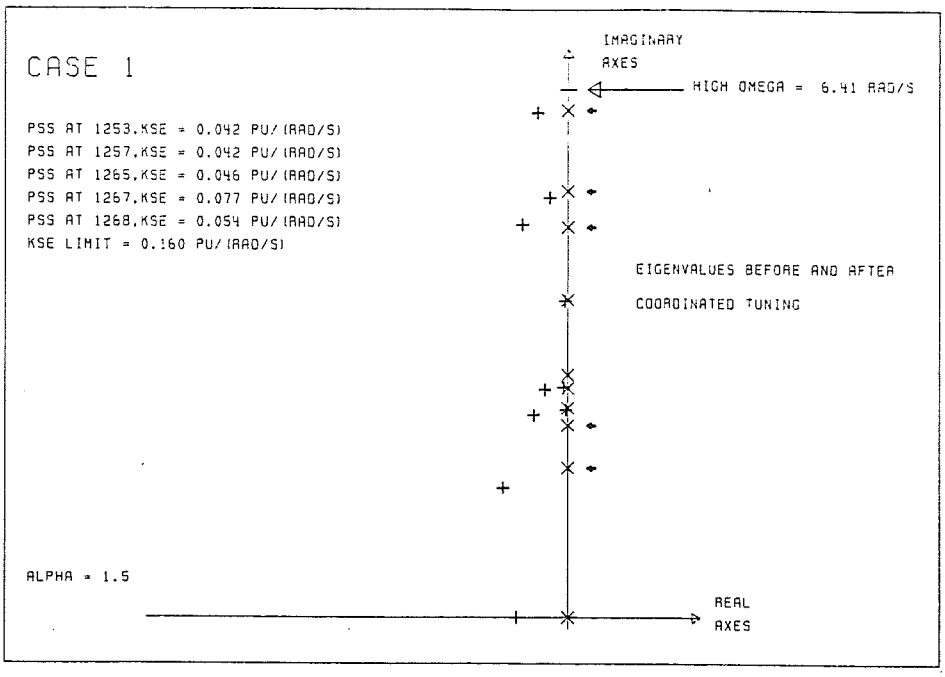

Figure 5.2 Eigenvalues for the slowest modes before (×) and after (+) the tuning ($\alpha = 1.5$, BLC, Case 1).

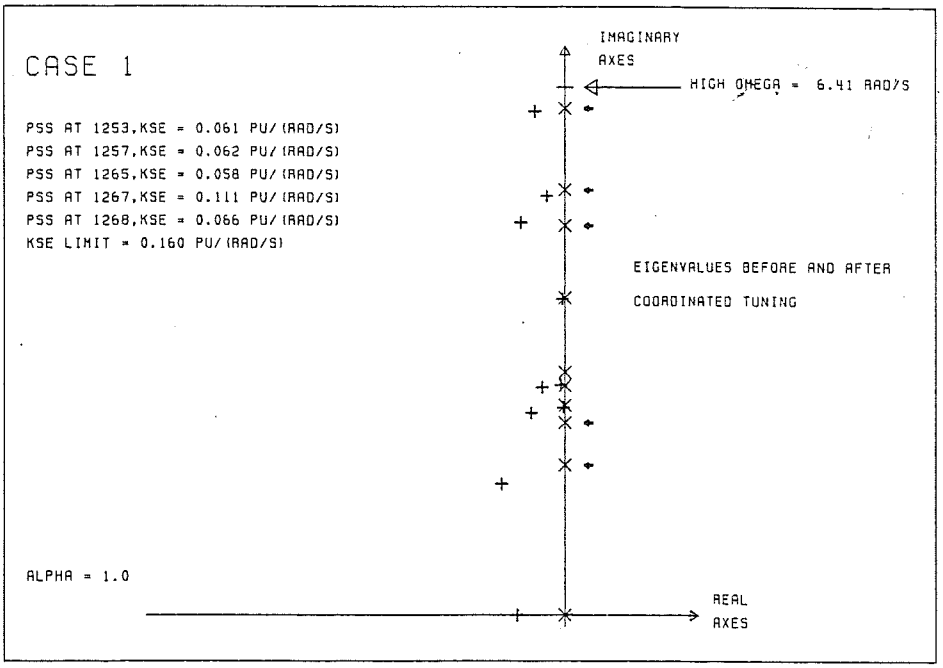

Figure 5.3 Eigenvalues for the slowest modes before (×) and after (+) the tuning ($\alpha = 1.0$, Case 1).

To do a complete analysis of siting and tuning of damping equipment in a large power system takes at least a man-year. In this perspective the author only will show some principle ideas applied to a large power system.

Result From the Optimization

The figures in this section show how the eigenvalues are moved into the left half plane. When the tuning starts, the eigenvalues are all on the imaginary axes. These eigenvalues are marked $\times$. The eigenvalues after the optimizations are marked $+$. The small arrows in the right half plane points out the modes that are chosen as slow and system wide modes.

The text tells where the damping equipment is placed and the values of the tuned parameters. The scaling is linear and the only way to get numerical values of the eigenvalues is to measure the distance from origin to the "high omega" line. The number at that position defines the actual scaling. The x- and y-axes have the same scaling.

Case 1

Figure 4.6 shows the robust sites with respect to all load characteristics and for chosen five system wide modes (Case 1, Table 3.2). The site 1254 is excluded because a PSS at that site has a minor impact on the damping of the chosen system wide modes. The site is approved though.

Figure 5.1 shows that the poles (eigenvalues) are moved into the left half plane when four PSSs are introduced. Only poles up to the "high omega" limit are shown. In order to get better damping for the three highest system wide modes we add a fifth PSS at bus 1268. This site is not approved for the CLC-load case for the second system wide mode. This is an extreme type of load characteristics. For load characteristics of concern, the siting analysis points out this site for the higher system frequencies. The result is shown in Fig. 5.2. It shows the augmented damping introduced by five PSSs. The load characteristic is BLC ($\alpha = 1.5$). Figures 5.3, 5.4 and 5.5 show what happens when α is reduced to 1.0 (constant current load), 0.5 and finally to 0 (CLC), respectively.

The following can be concluded: When α decreases, the K_{se_i}-parameters increase until some reach the limit 0.16 pu/(rad/s). K_{se_i} follows the relationship given in Eq. (5.7), i.e. K_{se_i} increases if α decreases.

The augmented damping can be maintained rather good until $\alpha = 0$. When the voltage dependence of the active load is zero it seems to be hard to add any damping, at least in this case.

An interesting property is that when α decrease, the pole for the rigid body (the pole on the real axes) moves towards origo. One pole is always located at origo. The explanation is as follows:

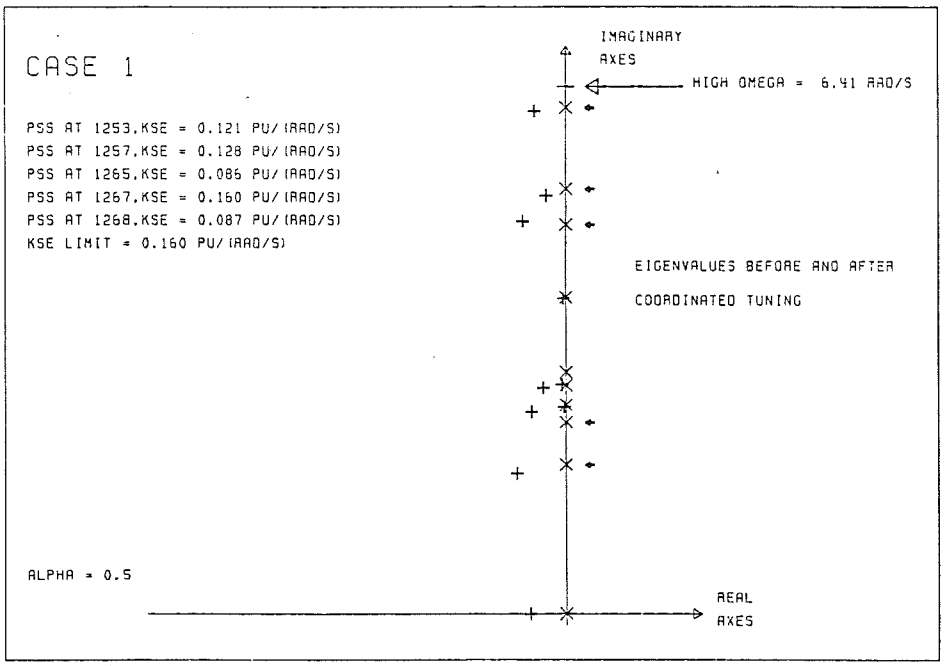

Figure 5.4 Eigenvalues for the slowest modes before (×) and after (+) the tuning ($\alpha = 0.5$, Case 1).

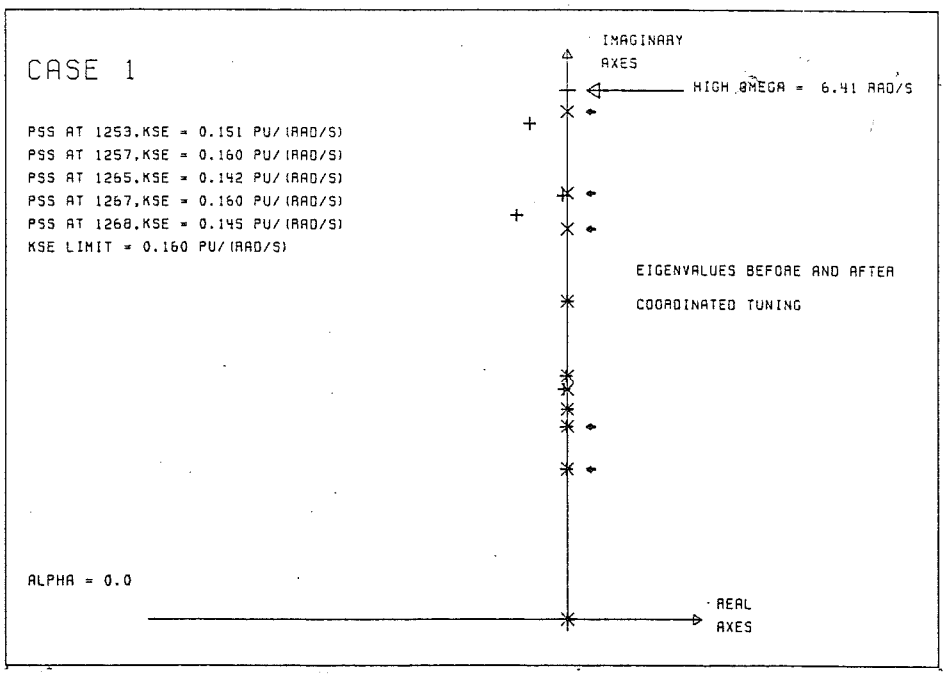

Figure 5.5 Eigenvalues for the slowest modes before (×) and after (+) the tuning ($\alpha = 0$, CLC, Case 1).

The equation of motion of mode i is

$$\left(M\lambda_i^2 + \tilde{D}\lambda_i + K\right) u_i = 0$$

One eigenvector can always be chosen as $u_0^T = (1, \ldots, 1)$, the eigenvector representing the rigid body motion. The structure of K is such that $Ku_0 = 0$, i.e.

$$\lambda_i^2 M u_0 + \lambda_i \tilde{D} u_0 = 0$$
$$\lambda_i(\lambda_i M u_0 + \tilde{D} u_0) = 0$$

The roots are $\lambda_1 = 0$ and $\lambda_2 M u_0 + \tilde{D} u_0 = 0$. To solve the last equation, we just multiply with u_0^T from the right:

$$\lambda_2 = -\frac{u_0^T \tilde{D} u_0}{u_0^T M u_0}$$

The expression $u_0^T \tilde{D} u_0$ summarizes all the elements in $\tilde{D}$. If D contains contribution from all kinds of damping equipment, it is easy to see that when all elements in $\tilde{D}$ are summarized, the only elements in the sum comes from

$$\frac{\partial P_{Li}}{\partial V_i} K_{se_i} \quad \text{and} \quad \frac{\partial P_{Lj}}{\partial V_j} K_{\text{SVC}_j}$$

So the eigenvalue of the rigid body is

$$\lambda_2 = \frac{u_0^T B \left(K_{se} + T_s^{\text{SVC}} K_{\text{SVC}} \left(T_m^{\text{SVC}}\right)^T\right) u_0}{u_0^T M u_0}$$

From Eq. (2.8) and the structure of B we get $\lambda_2 = 0$ when $\frac{\partial P_{Li}}{\partial V_i} = 0 \ \forall \ i$. This explains the motion and value of the left pole on the x-axis.

Now we continue to add one SVC and one HVDC link to the last configuration. The result can be seen in Figures 5.6 and 5.7. The result shows that the damping is improved for all system wide modes. The three highest are affected by the SVC and the two slowest system wide modes by the HVDC link. Sensitivity analysis shows clearly how the SVC and the HVDC link affects different modes. The chosen site for the SVC is taken from Fig. 4.7.

It is interesting to notice that we still have rather good damping for three of the system wide modes in Fig. 5.7 even if $\alpha = 0$. The HVDC link adds damping to the slowest system wide mode. The other two system wide modes are affected by the PSS at 1268 and the SVC, which was already seen in Fig. 5.2 (only PSSs). The HVDC-concept is not affected by α, so it is natural that the link can still add damping regardless of α. An explanation of the result in Figures 5.2 to 5.7

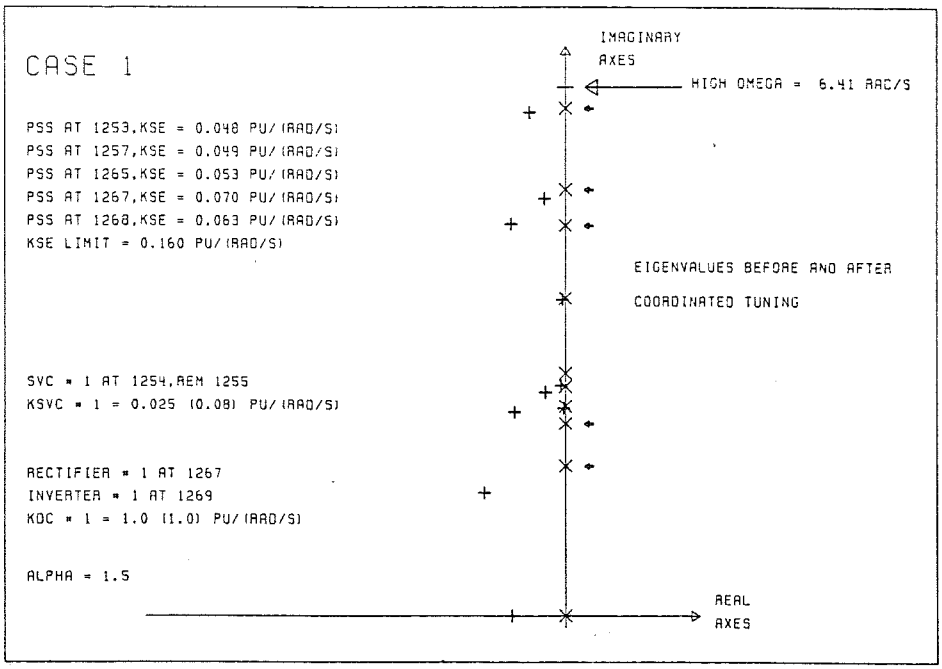

Figure 5.6 Eigenvalues before ($\times$) and after ($+$) the tuning. All damping equipment is included ($\alpha = 1.5$, Case 1).

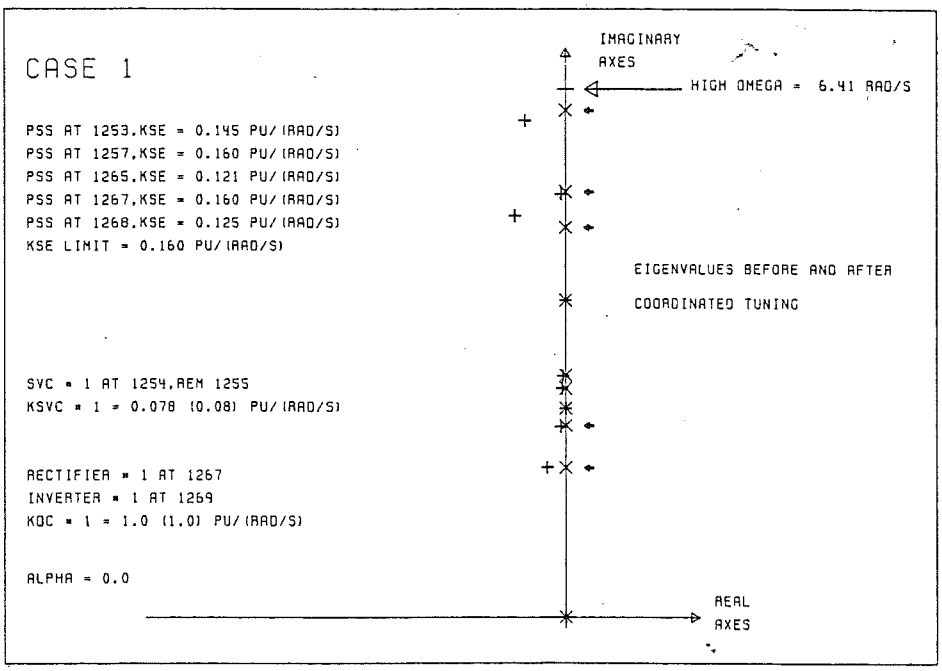

Figure 5.7 Eigenvalues before ($\times$) and after ($+$) the tuning. All damping equipment is included ($\alpha = 0$, Case 1).

may be like this. The site 1268 is in the north of Sweden, Norway and Finland. This area has relatively small load, but has a large surplus of power. Equation (5.8) suits this assumption. The expression

$$\frac{m_{ii}V_i}{2\sum_{j\neq i} P_{ij}}$$

might be of the same order as the limit of the K_{se_i}, i.e. 0.16 pu/(rad/s). This means that it is possible to add damping even when $\alpha = 0$. A check of this statement shows that $0.04 \leq K_{se} < 0.25$. The lower limit of K_{se} comes from Eq. (5.7) and the upper limit comes from (5.8).

Case 3

Now we turns to the more difficult case with 224 machines. The sites are selected from the siting analysis, Chapter 4. We only select a minimum configuration of PSSs for damping of the two slowest system wide modes. Figures 5.8 and 5.9 show the result for $\alpha = 1.5$ and $\alpha = 1.0$ respectively. Only twenty-one PSSs are chosen. The specifications are that the amplitude ought to be halved within 7 to 10 seconds.

The eigenvalues corresponding to the slowest modes are $\lambda_1 = -0.16 \pm j1.55$ and $\lambda_2 = -0.14 \pm j2.15$ respectively, after the optimization (Fig. 5.8). Initially, these eigenvalues were $\lambda_1 = \pm j1.56$ and $\lambda_2 = \pm j2.12$. The initial cycle times are 4.03 s and 2.96 s. This means that the amplitudes are halved within 1.1 period and 1.7 period respectively. This result is considered very good from operational people. The result fulfills the specification very well.

Further details can be seen in the report Eliasson (1989b).

5.8 Conclusions

The selected formulation of the optimization problem has excellent impact on the damping of the system. The eigenvalues are moved nearly straight into the left half plane, which means that the synchronous forces of the system are unchanged. This result is based on the sensitivity analysis. This analysis points out robust sites with respect to damping for selected slow and system wide modes. The other slow and local modes are easy to handle with local measures (Larsen and Swann (1981) Parts I, II & III). In Chapter 6 it is shown that augmented damping is introduced by use of feedback from the bus frequency deviation. This strengthen the need for using other signals than the conventional.

The optimization technique shows also that it is possible to tune roughly 100 PSSs, 20 SVCs and 10 HVDC links at the same time without running into

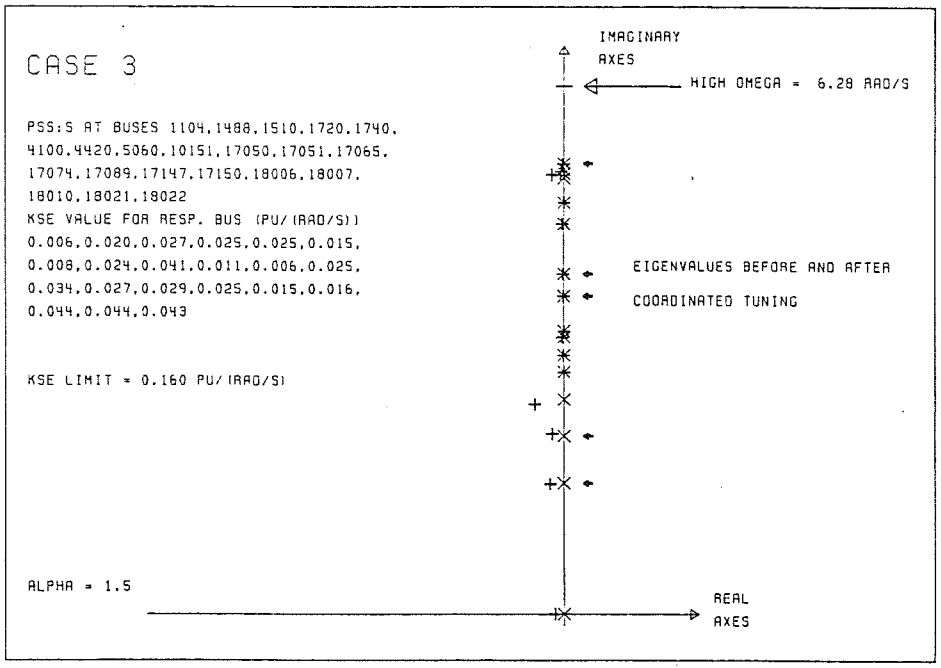

Figure 5.8 Eigenvalues before ($\times$) and after ($+$) the tuning ($\alpha = 1.5$, Case 3).

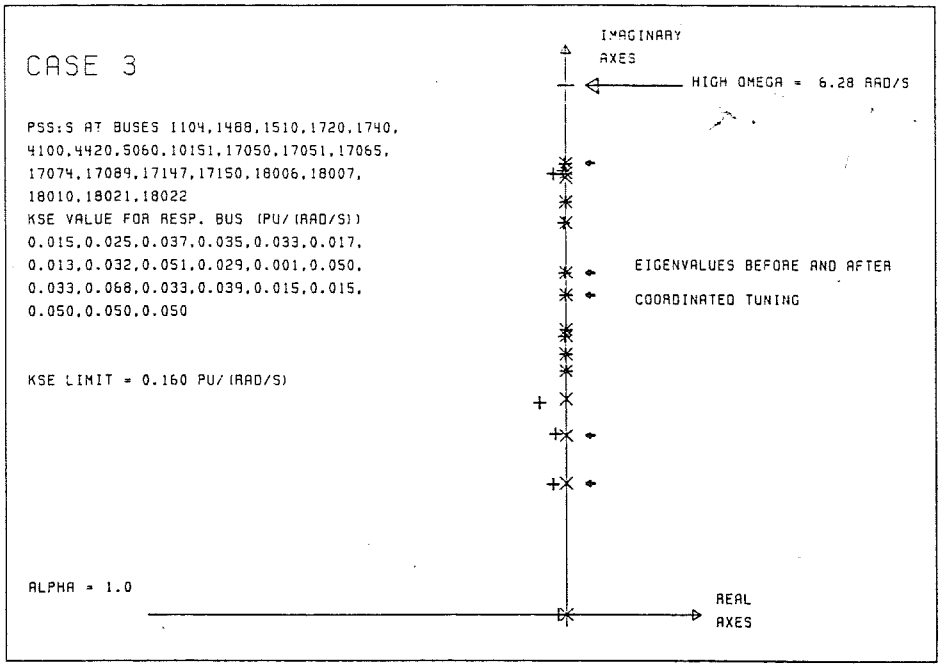

Figure 5.9 Eigenvalues before ($\times$) and after ($+$) the tuning ($\alpha = 1.0$, Case 3).

any computer time problems. A test was run for PSSs installed at all buses and the optimization worked well for Case 3 (224 PSSs). The most time consuming part is the calculation of the eigenvalues. The way it is implemented in the tuning package there is the need for two eigenvalue calculations, one before starting and one for checking that the system is globally stable after the tuning. The first calculation of the eigenvalues is much faster than the last one, because the squared eigenvalues are calculated (model (KM)). For a 224-machine case, the eigenvalues consumes $\approx$ 4 hours and the tuning of 100 parameters takes $\approx$ 0.5 hour.

It is worth emphasizing that all specifications of constraints, concerning real part, imaginary part or relative damping etc., can hardly lead to a successful optimization for large power systems. The reason is that the Jacobian matrix has to be updated in each iteration and it will take long computational time. Even if the eigenvalues are ordered with respect to the real and imaginary part, it is not clear what happens when two different trajectories are crossing.

To calculate the Jacobian matrix with constraints on the eigenvalues will overload any modern computer in the world of today.

The good damping results show that it is possible to use a simple two-state model for investigation of slow and system wide modes.

This choice of formulation of the optimization problem has many advantages:

- Easy to use.
- Extremely fast for large power systems.
- Easy to interpret.
- A nice trade-off between the values of the parameters with respect to

$$\left(\sum_{j\neq i} P_{ij} + V_i \frac{\partial P_{L_i}}{\partial V_i}\right)$$

  and the mass associated to the bus i for PSS-equipment.
- Robust design against change of load flow and voltage dependence of load.
- The tuning procedure adds positive damping to the low frequency modes.

Drawbacks:

- There is no guarantee that global stability is reached. A final check of the eigenvalues has to be done. Fortunately this has to be done only once, because it is very time consuming.

If unstable conditions should occur during the optimization, the upper limit u of $\Delta(\mathrm{tr}\, A^T A)$ must be reduced. Also investigation of the symmetric part of $\tilde{D}$ is of interest to do according to Eq. (4.22).

6

Verification of the Siting and Optimization Procedure

6.1 Introduction

The basic idea behind the model (KM), see Chapter 2, is that the bus voltage can be used as input signal. The reason is that the properties of modern AVRs (Automatic Voltage Regulator) are such that the rise time of the generator terminal voltage for a step response in the voltage reference is much shorter than the time of period of the interesting system modes. Simulations and verification of the model (KM) in Chapter 2 has also shown that this assumption holds quite well for slow and system wide modes. With this in mind, we investigate a PSS design with an extremely simple structure. We will use a feedback controller from the bus frequency deviation (Δf_i) and add the signal $K_{se_i} \cdot 2\pi \cdot \Delta f_i$ to the voltage reference for the good sites pointed out by the siting analysis.

Many PSSs designs use the electric power of the generators as input to the controller. If we assume that the mechanical torque is constant or changes slowly, it is possible to estimate $(\Delta\omega_i)$ from the electrical power deviations. It is also possible to estimate $(\Delta\dot{\omega}_i)$, but the estimates are, however, influenced by rapid changes in mechanical torque. The complexity of the controller increases and the parameters are difficult to tune in a MIMO-concept for a large power system.

Operational people state that a power system is acceptable damped if the

amplitude of a slow oscillation is reduced by 50% halved within 10 seconds. This implies that the real part of the eigenvalue should be approximately 0.07. The verifications given in this chapter put special emphasis on

- Design of PSSs dedicated for slow and system wide modes.
- Verification of augmented damping.

6.2 Verification of Augmented Damping

All real time simulations presented here are done with the power system simulation package PSS/E from PTI. During the simulations $\alpha = 1.5$ is used in the whole power system.

Data About the Simulated Systems

All information for siting of PSS- SVC- and HVDC-equipment is fetched from the siting analysis in Chapter 4 and the values of the parameters from Chapter 5. All data about the Nordel power systems used in this thesis is presented in Section 1.4, but below a summary is given:

21 machines (Case 1):	766	constants
	81	variables
	265	states
44 machines (Case 2):	1388	constants
	88	variables
	482	states
224 machines (Case 3):	7329	constants
	617	variables
	2518	states

As in Chapter 5 we only present results for Case 1 and Case 3 and the siting of the PSSs is according to Fig. 5.2 (Case 1) and Fig. 5.8 (Case 3).

The used PSS design is extremely simple. No such simple PSS-transfer function is available in the library of the simulation package. A special software had to be developed and linked to the simulation package. The value of K_{se_i} are taken directly from the optimization and then fed into the controller without changing a digit.

Explanation of the designation of the curves showing the machine angles:
Solid line = Uncontrolled system.
Dashed line = Controlled system with optimized parameters.
Dotted line = Controlled system with parameters not optimized for actual load specification.

Case 1

The load, located in south-western Norway, at bus 1257, Gen_06, is decreased with 100 MW. After 0.1 second it is increased again to its initial value. The two swing centers for the slowest and system wide mode are bus 1257 and bus 1267, Gen_18. The location of the buses can be seen in Fig.E.1, Appendix E.

The machine, 1267 (Gen_18), in southern Finland ought to swing with a frequency very close to the slowest system wide mode. See the solid line in Fig. 6.2. The eigenfrequency measured in Fig. 6.2 is 0.28 Hz. The nominal value of the eigenfrequency calculated by the model (KM) is 0.29 Hz. The first five figures, 6.1 to 6.5, show the angles of machines equipped with PSSs. Figure 6.6 represents angles for a machine not equipped with a PSS.

Figure 6.7 shows what happens if the values of the parameters of the controllers are doubled. The dotted line shows the angle of the machine, 1267. The solid curve represents the uncontrolled case and the dashed line represents the angle with optimized coefficients. The system is close to going unstable, when the values of the coefficients are doubled. The dominant angle frequence of the oscillation in Fig. 6.7 (the dotted line) is about 3.9 rad/s.

The eigenvalue calculation by the doubled values of the parameters indicates a poorly damped mode with the imaginary part of the eigenvalue equal to 3.82 rad/s and with the relative damping of about 0.007. This mode can also be seen in Fig. 5.2 (the sixth mode from bottom). The result from Fig. 6.7 indicates that this poorly damped mode can not be controlled by the chosen PSS-sites. But when the parameters are doubled the mode is energized. This phenomenon is further discussed in Case 3.

Figures 6.8 and 6.9 concern only the optimal controlled case. Figure 6.8 shows the angle (solid line) and the voltage (dashed line) for machine, 1267. Figure 6.9 shows the output signal from the PSS (solid line) and the voltage (dashed line) for machine, 1267.

The result in general must be considered good.

Case 3

The load at bus 4100, Tonsta 11, is decreased with 100 MW. After 0.1 second it is increased again to its initial value. The two swing centers for the slowest and system wide mode are bus 4100 and bus 18006, OL4G1. The location of the buses can be seen in Fig.E.3, Appendix E. This figure shows the aggregation of 224 machines into 21 machines.

It is worth to mention that the swing centers for Case 1, Case 2 and Case 3 for all selected slow and system wide modes are aggregated into each other throughout the hierarchy of models.

The estimated eigenfrequency in Fig. 6.10 (the first two swings) is 0.24 Hz. The nominal value of the eigenfrequency calculated by the model (KM) is 0.25 Hz. Figures 6.10 to 6.15 show the angle of selected machines in the Nordel

system. Only 21 PSSs are used. The values of the used parameters are shown in Fig. 5.8. These PSSs cover only the two slowest system wide modes. It is clearly shown in Figs. 6.10 to 6.15 that the introduced damping of the twentyone selected PSSs is considerable. Only the best sites from damping point of view are considered for the two slowest modes. It is also worth mentioning that the siting procedure and the tuning procedure take about the same time as doing one simulation of 224 machines under 40 seconds. In other words, by knowing good sites for PSSs the amount of work can drastically be reduced.

An interesting sequence of figures are Figures 6.16 to 6.20. Figures 6.16 and 6.17 show the uncontrolled (solid line), optimal controlled (dashed line) and controlled (dotted line), but the value of parameters in Fig. 5.8 are doubled. It is clearly seen that a poorly damped mode is energized. The frequency of the oscillation is estimated to 1.3 Hz. This oscillation can also be seen by calculating the eigenvalues of the used parameters.

The eigenvalue calculation of the closed loop system indicates too that an oscillative mode occurs. Two eigenvalues of 448 eigenvalues have the values, $\lambda_{1,2} = \pm j \cdot 8.82$, i.e. an oscillation of 1.40 Hz. This value of the imaginary parts of the eigenvalues can also be estimated by the following simplified calculation. From analysis of the load flow data and the involved machines, OL4G2 and OL4G1, we get the following equations to solve. The model (KM) gives for the two oscillating machines:

$$M = 0.305 \begin{pmatrix} 1 & 0 \\ 0 & 1 \end{pmatrix}$$

The machines have equal masses.

$$K = \frac{(0.99)^2}{0.0823} \begin{pmatrix} 1 & -1 \\ -1 & 1 \end{pmatrix} = 11.9 \begin{pmatrix} 1 & -1 \\ -1 & 1 \end{pmatrix}$$

The angles between the machines are zero. Define $\omega_0^2 = \frac{11.9}{0.305}$. The eigenvalues of $M^{-1}K$ are

$$\lambda_1 = 0, \quad \lambda_2 = \pm j\sqrt{2}\omega_0 = \pm j \cdot 2\pi \cdot 1.41 \text{ rad/s}$$

This rather simple calculation also gives a good result. The frequencies to compare are the frequency from the simulation, eigenvalue calculation of a second order model (448 states) and a simple KM-calculation (two states). The frequencies are 1.30 Hz, 1.40 Hz and 1.41 Hz, respectively.

Simulations show that even if the PSSs on these machines are taken away, the oscillations are still there. This indicates that a proportional controller is not sufficient to cope with this problem. A nice thing, though, is that we can use the eigenvalues from a second order model to get information of troublesome modes in a much more (six times in terms of number of states) complex model.

To be able to solve the occurred oscillation problem we might have to estimate some states or transfer information between the machines. This type of analysis is beyond the aim of this thesis. This thesis only treats slow and system wide modes.

Figures 6.18 to 6.20 show what happens if the parameters from Fig. 5.9 are used. The dotted line represents the values from Fig. 5.9. In general, the damping is somewhat better, but for one machine, LOG2 at bus 18010, the angle starts to increase in the end of the simulation. The solid line represents the uncontrolled system and the dashed line represents the optimal controlled system with parameters from Fig. 5.8. The stable controlled case and the dynamic simulation have the same load characteristics. The dotted line represents a mismatch in characteristics. The optimization is done for constant current load ($\alpha = 1.0$), but the dynamic model represents 50% constant impedance and 50% constant current load ($\alpha = 1.5$).

The estimated angle velocity in Fig. 6.20 is about 9.5 rad/s. From the eigenvalue calculation, it is shown that two eigenvalues are $\pm j \cdot 9.55$ rad/s. There are several eigenvalues with the real part equal to zero in the high frequency range. Presumably this mode is energized with this configuration of PSSs and chosen values of the parameters. In general, it can be stated that the PSS control law, Eq. (4.2), does not introduce any damping between the machines, if not special conditions are fulfilled. The HVDC control law, Eq. (4.5), does introduce damping between machines. The PSSs introduce mainly damping towards the ground (reference) via the voltage dependence of the load. This tells us, that the optimization is very sensitive to the voltage dependence of the load when only PSSs are used. It also indicates that the formulation of the optimization problem works very well. It takes roughly 8 CPU hours to simulate 40 seconds for the 224 machines case.

6.3 Conclusions

The simulations show that it is of great importance to choose proper sites for damping equipment for the slow and system wide modes and tune the parameters well. Only 21 PSSs sites are chosen to get the result. Today approximately 200 PSSs are installed in Nordel systems. Naturally, more than 21 PSSs are required to get the Nordel system well damped in the low frequency range. In combination with SVCs and the Fenno-Skan link maybe not more than 50 PSSs are needed. It is also clearly shown that the voltage dependence of the load plays a crucial role. The operational conditions are of great importance. This has to be considered for a specific site or within a certain area of the power system.

This analysis shows that the bus frequence deviation is a good signal to use in combination with a proportional controller for slow and system wide modes.

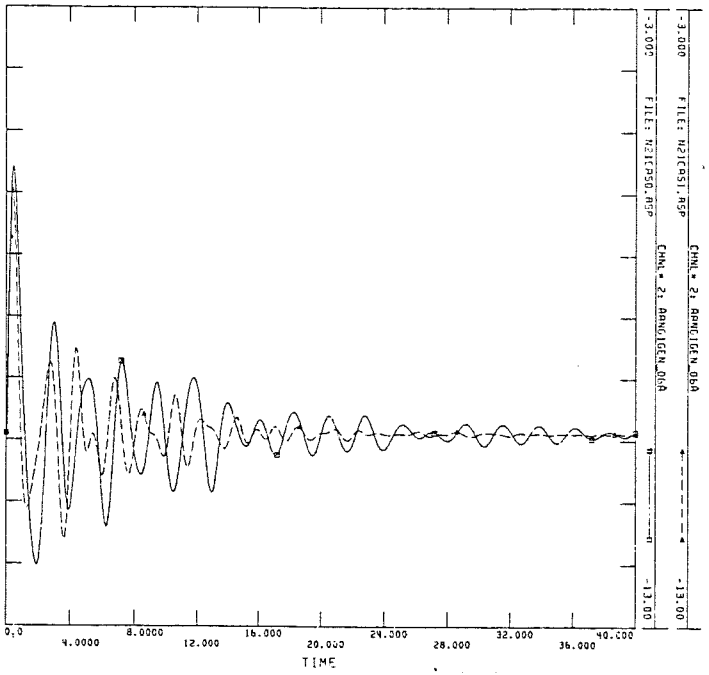

Figure 6.1 Dynamic response for inactive PSS (solid line) and active PSS (dashed line) for the disturbed machine, Gen_06, in southern Norway ($\alpha = 1.5$, Case 1).

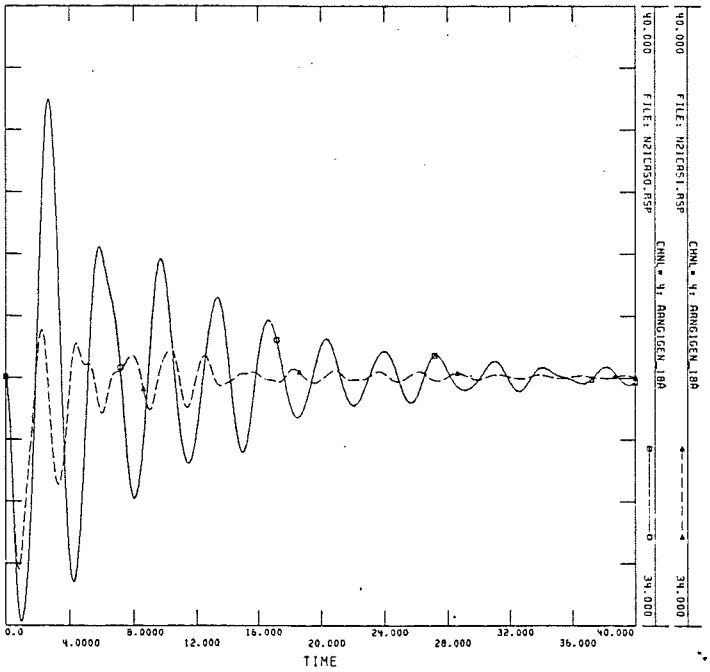

Figure 6.2 Dynamic response for inactive PSS (solid line) and active PSS (dashed line) of the machine, Gen_18, in southern Finland ($\alpha = 1.5$, Case 1).

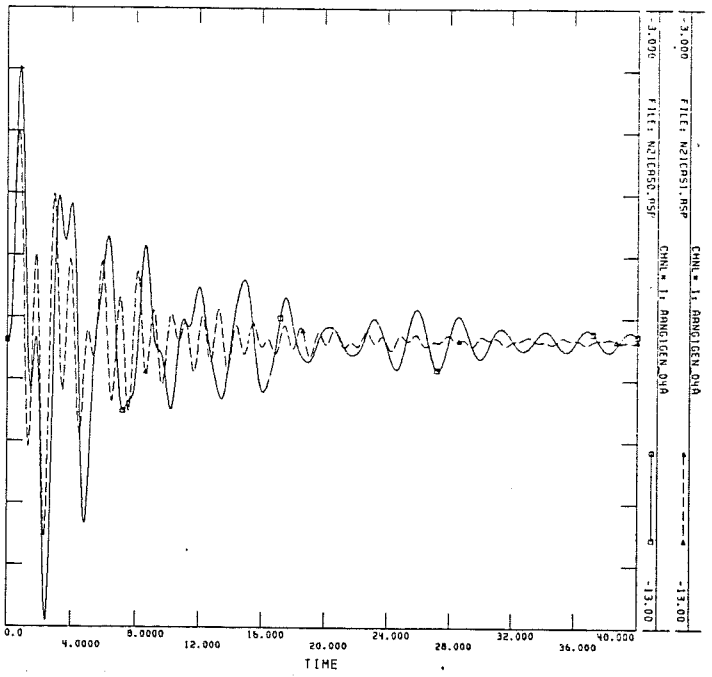

Figure 6.3 Dynamic response for inactive PSS (solid line) and active PSS (dashed line) of the machine, Gen_04, in Norway ($\alpha = 1.5$, Case 1).

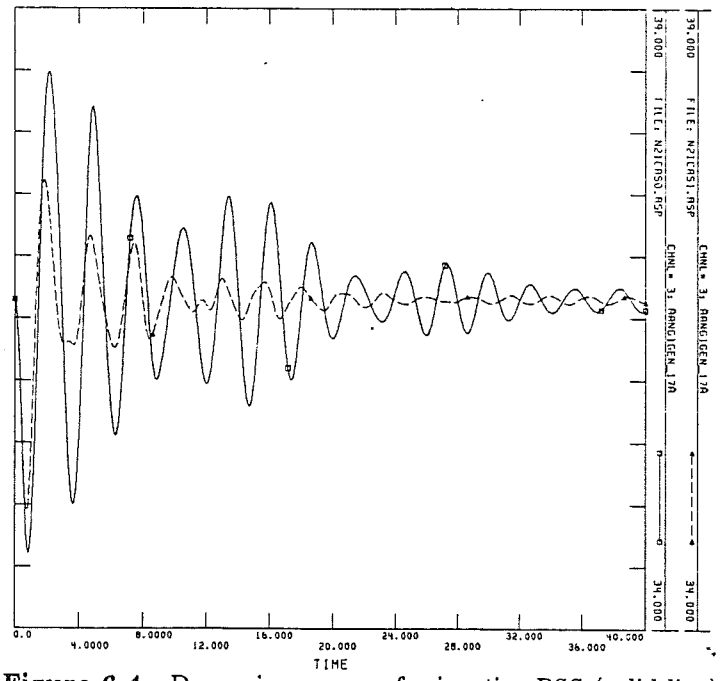

Figure 6.4 Dynamic response for inactive PSS (solid line) and active PSS (dashed line) of the machine, Gen_17, in northern Norway ($\alpha = 1.5$, Case 1).

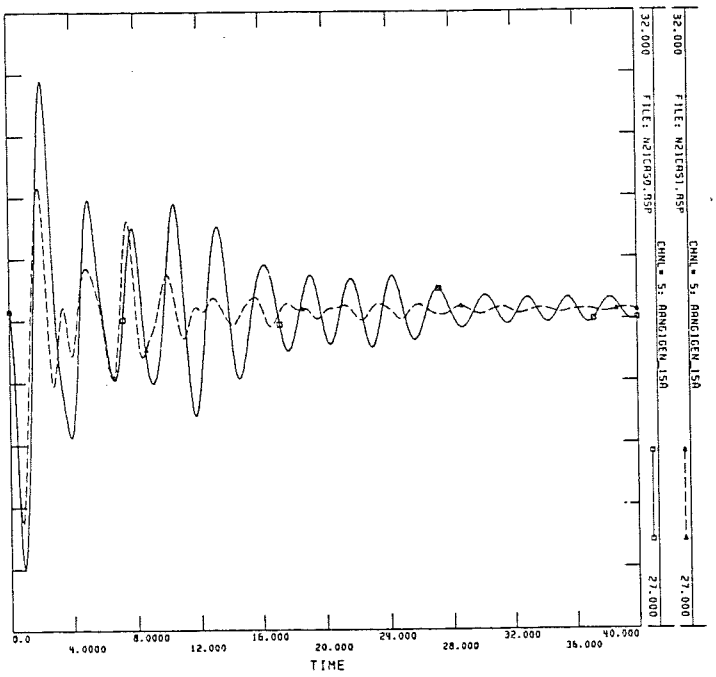

Figure 6.5 Dynamic response for inactive PSS (solid line) and active PSS (dashed line) of the machine, Gen_15, in northern Sweden ($\alpha = 1.5$, Case 1).

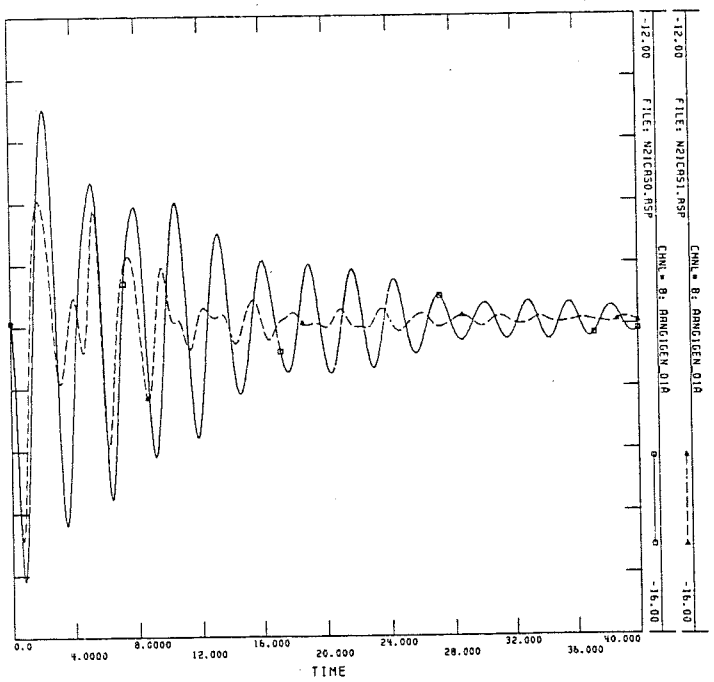

Figure 6.6 Dynamic response of the machine, Gen_01, in southern Sweden not equipped with any PSS ($\alpha = 1.5$, Case 1).

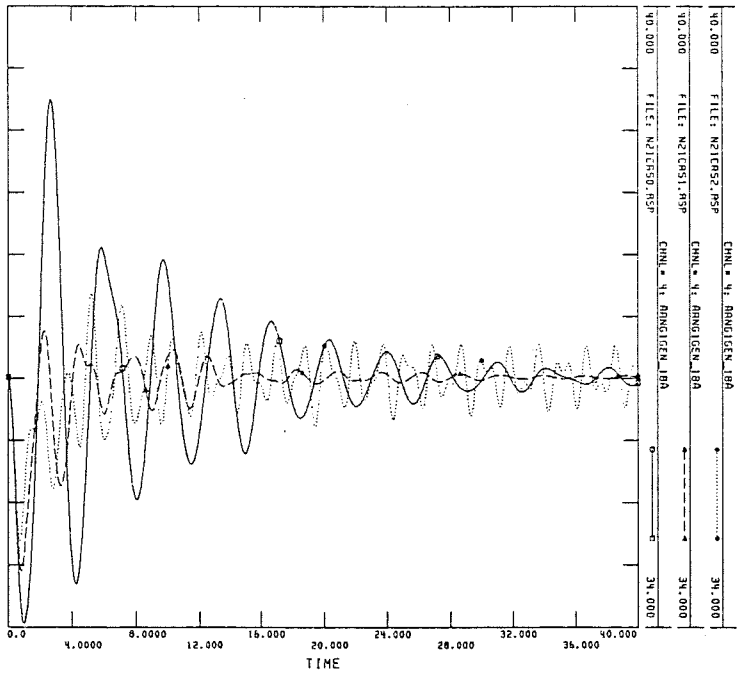

Figure 6.7 Dynamic response according to uncontrolled (solid line), controlled with optimal PSS (dashed line) and controlled with non-optimal PSS condition of the machine, Gen_18, in southern Finland ($\alpha = 1.5$, Case 1).

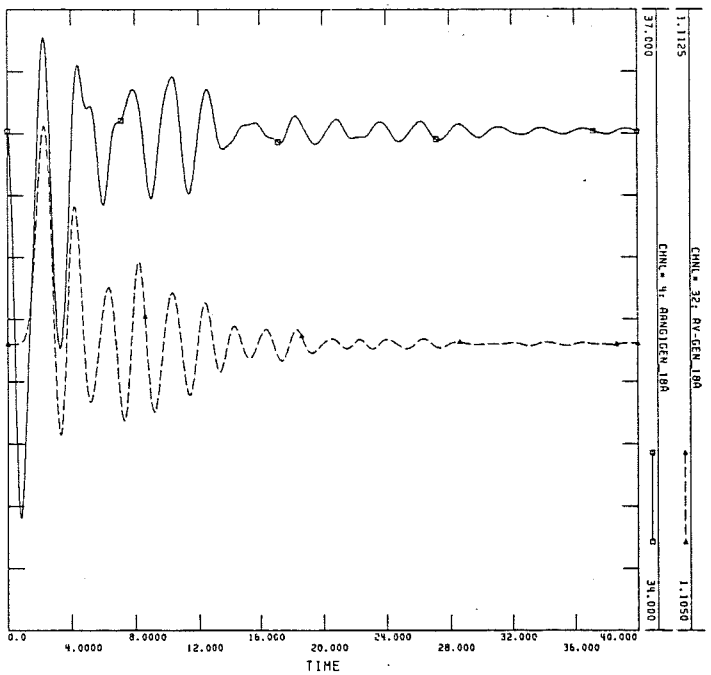

Figure 6.8 Dynamic response of the terminal voltage (dashed line) and the machine angle (solid line) for machine, Gen_18 (Bus #1267) ($\alpha = 1.5$, Case 1).

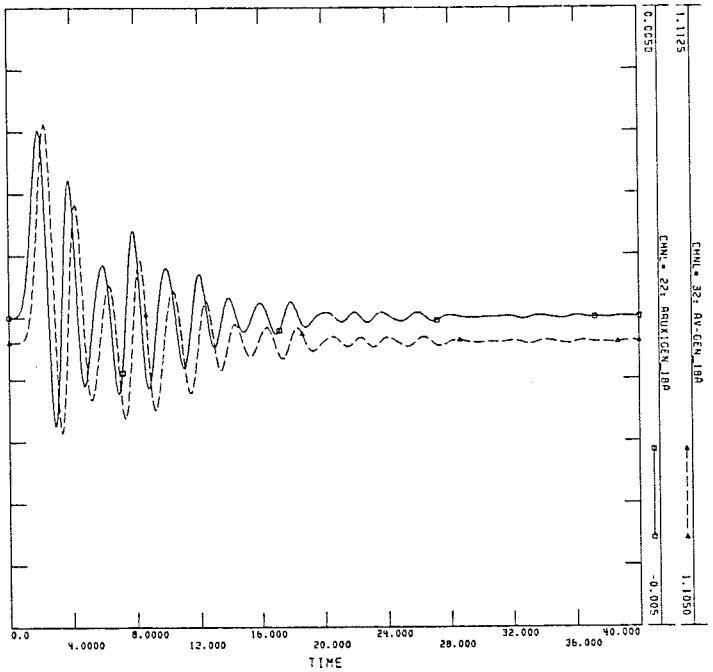

Figure 6.9 Dynamic response of the PSS output signal (solid line) and the terminal voltage (dashed line) for machine, Gen_18 (Bus #1267) ($\alpha = 1.5$, Case 1).

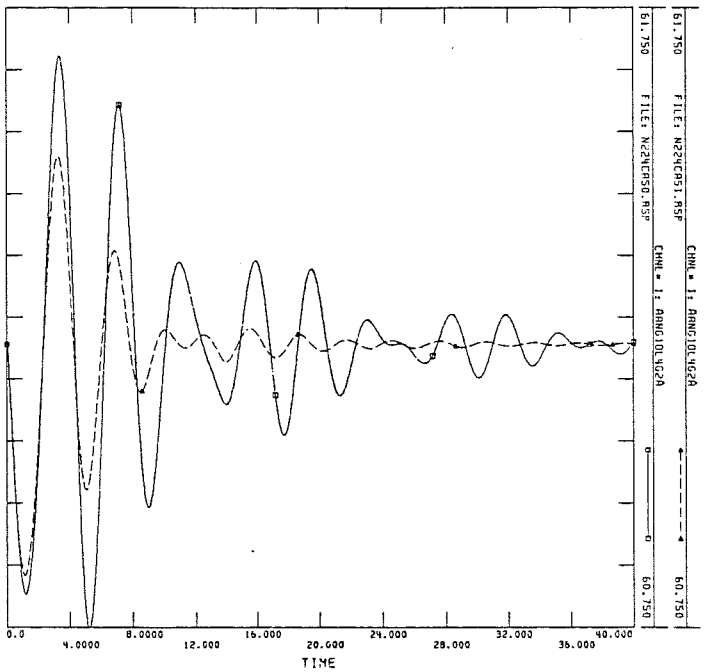

Figure 6.10 Dynamic response for inactive PSS (solid line) and active PSS (dashed line) of the machine, OL4G2, in south-western Finland ($\alpha = 1.5$, Case 3). Bus #18007.

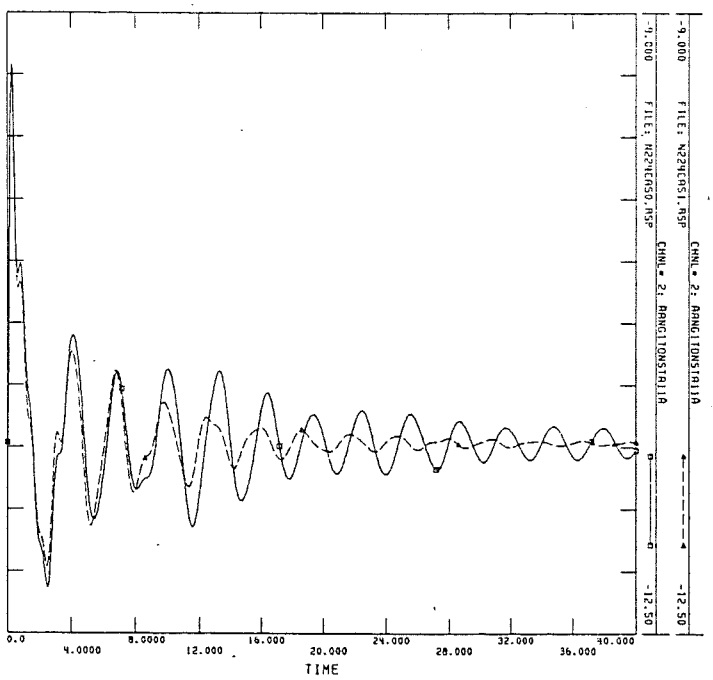

Figure 6.11 Dynamic response for inactive PSS (solid line) and active PSS (dashed line) of the disturbed machine in south-western Norway ($\alpha = 1.5$, Case 3). Bus #4100.

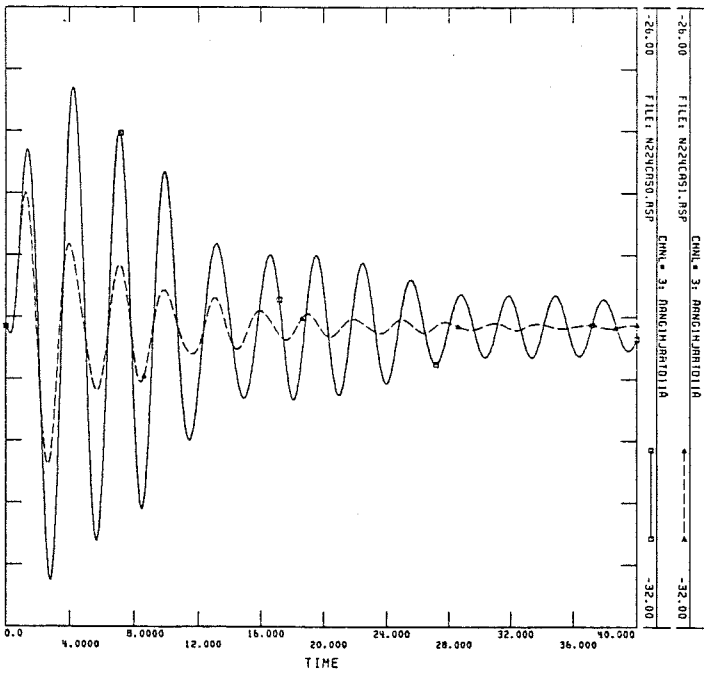

Figure 6.12 Dynamic response for inactive PSS (solid line) and active PSS (dashed line) of the machine, HJARTD11, in southern Norway ($\alpha = 1.5$, Case 3). Bus #1510.

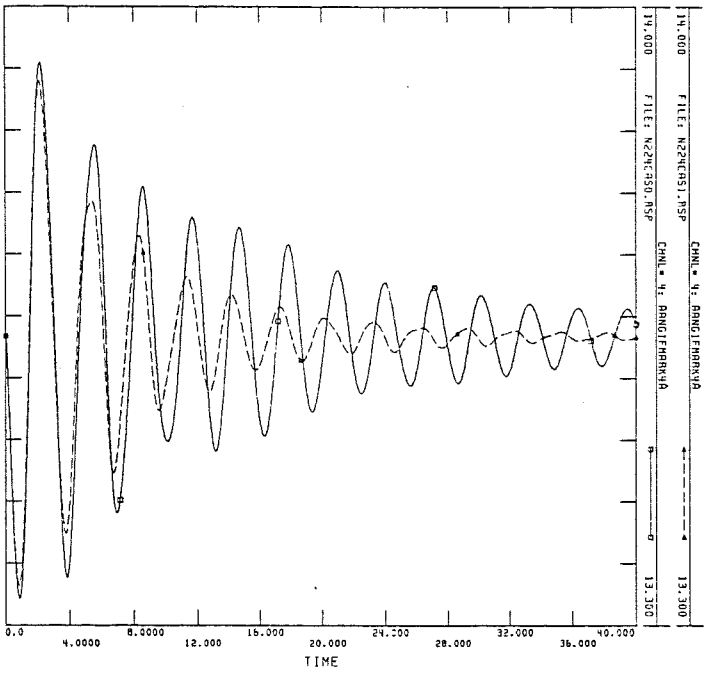

Figure 6.13 Dynamic response of the machine, FMARK4, in mid Sweden with no PSS ($\alpha = 1.5$, Case 3). Bus #20205.

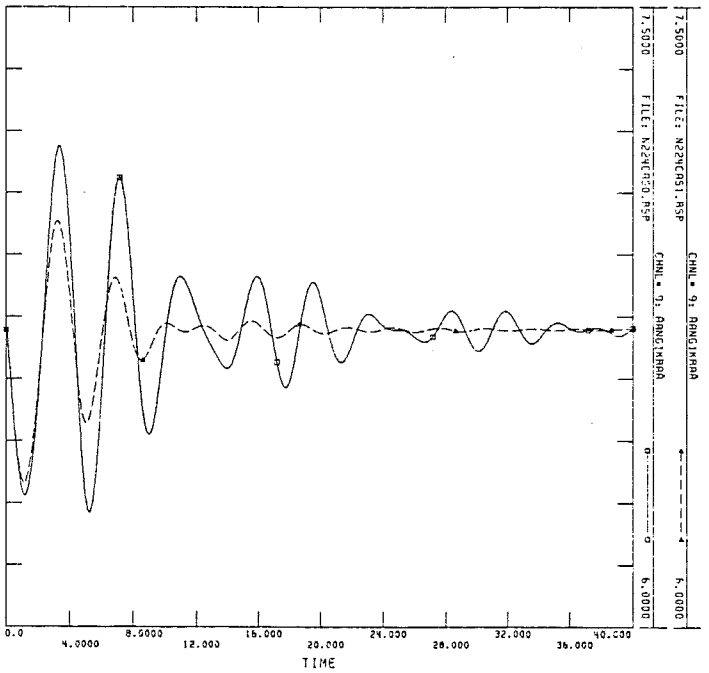

Figure 6.14 Dynamic response for inactive PSS (solid line) and active PSS (dashed line) of the machine, KRA, in southern Finland ($\alpha = 1.5$, Case 3). Bus #17051.

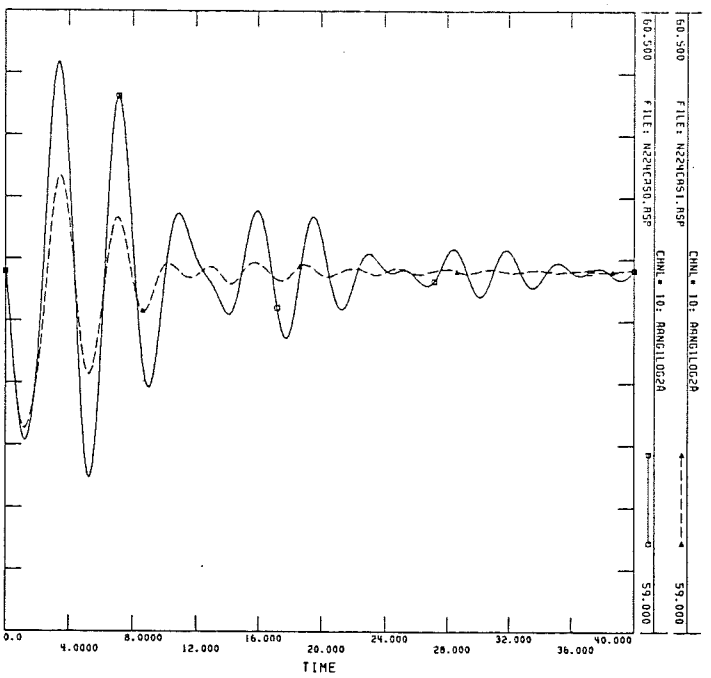

Figure 6.15 Dynamic response of the machine, LOG2, with no PSS ($\alpha = 1.5$, Case 3). Bus #18009.

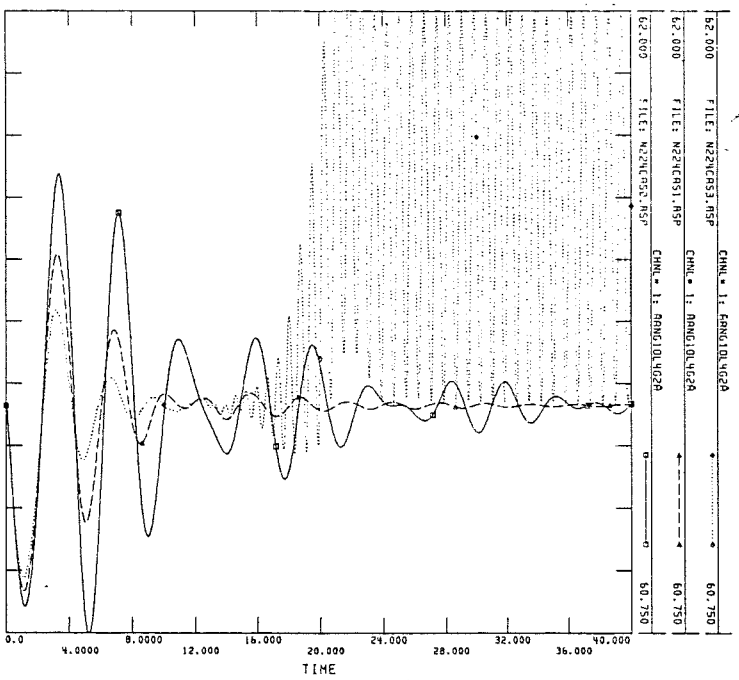

Figure 6.16 Dynamic response of the machine, OL4G2, for inactive PSS (solid line), active optimal PSS (dashed line) and active PSS with doubled value (dotted line) ($\alpha = 1.5$, Case 3). Bus #18006.

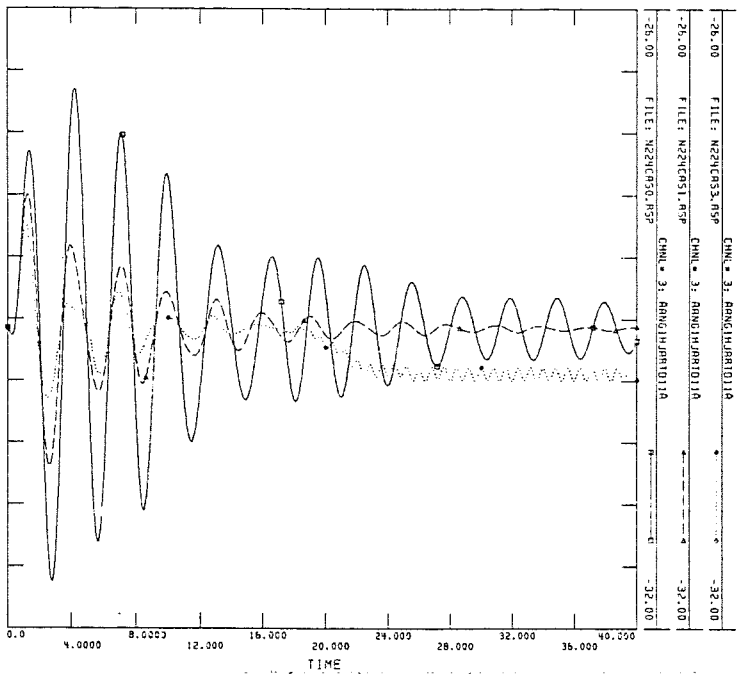

Figure 6.17 Dynamic response of the machine, HJARTD11, for inactive PSS (solid line), active optimal PSS (dashed line) and active PSS with doubled value (dotted line) ($\alpha = 1.5$, Case 3). Bus #1510.

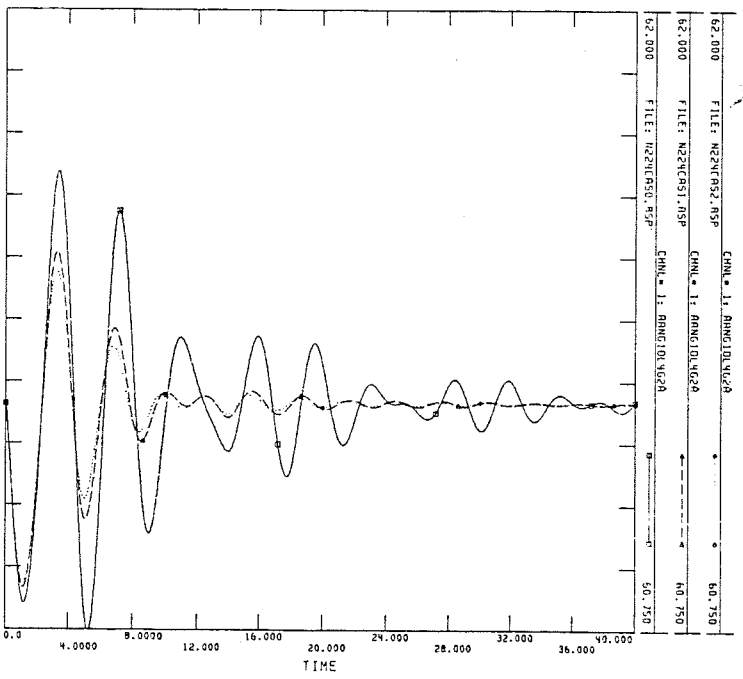

Figure 6.18 Dynamic response of the machine, OL4G2, for inactive PSS (solid line), active optimal PSS (dashed line) and active PSS with parameters corresponding to Fig. 5.9 ($\alpha = 1.0$, Case 3). Bus #18006.

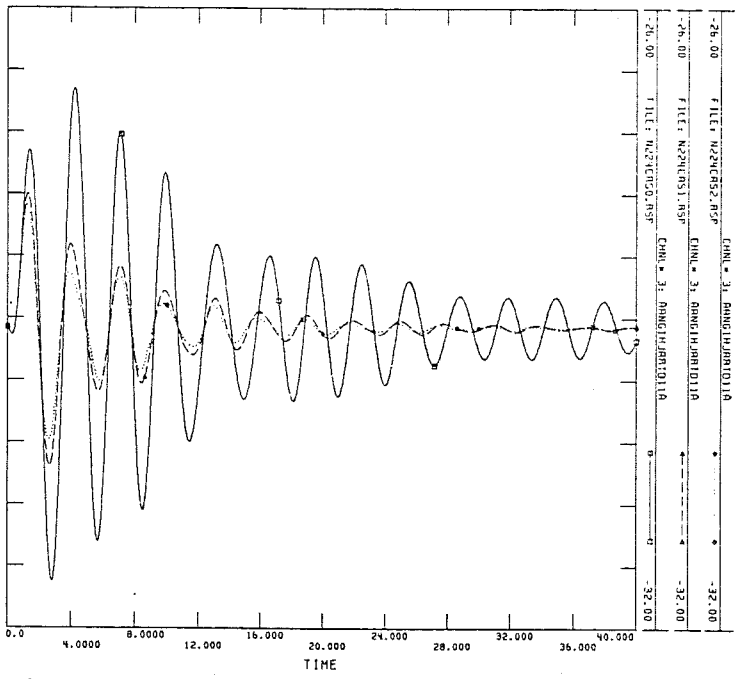

Figure 6.19 Dynamic response of the machine, HJARTD11, for inactive PSS (solid line), active optimal PSS (dashed line) and active PSS with parameters corresponding to Fig. 5.9 ($\alpha = 1.0$, Case 3). Bus #1510.

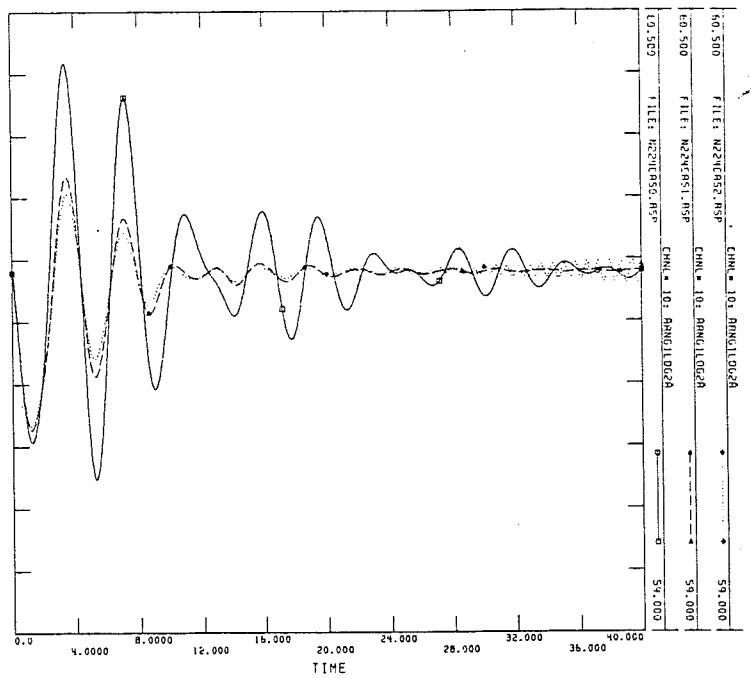

Figure 6.20 Dynamic response of the machine, LOG2, for inactive PSS (solid line), active optimal PSS (dashed line) and active PSS with parameters corresponding to Fig. 5.9 ($\alpha = 1.0$, Case 3). Bus #18009.

7

Summary

7.1 Model

The two-state model of the machines is enough to describe slow and system wide modes. The dynamics of the field winding, magnetization system and automatic voltage regulator were excluded from the model. The reason is that dynamics of the voltage control are much faster than the dynamics of slow and system wide modes. The dynamics of the governors are also excluded, because the dynamics of the fastest governors are 3 to 5 times slower than the dynamics of the slow modes. The result of the verification of the used model was good. An important advantage of the used model is the numerical checks of the value of eigenvalues and eigenvectors.

The model provides a technique to define slow and system wide modes. The model of the uncontrolled system matrix gives also an excellent fast procedure to calculate the left/right eigenvectors for the sensitivity analysis. The models also favors the slow modes because of the difference in stiffness for slow and fast modes. For the 224-machine model the stiffness of the slowest mode is ≈ 2 and the stiffness for the fastest mode is $\approx 10^5$ according to Eq. (2.21) (diagonal elements of $\tilde{K}$). With the control power available it will therefore only affect the slow modes.

7.2 Coherency

The definition of coherency is believed to be new. It has good preservation of the slow dynamics in large power systems. The major advantage is that the

definition does not depend on any excitation of the system. The hierarchy of models enables fast and reliable development and testing of programs.

Another basic idea was the possibilities to reduce the number of free parameters when coordinated tuning is performed.

7.3 Siting Analysis

The included damping equipments are Power System Stabilizers (PSSs), Static Var Compensators (SVCs) and High Voltage Direct Current links (HVDC).

To enhance the inherent damping of power systems due to generators and loads, a variety of stabilizer configurations can be used for the generators, SVCs and HVDC links. A study is made of how the overall damping matrix is built up from these contributions. This is used to develop a technique for systematic siting of damping equipment in power systems with several poorly damped modes in a given frequency window. This technique is applied to the Nordel system. Special emphasis is given to handling very large systems, voltage dependent loads and alternative measurement schemes.

The analysis also gave important information on where the damping equipment should be placed. Analytical expressions for siting of damping equipment are presented.

The PSSs shall be placed at sites with a net export of active power. In that case, the site is robust against voltage dependence of the load. More complicated expressions are derived for siting of SVCs.

The HVDC link will give positive contribution of damping if at least one of the frequency deviation signals are measured at either the inverter station or the converter station.

The most important results of this study are:

1. The voltage dependence of load has a major impact on the robust siting of PSSs and SVCs.
2. The calculated sites of PSSs and SVCs only concern slow and system wide modes.
3. Alternative measurement schemes are used for siting of SVCs and it is believed to be a new technique.
4. Alternative measurement schemes are also used to find the best point of measurement for a given site of a HVDC-link. This is also a new technique.
5. An analytical expression for robust siting of PSSs is derived according to the equations (4.15) and (4.16).

7.4 Coordinated Tuning and Verification of Augmented Damping

In these parts special emphasis is given to handle a large power system from optimization point of view. The verification shows the coordinated tuning result for 21, 44 and 224 machines. Existing techniques described in literature do not cover tuning of damping equipment in large power systems and especially not for slow and system wide modes.

The verification shows a good result concerning introduction of augmented damping in the slow and system wide modes.

The control law for the PSSs is very simple. A proportional controller with the bus frequency deviation as input is used.

The formulation of the optimization problem includes an important trade-off between actual export of power and the equivalent voltage dependence of the load at the PSSs-sites.

When the process gain is increased the parameter for the PSS is decreased. The optimization problem has no numerical instabilities and the used algorithm is extremely fast. It is a real MIMO-concept used for coordinated tuning of damping equipment in large power system.

The formulation of the optimization problem is new, at least when power systems are concerned. The choice of the constraint function was crucial for the damping of the slow modes. A qualitative explanation is also given.

7.5 New Contributions for Control and Tuning

The mathematical analysis of the structure of the system, minimum choice of states and inclusion of important system parameters are the key to success in doing this three stage analysis.

Many control people of today are working with ARMA-models and are losing insight to the physical behavior of a process. The physical analysis of the process is the key point to do any tuning and design in large power systems.

This thesis only treats the slow and system wide modes. These modes are known as the most troublesome to control and to damp. The verification of the augmented damping of the PSSs shows that a simple proportional controller using the frequency deviation as input is sufficient. For faster and local modes the active power is probably a better signal to use as input to the PSS.

The design of the PSS is not treated in detail in this thesis. The most important contribution from control point of view is the siting of damping equipment. The sites of the SVCs do really contribute with positive damping to the system. With conventional simulations it is a very time consuming thing to find proper sites for SVC equipment.

The formulation of the optimization problem works very well and the optimized parameters can be tuned for different voltage dependence of the load and different loadflows. This guarantees robust tuning. In the formulation of the optimization problem it is built in a natural trade-off between process gain of different areas and affected parameters for different sites. The optimization technique is new as far as the author knows.

7.6 Development of Software

Approximate 17 programs have been developed and tested. Fortran 77 is used in all programs. Number of lines written are approximate 43700, i.e. 10 000 to 15 000 Fortran statements. The largest load module is 5.7 megabytes, which cover 225 machines for siting of damping equipment.

The programs can be divided into three big groups:

1. Programs concerning coherency, mode presentation, verification of model, verification of coherency and graphic. Number of lines for these 7 programs are approximately 13350.
2. Programs concerning sensitivity derivatives in general, optimal siting of PSSs and SVCs, best points of measurement for HVDC links and verification programs. Number of lines for these 5 programs are approximately 22620.
3. Programs concerning the optimization. Number of lines for these 5 programs are approximately 7720.

7.7 Future Work

The author believes that two operational modes have to be considered for a robust PSS. In the high frequency range of oscillations it is also quite easy to exclude the slow disturbance from the mechanical torque.

For local and slow modes probably a Kalman filter should be used for estimation of the mechanical torque.

This means that a PSS with two input signals, frequency deviation and electric power, should be designed. One control mode is taking care of slow and system wide modes and the other control mode of the rest. The two modes can work in parallel, but there ought to be also a choice of one of the modes. One mode should take care of local oscillations, i.e. a certain frequency window has to be defined. One mode should take care of slow and system wide modes. If a machine participate in both slow local modes and slow system wide modes, it should be dedicated for one of the tasks. Other machines have to take care of the rest, because there always exist combinations of machines with opposite swing directions.

This thesis shows that the bus frequence deviation is a good signal to use for slow and system wide modes. This is also indicated by Larsen and Swann (1981), Part II. They also indicate that measurement of the power of the machine is good for local modes ($\geq$ 0.9 Hz). This is also emphasized by de Mello *et al.* (1980). The troublesome part, though, is the variation in the mechanical torque. The terminal frequency deviations at the machine might be a very good signal to use in this case. At least it works very well for slow and system wide modes.

The structure and properties of the damping matrix, $\tilde{D}$, in the system equations (5.1) is of great interest to study. It must be of great importance to find control structures and being able to show that the $\tilde{D}$-matrix is positive definite for a chosen frequency range. Transfer of measured values between dedicated machines must also be introduced in order to have the freedom to choose appropriate control structures.

8

References

Abdalla, O. H., S. A. Hassan and N. T. Tweig (1984): "Coordinated Stabilization of a Multimachine Power System," *IEEE Trans. Power Apparatus and Systems*, **PAS-103**, No 3, 483–492.

Andersson and Böiers (1984): *Ordinära Differentialekvationer*, Lunds Universitet, Matematiska institutionen, Lund, Sweden..

Anderson, P. M., and A. A. Fouad (1977): *Power System Control and Stability*, The Iowa State University Press, Ames, Iowa.

Akke, M. (1989): "Power System Stabilizers in Multimachine Systems," Lic Tech Thesis TFRT-3201, Department of Automatic Control, Lund Institute of Technology, Lund, Sweden.

Arnautovic, D., and J. Medanic (1987): "Design of Decentralized Multivariable Excitation Controllers in Multimachine Power System by Projective Controls," *IEEE Trans. Energy Conversion*, **EC-2**, Dec, 598–604.

Åström, K. J., and B. Wittenmark (1984): *Computer Controlled Systems*, Prentice-Hall, Englewoods Cliffs, New Jersey.

Bergen, A. R., and D. J. Hill (1981): "A Structure Preserving Model for Power System Stability Analysis," *IEEE Trans. Power Apparatus and Systems*, **PAS-100**, No 1, 25–35.

Brockett, R. W. (1970): *Finite Dimensional Linear Systems*, John Wiley and Sons, Inc, New York, USA.

Castro, J. C. *et al.* (1988): "Identification of Generating Units to be Equipped

with Stabilizers in a Multimachine Power System," *Automatica*, **24**, No 3, 405–409.

Chow, J. H., and J. J. Sanchez-Gasca (1989): "Pole-Placement Designs of Power System Stabilizers," *IEEE Trans. Power Systems*, **4**, 271–276.

Dahlquist, S. (1987): "Optimal Coordinated Tuning of Stabilizers in Power Systems," Report TFRT-5361, Department of Automatic Control, Lund Institute of Technology, Lund, Sweden, Department of Automatic Control, Lund Institute of Technology, Lund, Sweden.

deMello, F. P., and C. Concordia (1969): "Concepts of Synchronous Machine Stability as Affected by Excitation Control," *IEEE Trans. Power Apparatus and Systems*, **PAS-88**, Apr, 316–329.

deMello, F. P., and T. F. Laskowski (1975): "Concepts of Power System Dynamic Stability," *IEEE Trans. Power Apparatus and Systems*, **PAS-94**, No 3, 827–833.

deMello F. P., P. J. Nolan, T. F. Laskowski and J. M. Undrill (1980): "Coordinated Application of Stabilisers in Multimachine Power Systems," *IEEE Trans. Power Apparatus and Systems*, **PAS-99**, No 3, 892–901.

Dennis, J. E., Jr., and J. J. More (1977): "Quasi-Newton Methods, Motivation and Theory," *SIAM Review*, **19**, 46–89.

Dennis, J. E., Jr., and R. B. Schnabel (1981): "A New Derivation of Symmetric Positive Definite Secant Updates," in O. L. Mangasarian, R. R. Meyer, and S. M. Robinson (Eds.): *Nonlinear Programming 4*, Academic Press, London and New York, pp. 167–199.

Dennis, J. E., Jr., and R. B. Schnabel (1983): *Numerical Methods for Unconstrained Optimization and Nonlinear Equations*, Prentice-Hall Inc, Englewood Cliffs, New Jersey.

Edström, A. (1985): "Dynamic Equivalents for Stability Studies," Swedish Power State Board, Stockholm, Sweden.

Elgerd, O. I. (1971): *Electrical and Electronic Engineering*, McGraw-Hill Book Company, New York.

Elgerd, O. I. (1983): *Electric Energy Systems Theory*, Tata McGraw-Hill, New Delhi.

Eliasson, B. E. (1988): "A New Coherent Approach of Generators for Investigation of Slow and System Wide Oscillations in Large Power Systems," Report PDS-8808-26, Sydkraft AB.

Eliasson, B. E. (1989a): "Sensitivity and Siting Studies of Damping in Nordel

Power Systems," Technical report PDS-8903-31, Sydkraft AB, Malmö, Sweden.

Eliasson, B. E. (1989b): "Coordinated Tuning, Design and Verification of Augmented Damping in the Nordel Power System," Report PDS-8907-17, Sydkraft AB, Malmö, Sweden.

Eliasson, B. E., and D. J. Hill (1989): "Damping Structure in Power Systems," Technical report PDS-8903-29, Sydkraft AB, Malmö, Sweden.

Faddeev, D. K., and V. N. Faddeeva (1963): *Computational Methods of Linear Algebra*, W.H. Freeman and Company, San Francisco.

Fletcher, R. (1981): *Practical Methods of Optimization, Vol 2, Constrained Optimization*, John Wiley and Sons, New York and Toronto.

Franksen, O. E. (1967): *System Structures in Engineering*, Dept of Electric Power Engineering, DTH, Lyngby, Denmark.

Friedland, B. (1986): *Control System Design*, McGraw-Hill, New York.

Fujiwara, R., S. Abe, and S. Takeda (1981): "Dynamic Stability Improvement of Power System by Means of Static Var System," *Electrical Engineering in Japan*, **101**, 119–126.

Gallai, A. M. and R. J. Thomas (1982): "Coherency Identification for Large Electric Power Systems," *IEEE Trans. Circuits and Systems*, **CAS-29**, No 11, 777–782.

Geeves, S. (1988): "A Model-Coherency Techniqe for Deriving Equivalents," *IEEE Trans. Power Apparatus and Systems*, **PAS-3**, No 1, 44–51.

Germod, A. J., and R. Podmore (1978): "Dynamic Aggregation of Generating Unit Models," *IEEE Trans. Power Apparatus and Systems*, **PAS-97**, 1060–1069.

Gill, P. E., W. Murray, and M. H. Wright (1981): *Practical Optimization*, Academic Press, London and New York.

Gill, P. E., W. Murray, M. A. Saunders, and M. H. Wright (1986): "Some Theoretical Properties of an Augmented Lagrangian Merit Function," Technical Report SOL 86-6R, Department of Operations Research, Stanford University.

Goldstein, H. (1970): *Classical Mechanics*, Addison-Wesley, Inc, Reading, Mass.

Golub, G. H., and C. F. Van Loan (1983): *Matrix Computations*, The John Hopkins University Press, Baltimore, Maryland.

Halmos, P. R. (1968): *Finite-Dimensional Vector Spaces*, D. Van Nostrand Company, Inc, Princeton, New Jersey.

Heffron, W. G., and R. A. Phillips (1952): "Effect of Modern Amplidyne Voltage Regulator on Underexcited Operation of Large Turbine Generators," *AIEE Trans. Power Apparatus and Systems*, **VOL-71**, Aug, 692–697.

Hill, D. J., and T. S. Bhatti (1987): "A Multimachine Heffron-Phillips Model for Power Systems with Frequency and Voltage Dependent Loads," Technical report EE8739, Department of Electrical and Computer Engineering, University of Newcastle, Australia.

Kailath, T. (1980): *Linear Systems*, Prentice-Hall, Englewood Cliffs, New Jersey.

Kinoshita, H. (1979): "Improvement of Power System Dynamic Stability by Static Shunt Var System," *Electrical Engineering in Japan*, **99**, 81–88.

Larsen, E. V., and D. A. Swann (1981): "Applying Power System Stabilizers – Parts I, II, III," *IEEE Trans. Power Apparatus and Systems*, **PAS-100**, No 6, 3017–3046.

Ledwich, G. (1983): "Control Algorithms for Shunt VAR Systems," *Electric Power Systems Research*, **6**, 141–146.

Ledwich, G., and T. Jordan (1982): "Placement of Shunt VAR Systems," *Electric Power Systems Research*, **5**, 299–306.

Lefebvre, S. (1983): "Tuning of Stabilizers in Multimachine Power Systems," *IEEE Trans. Power Apparatus and Systems*, **PAS-102**, No 2.

Luenberger, D. G. (1984): *Linear and Nonlinear Programming*, Addison-Wesley, Reading, Mass.

Lysfjord, T. *et al.* (1982): "Förbättrad dämpning av effektpendlingar i Nordelnätet genom optimering av inställbara reglerparametrar för dämptillsatser," Report 1982-06-15, NORDEL.

NAG, Fortran Library – Mark 13 (1988): "Volumes 3 and 4," Nag Ltd, Wilkinson House, Jordan Hill Road, Oxford, UK.

Nolan, P. J., N. K. Sinha and R. T. H. Alden (1976): "Eigenvalue Sensitivities of Power Systems Including Network and Shaft Dynamics," *IEEE Trans. Power Apparatus and Systems*, **PAS-95**, No 4, 1318–1324.

Oshawa and M. Hayashi (1978): "Coherency Recognition for Transient Stability Equations using Lyapunov Function," *IPC Sci Technol Press, Guildford, Surrey, England*, 815–818.

Padiyar, K. R., M. A. Pai and C. Radhakrishna (1981): "A Versatile System Model for the Dynamic Stability Analysis of Power Systems Including HVDC Links," *IEEE Trans. Power Apparatus and Systems*, **PAS-100**, No 4, 1871–1879.

Padiyar, K. R., and C. Radhakrishna (1986): "Dynamic Stabilization of Power Systems through Reactive Power Modulation," *Electric Machines and Power Systems*, **11**, 281–293.

Podmore, R. (1978): "Identification of Coherent generators for Dynamic Equivalents," *IEEE Trans. Power Apparatus and Systems*, **PAS-97**, 1344–1354.

Powell, M. J. D. (1974): "Introduction to Constrained Optimization," in P. E. Gill and W. Murray (Eds.): *Numerical Methods for Constrained Optimization*, Academic Press, London and New York, pp. 1–28.

Rudnick, H., F. M. Hughes and A. Brameller (1983): "Steady State Instability: Simplified Studies in Multimachine Power Systems," *IEEE Trans. Power Apparatus and Systems*, **PAS-102**, No 12, 3859–3867.

Siwakumar, S., A. M. Sharaf and H. G. Hamed (1985): "Coordinated Tuning of Power System Stabilizers in Multimachine Power Systems," *Electric Power Systems Research*, No 8, 275–284.

Uhlhorn, U. (1986): *Analytic Mechanics*, Dept. of Mechanics, LTH, Lund, Sweden.

Vournas, C. D., and R. J. Fleming (1978): "Generalisation of the Heffron-Phillips Model of a Synchronous Generator," *IEEE PES Summer Meeting*, paper A 78 534-0, Los Angeles.

Vournas, C. D., and B. Papadias (1987): "Power System Stabilization via Parameter Optimization – Application to the Hallenig Interconnected System," *IEEE Trans. Power Systems*, **PWRS-2**, No 3, 615–623.

Wilkinson, J. H. (1965): *The Algebraic Eigenvalue Problem*, Oxford University Press, London.

Wilson, W. J., and J. D. Aplevich (1986): "Coordinated Governor/Exciter Stabilizer Design in Multi-Machine Power Systems," *IEEE Trans. Energy Conversion*, **EC-1**, Sep, 61–67.

Wu, F. F., and C.-C. Liu (1986): "Characterization of Power System Small Disturbance Stability with Models Incorporating Voltage Variation," *IEEE Trans. Circuits and Systems*, **CAS-33**, No 4, 406–417.

Wu, F. F., and N. Narasimhamurthi (1983): "Coherency Identification for Power System Dynamic Equivalents," *IEEE Trans. Circuits and Systems*, **CAS-30**, No 4, 140–147.

Young, H. *et al.* (1988): "Observable Island Identification for State Estimation Using Incidence Matrix," *Automatica*, **Vol 24**, No 1, 71–75.

Yu, Y. N. (1983): *Electric Power System Dynamics*, Academic Press, New York.

Zhou, R. J. *et al.* (1985): "Coherency Analysis of Large Electric Power Systems," *IREE Aust. Journal of Electrical and Electronics Engineering Australia*, **Vol 5**, No 1, 92–99.

A

Basic Multimachine Model

In this appendix, the basic multimachine model is derived. The steps taken in deriving the model are similar to less general exercises carried out in Bergen and Hill (1981) and Wu and Liu (1986).

Suppose there are m generators which are interconnected by a network of transmission lines and transformers. The network has a total of n buses. The $n-m$ buses without generation only have power injection from loads. Let the generator terminal buses be numbered as $i = 1, \ldots m$ and the load buses as $i = m+1, \ldots n$. Let δ_j be the rotor angle of the j:th generator with respect to a synchronously rotating reference frame. Then $\omega_j = \dot{\delta}_j$ is the frequency deviation from the synchronous frequency.

The dynamics of each generator is given by the swing equation

$$M_i \frac{d\omega_i}{dt} + D_i\omega_i = P_{m_i} - P_{gi} \tag{A.1}$$

where M_i is the inertia constant, D_i the damping coefficient, P_{m_i} the mechanical power input and P_{gi} is the electrical power generated. To simplify calculation of P_{gi}, we make a number of assumptions:

1. The network is assumed to be in sinusoidal steady-state with transmission lines represented by series impedances.
2. Each generator is modeled as an internal voltage source E'_j behind a transient reactance X'_{dj}.

3. The phase angle of the internal machine voltage E_i' coincides with the rotor angle δ_i.
4. The powers P_{mi} are constant.
5. The transmission lines are assumed to be lossless.
6. The loads are modeled as real and reactive power demands which are a function of the magnitude of the bus voltage.
7. Q_{ei} is a known characteristic of the excitation system.

Assumptions 1–5 are standard in simplified models for power system stability analysis, see Anderson and Fouad (1977). The generator model is often further simplified to a constant voltage $|E_i'|$ behind transient reactance. The present model is motivated by problems which are caused by the use of fast excitation systems. These attempt to regulate the terminal voltages to set values via fast changes in $|E_i'|$.

Assumption 4 requires that the frequency control system occupies a different (lower in practice) bandwidth than the voltage control system. This is not always the case, but seems to be the preferred situation.

It is also common to simplify the model by assuming the loads are impedances. In general the load powers are nonlinear functions of frequency and voltage of the load bus. The frequency dependence of loads is often neglected. This practice will be followed here according to Assumption 6.

From Assumption 1, there are four variables to consider at each network bus, namely, the voltage magnitude $|V_i|$, the voltage phase angle θ_i, the real power injection P_i and the reactive power injection Q_i. Let $\delta = \left[\delta_1, \delta_2, \ldots, \delta_m\right]^t$, $|E'| = \left[|E_1'|, |E_2'|, \ldots, |E_m'|\right]^t$, $\theta = \left[\theta_1, \theta_2, \ldots, \theta_n\right]^t$, and $|V| = \left[|V_1|, |V_2|, \ldots, |V_n|\right]^t$. It is useful to write $|V| = \left[|V_g|^t |V_l|^t\right]$, where V_g denotes generator terminal voltages and V_l the load bus voltages.

In the formulation of models it is sometimes convenient to regard the internal generator voltages E_j' as corresponding to fictitious network buses in an augmented network (Bergen and Hill, 1981). These are then numbered $i = n+1, \ldots, n+m$ and $V_i = E_{i-n}'$, $i = n+1, \ldots, n+m$. We use the notation $|V_a| := \left(|V|, |E|\right)$ and $\delta_a := (\delta, \theta)$.

From Assumptions 1 and 5 all transmission lines are represented as pure reactances. Thus in the overall augmented network all buses are conneted by reactances. (Assumption 2 gives that each fictitious bus is attached to a generator terminal bus through the transient reactance.) Let the bus admittance matrix for the transmission network and the augmented network by Y and Y_a, respectively. Y_a is obtained from Y in the form

$$Y_a = \begin{pmatrix} Y & 0 \\ 0 & 0 \end{pmatrix} + Y_d$$

where Y_d has every row (and column) containing the terms $\pm j(1/X'_{dj})$ in the pattern of an admittance matrix. Both Y and Y_a are purely imaginary with Y having elements $Y_{ij} = jB_{ij}$, where B_{ij} is the susceptance between buses i and j.

At each bus, real and reactive power is exchanged between some of the generators, loads and/or transmission lines. At an internal generator bus, we have real power balance given by (A.1) with

$$P_{gi}(\delta, \theta, |V|) = \frac{|E'_i|\,|V_i^0|}{X'_{di}} \sin(\delta_i - \theta_i) \tag{A.2}$$

The reactive power balance is given by

$$Q_{gi}(\delta, \theta, |V|) + Q_{ei}(|E'_i|, |V_i|) = 0 \tag{A.3}$$

where Q_{ei} is the reactive power injected at the generator internal bus and Q_{gi} is given by

$$Q_{gi}(\delta, \theta, |V|) = \frac{|E'_i|\,|V_i^0|}{X'_{di}} \cos(\delta_i - \theta_i) - \frac{|V_i^0|^2}{X'_{di}} \tag{A.4}$$

If we adopt the classical model where the $|E'_i|$ are constant, the internal generator buses become PV buses in the usual load flow sense. In this case, the reactive power equation (A.3) is not needed. The terminal buses are PQ buses. For fast excitation systems, it makes more sense to require the terminal voltages $|V_g|$ to be constant (Wu and Liu, 1986). The terminal buses are then PV buses (with their reactive power injection to be determined).

The remaining network buses have no generation attached. The injected powers are determined by loads and control devices.

At each network bus, the injected powers are balanced by powers entering transmission lines. We use the augmented network view. Let P_{bi} and Q_{bi} denote the total real and reactive powers leaving the i:th bus via transmission lines. Then

$$\begin{aligned} P_{bi}(\delta_a, |V_a|) &= \sum_{j=1}^{n+m} |V_i|\,|V_j|\,B_{aij} \sin(\delta_i - \delta_j) \\ Q_{bi}(\delta_a, |V_a|) &= -\sum_{j=1}^{n+m} |V_i|\,|V_j|\,B_{aij} \cos(\delta_i - \delta_j) \end{aligned} \tag{A.5}$$

For specific bus types, these compact expressions can be rewritten in terms of δ, θ and so on. For instance, at a generator terminal bus, the real power balance is given by

$$\begin{aligned} P_i(\delta, \theta, |E'|, |V|) &= P_{bi}(\delta_a, |V_a|) \\ &= \frac{|E'_i|\,|V_i^0|}{X'_{di}} \sin(\theta_i - \delta_i) + \sum_{j=1}^{n} |V_i|\,|V_j|\,B_{ij} \sin(\theta_i - \theta_j) \\ & \qquad i = 1, 2, \ldots, m \end{aligned} \tag{A.6a}$$

where P_i is the nett power injected into bus i from loads and/or control devices. A similar expression for Q_i can be easily stated. At the remaining load buses, we have

$$P_i(\delta, \theta, |E'|, |V|) = \sum_{j=1}^{n} |V_i|\,|V_j|\,B_{ij}\sin(\theta_i - \theta_j) \qquad \text{(A.6b)}$$
$$i = m+1, \ldots, n$$

Combining (A.1), (A.3) and power balance at terminal and load buses, it is clear that a model can be written in the form

$$\begin{aligned} P_n(\delta, \theta, |E'|, |V|) &= P_1 \\ M_g\omega_g + D_g\omega_g + P_g(\delta, \theta, |E'|, |V|) &= P_2 \end{aligned} \qquad \text{(A.7)}$$

$$\begin{aligned} Q_n(\delta, \theta, |E'|, |V|) &= Q_1 \\ Q_g(\delta, \theta, |E'|, |V|) &= Q_2 \end{aligned} \qquad \text{(A.8)}$$

where $M_g = \text{diag}\{M_i\}$, $D_g = \text{diag}\{D_i\}$, $P_1 = [P_1, P_2, \ldots, P_m]^T$, and other terms are defined in the obvious way. P_n, Q_n refer to bus powers for network buses.

Now assume an operating point $(\delta^0, \theta^0, |E^{0\prime}|, |V^0|)$ is known. Suppose small deviations occur under the influence of small disturbances. At such an operating point, we have $\omega_g^0 = 0$ and (A.7), (A.8) reduce to standard load flow equations (for the augmented network). Since these equations have translational symmetry, it is standard to refer the angles to a reference which can be taken here as $\delta_m(= \delta_{an}) = 0$.

Small disturbance stability is studied via linearization of equations (A.7), (A.8) about the operating point. In setting up the linearized equations, we make use of the Jacobian J of the load flow equations. We have

$$\begin{pmatrix} P_{n\delta} & P_{n\theta} & \vdots & P_{ne} & P_{nv} \\ P_{g\delta} & P_{g\theta} & \vdots & P_{ge} & P_{gv} \\ \cdots & \cdots & \cdots & \cdots & \cdots \\ Q_{n\delta} & Q_{n\theta} & \vdots & Q_{ne} & Q_{nv} \\ Q_{g\delta} & Q_{g\theta} & \vdots & Q_{ge} & Q_{gv} \end{pmatrix} := \begin{pmatrix} J_{11} & J_{12} \\ J_{21} & J_{22} \end{pmatrix} \qquad \text{(A.9)}$$

where

$$P_{n\delta} = \frac{\partial P_n}{\partial \delta}$$

and so on in the obvious way. Then $J^0, P_{n\delta}^0$ etc denote these matrices evaluated at the operating point. The components of the various submatrices in J are

easily built up using (A.5) or (A.6). From (A.6), we see that elements of $P_{n\delta}$ are given by

$$J_{ij} = \begin{cases} -\dfrac{|E_i'||V_i^0|}{X_{di}'} \cos\left(\theta_i^0 - \delta_i^0\right) & ; \quad 1 \le i \le m, j = 1 \\ 0 & ; \quad \text{otherwise for } 1 \le i \le n, 1 \le j \le m \end{cases}$$

Now consider the block $P_{n\theta}$. The corresponding elements are given by (A.6) as

$$J_{ij} = \begin{cases} \dfrac{|E_i'||V_i^0|}{X_{di}'} \cos\left(\theta_i^0 - \delta_i^0\right) + \displaystyle\sum_{j=1}^{n} |V_i^0||V_j^0| B_{ij} \cos\left(\theta_i^0 - \delta_j^0\right) & ; \\ & 1 \le i \le m, j = 1 \\ \displaystyle\sum_{j=1}^{n} |V_i^0||V_j^0| B_{ij} \cos\left(\theta_i^0 - \delta_j^0\right) & ; \quad m+1 \le i \le n, j = 1 \\ |V_i^0||V_j^0| B_{ij} \cos\left(\theta_i^0 - \delta_j^0\right) & ; \quad \text{otherwise for } 1 \le i \le n, 1 \le j \le n \end{cases}$$

We should note that the nonzero terms in J are closely related to the network structure. They correspond to a physical connection between buses. The elements of J can clearly be expressed in a more compact way using (A.5). For instance, the submatrix J_{11} which relates real power to angles is given by

$$J_{ij} = \begin{cases} \displaystyle\sum_{j=1}^{n+m} |V_i^0||V_j^0| B_{aij} \cos\left(\delta_{ai}^0 - \delta_{aj}^0\right) & ; \quad i = j \\ -|V_i^0||V_j^0| B_{aij} \cos\left(\delta_{ai}^0 - \delta_{aj}^0\right) & ; \quad i \ne j \end{cases}$$

The linearized version of (A.7) and (A.8) can now be written as

$$P_{n\delta}\delta + P_{n\theta}\theta + P_{ne}|E'| + P_{nv}|V| = P_1 \qquad \text{(A.10a)}$$

$$M_g\dot{\omega}_g + D_g\omega_g + P_{n\delta}\delta + P_{n\theta}\theta + P_{ge}|E'| + P_{gv}|V| = P_2 \qquad \text{(A.10b)}$$

$$Q_{n\delta}\delta + Q_{n\theta}\theta + Q_{ne}|E'| + Q_{nv}|V| = Q_1 \qquad \text{(A.11a)}$$

$$Q_{g\delta}\delta + Q_{g\theta}\theta + Q_{ge}|E'| + Q_{gv}|V| = Q_2 \qquad \text{(A.11b)}$$

where $\delta, \theta, |E'|, |V|, \omega_g$ now refer to perturbations from the operating values. (For convenience of notation, we have not introduced new symbols for the perturbation variables.)

We now include the effect of nonlinear loads at the network buses. From Assumption 6, we can write

$$\begin{aligned} P_1 &= -N_1|V| + \tilde{P}_1 \\ Q_1 &= -N_2|V| \end{aligned} \qquad \text{(A.12)}$$

where $\tilde{P}_1$ refers to other real power sources at the buses. For example, suppose the load demand characteristics have the exponential form

$$P_{Li} = a_i|V_i|^{p_i}$$
$$Q_{Li} = b_i|V_i|^{q_i}$$

Then $N_1 = \text{diag}\left\{a_i p_i |V_i|^{p_i - 1}\right\}$ and $N_2 = \text{diag}\left\{b_i q_i |V_i|^{q_i - 1}\right\}$.

Substituting (A.12) into (A.10a), (A.11a) gives

$$\begin{pmatrix} P_{n\theta} & P_{nv} + N_1 \\ Q_{n\theta} & Q_{nv} + N_2 \end{pmatrix} \begin{pmatrix} \theta \\ |V| \end{pmatrix} = - \begin{pmatrix} P_{n\delta} & P_{ne} \\ Q_{n\delta} & Q_{ne} \end{pmatrix} \begin{pmatrix} \delta \\ |E'| \end{pmatrix} + \begin{pmatrix} \tilde{P}_1 \\ 0 \end{pmatrix} \quad \text{(A.13)}$$

We now consider the condition:

$$\text{The matrix } \begin{pmatrix} P_{n\theta} & P_{nv} + N_1 \\ Q_{n\theta} & Q_{nv} + N_2 \end{pmatrix} \text{ is nonsingular.}$$

Under this condition, (A.13) can be solved to yield $\theta, |V|$. On substitution into (A.10b), it is straightforward to check that this yields the form

$$M_g\dot{\omega}_g + D_g\omega_g + K_1\delta + K_2|E'| = P_2 + L\tilde{P}_1 := P_2^* \quad \text{(A.14)}$$

Note that the matrices K_1, K_2, and L can be readily obtained in practice from a linear load flow solution of the network.

In (A.14), we have maintained $|E'|$ as an independent input. Thus, it has the general character of a PV bus and equation (A.11b) is not used. Sometimes, we also need $|V|$ as a controlled variable. Then equation (A.11a) is also redundant. The condition of interest is then:

$$\text{The matrix } P_{n\theta} \text{ is nonsingular.}$$

The elements of $P_{n\theta}$ were given above. From equations (A.10), we obtain

$$M_g\dot{\omega}_g + D_g\omega_g + P_{g\delta}^*\delta + P_{ge}^*|E'| + P_{gv}^*|V| = P_2^* \quad \text{(A.15)}$$

where

$$\begin{aligned} P_{g\delta}^* &= P_{g\delta} - P_{g\theta}P_{n\theta}^{-1}P_{n\delta} \\ P_{ge}^* &= P_{ge} - P_{g\theta}P_{n\theta}^{-1}P_{ne} \\ P_{gv}^* &= P_{gv} - P_{g\theta}P_{n\theta}^{-1}P_{nv} \\ P_2^* &= P_2 - P_{g\theta}P_{n\theta}^{-1}P_1 \end{aligned} \quad \text{(A.16)}$$

The use of the notation K_1, K_2 in (A.14) is consistent with earlier discussion based on reduced network models. See deMello *et al.* (1980).

There are special cases of interest which simplify the models (A.14) and (A.15). One which we use later is suggested by Lysfjord et al. (1982). Suppose system reduction has been used and each M_i represents several generators in parallel. Then a reasonable approximation is to ignore the X'_{di} relative to other reactances. Further, each bus in the reduced system may have both generation and load attached. Then we have $\delta = \theta$ and $|E'| = |V|$. Model (A.15) can be simplified with

$$P^*_{g\delta} = P_{g\delta} \qquad P^*_{ge} = P_{ge}$$
$$P^*_{gv} = 0 \qquad P^*_2 = P_2$$

We henceforth refer to this case as the aggregation system model.

Of course, it may happen that some $|E'_i|$ and some $|V_i|$ are controlled by stabilisers. Then clearly parts of (A.11) and (A.10a) are to be solved. For simplicity, we will only give details here for the cases given above.

A further case of interest is where we allow for load frequency dependence. This has influence on the overall damping matrix. Then (A.12) are written

$$\begin{aligned} P_1 &= -N_1|V| - D_{lp}\omega_l + \tilde{P}_1 \\ Q_1 &= -N_2|V| - D_{lq}\omega_l \end{aligned} \tag{A.17}$$

where D_{lp}, D_{lq} are diagonal matrices corresponding to frequency dependence in real, reactive loads respectively. Each element of these matrices is taken to be nonzero. We suppose that load buses are not voltage controlled for simplicity. Substituting (A.17) into (A.10a), (A.11a) gives

$$\begin{pmatrix} D_{lp} & P_{nv} + N_1 \\ D_{lp} & Q_{nv} + N_2 \end{pmatrix} \begin{pmatrix} \omega_1 \\ |V| \end{pmatrix} = - \begin{pmatrix} P_{n\delta} & P_{n\theta} & P_{ne} \\ Q_{n\delta} & Q_{n\theta} & Q_{ne} \end{pmatrix} \begin{pmatrix} \delta \\ |\theta| \\ |E'| \end{pmatrix} + \begin{pmatrix} \tilde{P}_1 \\ 0 \end{pmatrix} \tag{A.18}$$

The relevant solvability condition is:

$$\text{The matrix } \begin{pmatrix} D_{lp} & P_{nv} + N_1 \\ D_{lq} & Q_{nv} + N_2 \end{pmatrix} \text{ is nonsingular.}$$

Under this condition, (A.18) can be solved to give $\omega_l, |V|$. We then have from (A.10)

$$\begin{aligned} D_{lp}\dot{\theta} + P^*_{n\delta}\delta + P^*_{n\theta}\theta + P^*_{ne}|E'| &= L_1\tilde{P}_1 := P^*_1 \\ M_g\dot{\omega}_g + D_g\omega_g + P^*_{g\delta}\delta + P^*_{g\theta}\theta + P^*_{ge}|E'| &= P_2 + L_2\tilde{P}_1 := P^*_2 \end{aligned} \tag{A.19}$$

where $P^*_{n\delta}$, other starred matrices, L_1 and L_2 are all derived from solving (A.18) and substitution. Clearly, θ is now a part of the system state.

If we need $|V|$ as independent variables, then set $N_1 = 0$, $N_2 = 0$ in (A.17); only the frequency dependent component of the loads is relevant. Then we have in place of (A.19)

$$\begin{aligned} D_{lp}\dot{\theta} + P_{n\delta}\delta + P_{n\theta}\theta + P_{ne}|E'| + P_{nv}|V| &= \tilde{P}_1 \\ M_g\dot{\omega}_g + D_g\omega_g + P_{g\delta}\delta + P_{g\theta}\theta + P_{ge}|E'| + P_{g\theta}|V| &= \tilde{P}_2 \end{aligned} \tag{A.20}$$

Typically, these equations would accommodate some network buses as controlled and others uncontrolled (regular load buses).

B

Orthogonality of the Eigenvectors of the model (KM)

The matrices K and M are defined according to Eq. (2.8). The following two statements are now going to be proved:

(1) K is positive semidefinite.

(2) The eigenvectors of the KM-model are K and M orthogonal.

LEMMA B.1
Consider the $n \times n$ symmetric $K \in R^{n \times n}$ matrix, where

$$k_{ij} = -\frac{V_i V_j}{x_{ij}} \cos(\theta_i - \theta_j) \leq 0 \quad \forall i \neq j = 1, \ldots, n$$

and

$$k_{ii} = -\sum_{i \neq j} k_{ij}$$

Then all the eigenvalues of K are real and greater than or equal to zero.

Proof: K is symmetric $\Longrightarrow$ real eigenvalues.

Let

$$\rho_i = \sum_{i \neq j}^{n} |k_{ij}|, \quad i = 1, \ldots, n$$

then, by using Geršgorin's theorem, every eigenvalue of K lies in a section

$$|x - k_{ii}| \leq \rho_i, \quad i = 1, \ldots, n$$

This specific $K \Longrightarrow x \geq 0$, because $k_{ii} = \rho_i$.
Thus K is positive semidefinite. □

Remark 1. The matrix, K, can be written as $A^T K_{prim} A$, where A is the arc-node incidence matrix of the net topology.
$K_{prim} = \text{diag}(-k_{12}, \ldots, -k_{1n}, \ldots, -k_{n-1,n})$. Ground is the datum node. All $-k_{ij}$, $(i < j = 2, \ldots, n)$ are ≥ 0 and $\in K$, i.e. all eigenvalues of K are ≥ 0. See also Franksen (1967) page 94. □

Remark 2. The stiffness matrix, K, can be written as the Hessian matrix, with respect to θ, of

$$F(\overline{V}, \overline{\theta}) = \frac{1}{2} \sum_{i=1}^{n} \sum_{j=1}^{n} \frac{V_i V_j}{x_{ij}} \cos(\theta_i - \theta_j)$$

The scalar function $F(\overline{V}, \overline{\theta})$ can be interpreted as a generalized energyfunction or Liapunov-function. For stable systems it holds that the hessian matrix must be positive semidefinite. See, e.g., Andersson and Böiers (1984), Åström and Wittenmark (1984), Yu (1983). □

LEMMA B.2
The eigenvectors of Eq. (2.11) (u is dropped)

$$(\lambda_i^2 M + K)\, u_i = \overline{0} \tag{B.1}$$

are K and M orthogonal.

Proof: The diagonal matrix, M, is positive definite according to Eq. (2.8). Let $s_i = -\lambda_i^2$. Thus

$$M^{-1} K\, \overline{u}_i = s_i\, \overline{u}_i \iff K\, \overline{u}_i = s_i\, M\, \overline{u}_i$$

Define $k(\overline{x}) = \overline{x}^T K\, \overline{x}$ and $m(\overline{x}) = \overline{x}^T M\, \overline{x}$, where $m(x)$ is positive definite. Let $(m_1, \ldots, m_n)$ be given positive real numbers. According to Cholesky decomposition and the spectral theorem (Halmos (1958), Gene *et al.* (1983)) there exist real constants $(k_1, \ldots, k_n)$ and an invertible $n \times n$-matrix, U, so that

$$U^T K U = k, \quad k = \text{diag}(k_1, \ldots, k_n) \tag{B.2}$$
$$U^T M U = m, \quad m = \text{diag}(m_1, \ldots, m_n) \tag{B.3}$$

or

$$\overline{u}_i^T K \overline{u}_j = k_i \delta_{ij}, \quad i, j = 1, \ldots, n \tag{B.4}$$
$$\overline{u}_i^T M \overline{u}_j = m_i \delta_{ij}, \quad i, j = 1, \ldots, n \tag{B.5}$$

which gives $s_i = \frac{k_i}{m_i}$.

According to Eqs. (B.2), (B.3) and (B.1) the matrix U contains the eigenvectors $\overline{u}_i$ as columns. Equations (B.4) and (B.5) proves the orthogonality statement. □

Properties of the Stiffness Matrix of a General Network

The matrix K_{22} is nonsingular for stable power systems. According to Lemma B.1 the stiffness matrix

$$K = \begin{pmatrix} K_{11} & K_{12} \\ K_{12}^T & K_{22} \end{pmatrix} \qquad \begin{matrix} \dim(K_{11}) = m \times m \\ \dim(K_{22}) = l \times l \end{matrix}$$

is symmetric and the quadratic form is positive semidefinite. Furthermore, the sum of the elements in each row and each column is zero and the rank of K is $m + l - 1$ for a properly connected network. Only one eigenvalue is zero. These properties of K imply that K_{22} is symmetric.

The matrix K_{22} concerns only the load areas, but all the load areas are connected via power lines to one or several generators. Assume now that the load areas are divided in q different areas with no direct interconnection. The load areas are naturally electrically connected via the generator nodes.

If we now select a proper sequence of numbering of the nodes within the load areas, we can block the matrix, K_{22}, into q invariant blocks. All the blocks have the same mathematical properties. The theory of invariant subspaces tells us that, if the restriction of K_{22} to block j is nonsingular, this implies that K_{22} is nonsingular.

The proof is therefore restricted to a general block (load area), K_{22}^j, except when all loads are radially connected to one or several generators. With radial load, we mean that the load area has no internal network.

From above we can write:

$$K_{22} = K_{22}^1 \oplus \ldots \oplus K_{22}^q$$

where $\dim(K_{22}^1) + \ldots + \dim(K_{22}^q) = l$. According to the property of K we can write each block of K_{22} as

$$K_{22}^j = K_0^j + \sum_{n_i=1}^{r_j} \sigma_{n_i}^j e_{n_i}^j (e_{n_i}^j)^T$$

The sequence n_i $(i = 1, \ldots, r_j)$ represents all the rows of K_{22}^j which have the sum of the row elements greater than zero. The vector, $e_{n_i}^j$, has the n_i:th element

equal to one and all other elements are zero. The value of $\sigma^j_{n_i}$ is greater than zero for all n_i.

The matrix K^j_0 has the same properties as the matrix K, i.e. rank $= l_j - 1$ (for dim ≥ 2), symmetric and positive semidefinite. We know that there exists T^j such that

$$(T^j)^T K^j_0 T^j = \text{diag}(K^j_{0_1}, \ldots, K^j_{0_{l_j-1}}, 0) \tag{B.6}$$

From (B.6) we can define the range of K^j_0 and the null space K^j_0 as:

$$R(K^j_0) = \text{span}\,\{T^j_1, \ldots, T^j_{l_j-1}\}$$
$$N(K^j_0) = \text{span}\,\{T^j_{l_j}\} = \text{span}\,\{(1, \ldots, 1)^T\}$$

where T^j_i is the i:th column of T^j. Equation (B.6) implies that

$$K^j_0 = \sum_{i=1}^{l_j-1} K^j_{0_i} T^j_i (T^j_i)^T$$

Now we can write K^j_{22} as

$$K^j_{22} = \sum_{i=1}^{l_j-1} K^j_{0_i} T^j_i (T^j_i)^T + \sum_{n_i=1}^{r_j} \sigma^j_{n_i} e^j_{n_i} (e^j_{n_i})^T$$

LEMMA B.3
For proper electrically connected and stable power systems the matrix, K_{22}, is nonsingular, where the stiffness matrix (K) of the general power system is

$$K = \begin{pmatrix} K_{11} & K_{12} \\ K^T_{12} & K_{22} \end{pmatrix}$$

Proof: If all loads are radially connected to certain generators, the matrix, K_{22}, is

$$K_{22} = \sum_{i=1}^{l} \sigma_i e_i e_i^T$$

where all σ_i:s are greater than zero. In this case we are through. In the general case we can block K_{22} into q invariant subspaces. For each subspace the following is valid:

$$K^j_{22} = K^j_0 + \sum_{n_i=1}^{r_j} \sigma^j_{n_i} e^j_{n_i} (e^j_{n_i})^T; \qquad \sigma^j_{n_i} > 0 \;\forall\; n_i,\; j = 1, \ldots, q$$

If we can prove that

$$\left(K_0^j + \sigma_{n_1}^j e_{n_1}^j (e_{n_1}^j)^T\right)^{-1} \ \exists$$

we are through.

Take $x^j \in R^{l_j}$ arbitrarily. We can write

$$x^j = x_R^j + x_N^j$$

where $x_R^j \in R(K_0^j)$ and $x_N^j \in N(K_0^j)$. We know from the property of K_{22} that, if $x_R^j \neq 0$, the quadratic form

$$(x_R^j)^T K_{22}^j x_R^j > 0 \qquad \text{and} \qquad (x_R^j)^T K_{22}^j x_N^j = 0$$

The interesting thing is the value of

$$(x_N^j)^T K_{22}^j x_N^j \quad \text{for} \quad x_N^j \neq 0$$

We can write

$$(x_N^j)^T K_{22}^j x_N^j = (x_N^j)^T K_0^j x_N^j + (x_N^j)^T \sigma_{n_1}^j e_1^j (e_1^j)^T x_N^j = 0 + (\beta_N^j)^2 \sigma_{n_1}^j > 0$$

where

$$x_N^j = \beta_N^j T_{l_j}^j; \qquad \beta_N^j \in R$$

This implies that

$$(x^j)^T K_{22}^j x^j > 0 \quad \forall \ x^j \neq 0$$

i.e., all the eigenvalues of K_{22}^j are greater than zero. This completes the proof. □

C

Notations

$\overline{a}$	$n \times 1$ vector $\in R^n$	
α_i	angular velocity of principle mode i	rad/s
D_i	damping internal generator i	p.u./(rad/s)
δ_i	angle of machine i	rad
δ_{i_j}	chroneckers delta	
E_i	voltage behind transient reactance of machine i	p.u.
E_{k_i}	kinetic energy for generator i at ω_0	Nm
H_i	inertia constant for generator i	s
m_{ii}	$= \frac{2H_i \cdot S_{r_i}}{\omega_0 S}$ mass of machine i	s/rad
$\overline{\nabla}_\omega$	nabla operator with respect to $\overline{\omega}$	
$\overline{\nabla}_\theta$	$= \left(\frac{\partial}{\partial\theta_1}, \frac{\partial}{\partial\theta_2}, \ldots, \frac{\partial}{\partial\theta_n}\right)$ nabla operator with respect to $\overline{\theta}$	
$\overline{\nabla}_V$	nabla operator with respect to $\overline{V}$	
ω_i	$= \frac{d\theta_i}{dt}$ angular velocity at bus i	rad/s
ω_0	rated electrical angular velocity	rad/s
P_{m_i}	mechanical power input to generator i	p.u. of S
S	system base	MVA
S_{g_i}	apparent power from generator i to bus i	p.u. of S
S_{g_i}	$= P_{g_i} + j\,Q_{g_i}$	
S_i	apparent injection to the net at bus i	p.u. of S
S_i	$= P_i + j\,Q_i$	
S_{L_i}	complex load at bus i	p.u. of S
S_{L_i}	$= P_{L_i} + j\,Q_{L_i}$	
S_{r_i}	rated apparent power for generator i	MVA
θ_i	phase angle of voltage at bus i	rad
V_i	absolute value of voltage at bus i	p.u. of V_{bas}

X_{ij}	series reactance of power line between bus i and j	p.u. ohm
Z_{bas}	base impedance V_{bas}^2/S	ohm

We define

$$\partial_\theta(\overline{a}) = \frac{\partial(\overline{a})}{\partial\theta} \triangleq \left(\frac{\partial a_i}{\partial\theta_j}\right); \quad \text{Jacobian matrix}$$

Subscript '0' indicates the quantities evaluated at the equilibrium point.

D

Calculation of the Gradient and the Jacobian Matrix

D.1 The Gradient of the Objective Function

In this section we derive the gradients analytically which are used by numerical algorithms. Equation (5.1) gives

$$\operatorname{tr}(A) = -\operatorname{tr}(M^{-1}\tilde{D})$$

where

$$\tilde{D} = T_s^{\mathrm{DC}} K_{\mathrm{DC}} (T_m^{\mathrm{DC}})^T - BK_{se} - BT_s^{\mathrm{SVC}} K_{\mathrm{SVC}} (T_m^{\mathrm{SVC}})^T$$

A variation analysis of $\operatorname{tr} A$ with respect to the parameters gives:

$$\delta(\operatorname{tr} A) = -\operatorname{tr} \delta(M^{-1}\tilde{D}) = -\operatorname{tr} M^{-1}(\delta(\tilde{D})) \tag{D.1}$$

Finally,

$$\delta(\tilde{D}) = T_s^{\mathrm{DC}} \delta(K_{\mathrm{DC}})(T_m^{\mathrm{DC}})^T - B\delta(K_{se}) - BT_s^{\mathrm{SVC}} \delta(K_{\mathrm{SVC}})(T_m^{\mathrm{SVC}})^T$$

Equation (D.1) becomes

$$\delta(\operatorname{tr} A) = -\operatorname{tr}\Big(M^{-1}\big(T_s^{\mathrm{DC}}\delta(K_{\mathrm{DC}})(T_m^{\mathrm{DC}})^T - B\delta(K_{se}) - BT_s^{\mathrm{SVC}}\delta(K_{\mathrm{SVC}})(T_m^{\mathrm{SVC}})^T\big)\Big) \tag{D.2}$$

The partial derivative with respect to K_{se_i}:

$$\frac{\partial(\operatorname{tr} A(\Theta))}{\partial K_{se_i}} = \operatorname{tr}\left\{M^{-1}\begin{pmatrix} 0 & \dots & B(1,i) & \dots & 0 \\ \vdots & & \vdots & & \vdots \\ 0 & \dots & B(n,i) & \dots & 0 \end{pmatrix}\right\} \tag{D.3}$$

The gradient restricted to the HVDC-parameters: Assume that the rectifier is placed at bus i and the measurement of $\Delta\omega$ takes place at bus l. Furthermore, assume that the inverter is placed at bus j and the measurement of $\Delta\omega$ takes place at bus k. The tuning parameter for this HVDC-system is designated by K_{DC_r}.

$$\frac{\partial(\operatorname{tr} A(\Theta))}{\partial K_{\mathrm{DC}_r}} = -\operatorname{tr}\left\{M^{-1}\begin{pmatrix} 0 & \dots & 0 & \dots & 0 & \dots & 0 \\ \vdots & & & & & & \vdots \\ 0 & \dots & 1_{il} & \dots & -1_{ik} & \dots & 0 \\ \vdots & & & & & & \vdots \\ 0 & \dots & -1_{jl} & \dots & 1_{jk} & \dots & 0 \\ \vdots & & & & & & \\ 0 & \dots & 0 & \dots & 0 & \dots & 0 \end{pmatrix}\right\} \tag{D.4}$$

$k \neq i,\ l \neq j$

The gradient restricted to the SVC-parameters: Assume that an SVC is placed at bus i and the measurements take place at bus l ($\Delta\omega_l$) and bus k ($-\Delta\omega_k$).

$$\frac{\partial(\operatorname{tr} A(\Theta))}{\partial K_{\mathrm{SVC}_i}} = \operatorname{tr}\left\{M^{-1}\begin{pmatrix} & & l & & k & & \\ 0 & \dots & B(1,i) & \dots & -B(1,i) & \dots & 0 \\ \vdots & & \vdots & & \vdots & & \vdots \\ 0 & \dots & B(n,i) & \dots & -B(n,i) & \dots & 0 \end{pmatrix}\right\} \tag{D.5}$$

$l \neq k$

D.2 The Jacobian Matrix of the Constraint Function

The system matrix:

$$A = \begin{pmatrix} 0 & I \\ -M^{-1}K & -M^{-1}\tilde{D} \end{pmatrix}; \quad K^T = K$$

$$A^T A = \begin{pmatrix} (M^{-1}K)^T M^{-1}K & (M^{-1}K)^T M^{-1}\tilde{D} \\ (M^{-1}\tilde{D})^T M^{-1}K & I + (M^{-1}D)^T M^{-1}\tilde{D} \end{pmatrix}$$

$$\operatorname{tr} A^T A = \operatorname{tr}\left((M^{-1}K)^T M^{-1}K\right) + \operatorname{tr}\left((M^{-1}\tilde{D})^T M^{-1}\tilde{D}\right) + n$$

n = number of buses

A variation analysis of $\operatorname{tr} A^T A$ with respect to the parameters gives (first order approximation):

$$\begin{aligned}\delta\left(\operatorname{tr} A^T(\Theta)A(\Theta)\right) = \operatorname{tr}&\left(\delta(M^{-1}K)^T M^{-1}K\right) + \operatorname{tr}\left((M^{-1}K)^T \delta(M^{-1}K)\right) \\ &+ \operatorname{tr}\left(\delta(M^{-1}\tilde{D})^T M^{-1}\tilde{D}\right) + \operatorname{tr}\left((M^{-1}\tilde{D})^T \delta(M^{-1}\tilde{D})\right)\end{aligned}$$

Let C be a real general matrix, then it is easy to show that the first order approximation gives:

$$\delta(\operatorname{tr} C^T C) = 2\operatorname{tr} C^T \delta C = 2\operatorname{tr}((\delta C)^T C)$$

This will shorten the calculations. The matrix $\delta(M^{-1}\tilde{D})$ is already calculated, see the previous section. The matrix $M^{-1}K$ is constant.

Summary of the variation analysis:

$$\begin{aligned}\delta\left(\operatorname{tr} A^T(\Theta)A(\Theta)\right) = 2\operatorname{tr}\Big(&M^{-1}\Big(T_s^{\mathrm{DC}}\delta(K_{\mathrm{DC}})(T_m^{\mathrm{DC}})^T \\ &- B\delta(K_{se}) - BT_s^{\mathrm{SVC}}\delta(K_{\mathrm{SVC}})(T_m^{\mathrm{SVC}})^T\Big)\Big)^T M^{-1}\tilde{D}\end{aligned} \tag{D.6}$$

Now it is easy to calculate the Jacobian matrix. In this case, it is only a row vector with dimension $1 \times m$ (m number of parameters).

The partial derivatives are calculated in the same manner as for the gradient of the objective function.

D.3 Properties of the Optimization Problem

After some investigation of the general system, it become obvious that the influence on the damping from the K_{sed}-parameters was poor.

Variation of the K_{sed}-parameters mainly affects the imaginary part of the eigenvalues. That is why this appendix is devoted to the optimization problem with $K_{sed} = 0$ (matrix).

Both $\overline{\nabla}_{\Theta}\big(\operatorname{tr} A(\Theta)\big)$ and the Jacobian matrix of $\operatorname{tr} A^T(\Theta)A(\Theta)$ will be as follows.

PSS-equipment: Equation (D.3) gives:

$$\frac{\partial\big(\operatorname{tr} A(\Theta)\big)}{\partial K_{se_i}} = \frac{B(i,i)}{m_{ii}} \tag{D.7}$$

where m_{ii} is defined in Appendix C.

$$M = \operatorname{diag}\big(m_{ii}\big), \quad i = 1, \ldots, n$$

HVDC links: Equation (D.4) gives:

$$\frac{\partial\big(\operatorname{tr} A(\Theta)\big)}{\partial K_{\mathrm{DC}_r}} = -\left(m_{il}^{-1} + m_{jk}^{-1}\right) \tag{D.8}$$

This means no damping, if the measurements are taken strictly outside the siting of the rectifier and the inverter.

If the measurements are taken at the stations, then the

$$\frac{\partial\big(\operatorname{tr} A(\Theta)\big)}{\partial K_{\mathrm{DC}_r}} = -\left(m_{ii}^{-1} + m_{jj}^{-1}\right)$$

Finally, if one of the measurements are taken outside the station, e.g., the inverter station, then

$$\frac{\partial\big(\operatorname{tr} A(\Theta)\big)}{\partial K_{\mathrm{DC}_r}} = -m_{ii}^{-1}$$

SVC equipment: Equation (D.5) gives:

$$\frac{\partial\big(\operatorname{tr} A(\Theta)\big)}{\partial K_{\mathrm{SVC}_i}} = \frac{B(l,i)}{m_{ll}} - \frac{B(k,i)}{m_{kk}} \tag{D.9}$$

If the positive $\Delta\omega$-measurement is taken at the siting bus, the partial derivatives becomes

$$\frac{\partial\big(\operatorname{tr} A(\Theta)\big)}{\partial K_{\mathrm{SVC}_i}} = \frac{B(i,i)}{m_{ii}} - \frac{B(k,i)}{m_{kk}} \tag{D.10}$$

Similar expressions can be derived for the Jacobian matrix (vector) for the constraint function.

PSS equipment:

$$\frac{\partial \operatorname{tr}\left(\operatorname{tr} A^T(\Theta)A(\Theta)\right)}{\partial K_{se_i}} = -2\operatorname{tr}\left\{\begin{pmatrix} 0 & \dots & 0 \\ \vdots & & \vdots \\ \frac{B(1,i)}{m_{11}^2} & \dots & \frac{B(n,i)}{m_{nn}^2} \\ \vdots & & \vdots \\ 0 & \dots & 0 \end{pmatrix} \tilde{D}\right\}$$

If no incident on other equipment in the system occur, then

$$\frac{\partial\left(\operatorname{tr} A^T(\Theta)A(\Theta)\right)}{\partial K_{se_i}} = 2K_{se_i}\sum_{j=1}^{n}\frac{\left(B(j,i)\right)^2}{m_{jj}^2} \tag{D.11}$$

HVDC links:

$$\frac{\partial\left(\operatorname{tr} A^T(\Theta)A(\Theta)\right)}{\partial K_{\mathrm{DC}_r}} = 2\operatorname{tr}\left\{\begin{array}{c} \\ \end{array}\right.$$

$$\begin{array}{c} \\ l \\ k \end{array}\begin{array}{c} \begin{array}{cccc} i & & j & \end{array} \\ \begin{pmatrix} 0 & 0 & 0 & 0 \\ 0 & m_{ii}^{-1} & -m_{jj}^{-1} & 0 \\ 0 & -m_{ii}^{-1} & m_{jj}^{-1} & 0 \\ 0 & 0 & 0 & 0 \end{pmatrix} \end{array} \tilde{D}\left.\begin{array}{c} \\ \end{array}\right\}$$

If no incident on other damping equipment occur in the power system, then

$$\frac{\partial \operatorname{tr}\left(A^T(\Theta)A(\Theta)\right)}{\partial K_{\mathrm{DC}_r}} = 4K_{\mathrm{DC}_r}\left(m_{ii}^{-2} + m_{jj}^{-2}\right) \tag{D.12}$$

SVC equipment:

$$\frac{\partial\left(\operatorname{tr} A^T(\Theta)A(\Theta)\right)}{\partial K_{\mathrm{SVC}_i}} = -2\operatorname{tr}\left\{\begin{array}{c} \\ \end{array}\right.$$

$$\begin{array}{c} \\ l \\ \\ k \end{array}\begin{pmatrix} 0 & \dots & 0 \\ \vdots & & \vdots \\ \frac{B(1,i)}{m_{11}^2} & \dots & \frac{B(n,i)}{m_{nn}^2} \\ \vdots & & \vdots \\ -\frac{B(1,i)}{m_{11}^2} & \dots & -\frac{B(n,i)}{m_{nn}^2} \\ \vdots & & \vdots \\ 0 & \dots & 0 \end{pmatrix} \tilde{D}\left.\begin{array}{c} \\ \end{array}\right\}$$

If no incident on other equipment exists in the system, then

$$\frac{\partial(\operatorname{tr} A^T(\Theta)A(\Theta))}{\partial K_{\mathrm{SVC}_i}} = 4K_{\mathrm{SVC}_i} \sum_{j=1}^{n} \frac{\left(B(j,i)\right)^2}{m_{jj}^2} \tag{D.13}$$

From Eqs. (D.11), (D.12) and (D.13) we get the values on the diagonal of the Hessian matrix by derivation. The diagonal elements (h_{ii}) are for the different equipments:

$$h_{ii} = \begin{cases} 2\sum_{j=1}^{n} \frac{\left(B(j,i)\right)^2}{m_{jj}^2} & \text{with a PSS at nod } i \\ 4\left(m_{ii}^{-2} + m_{jj}^{-2}\right) & \text{with the rectifier at nod } i \text{ and the inverter at nod } j \\ 4\sum_{j=1}^{n} \frac{\left(B(j,i)\right)^2}{m_{jj}^2} & \text{with a SVC at nod } i \end{cases}$$

$$B(i,i) = \sum_{j \neq i} \sin\left(\theta_j - \theta_i\right) \frac{V_j}{X_{ij}} - \frac{\partial P_{L_i}}{\partial V_i}$$

$$B(l,i) = -\sin\left(\theta_l - \theta_i\right) \frac{V_l}{X_{il}}$$

E

Coherent Groups of the Nordel Power System

The coherency technique described in Chapter 3 is used for reduction of a large power system, Case 3, into two coherent power systems, Case 2, and Case 1.

Figure E.1 shows Case 1. The generator names and bus numbers are marked on the top of the buses.

Figure E.2 shows Case 2. The numbers within parenthesis are the designation of the group in Case 1. The groups are surrounded by solid lines. The generator names and bus numbers are marked on the top of the buses.

Figure E.3 contains four figures. The solid lines surrounds 21 groups, i.e. the figure describes how Case 3 is aggregated into Case 1. The numbers within the parentheses are the designation of corresponding buses in Case 1.

Figure E.4 contains four figures. The solid lines surrounds 44 groups of generators, i.e. the figure describes how Case 3 is aggregated into Case 2. The numbers within the parentheses are the designation of corresponding buses in Case 2.

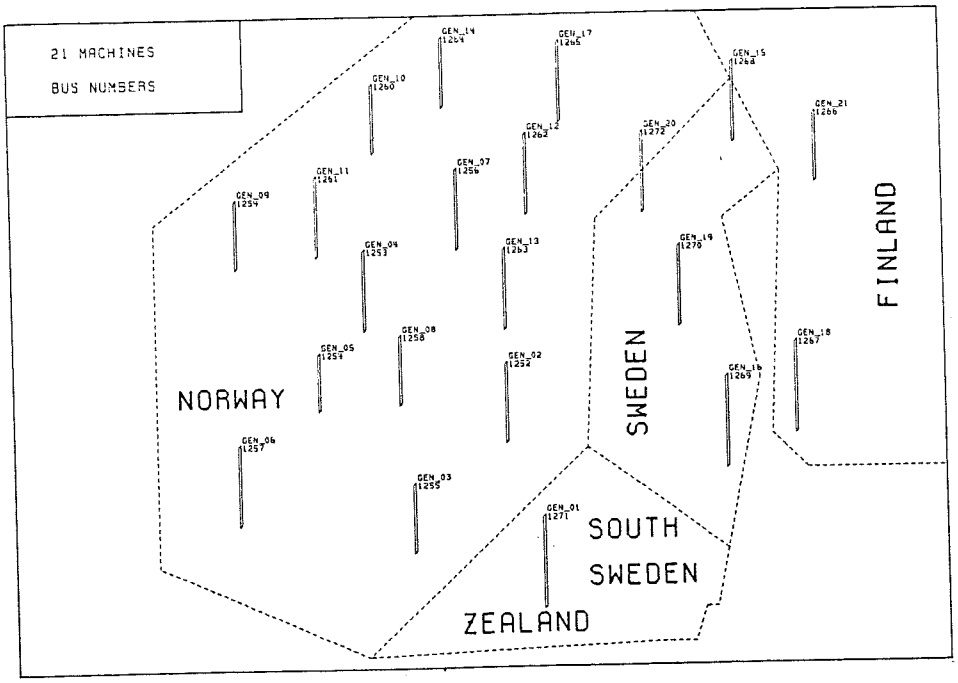

Figure E.1 21 coherent generators out of 224 generators.

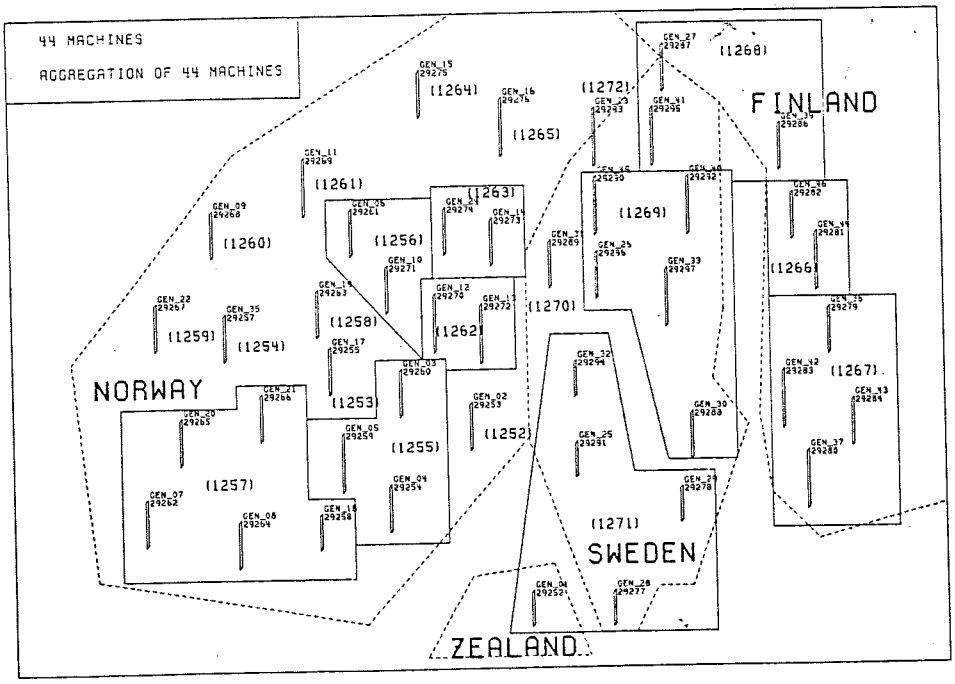

Figure E.2 Aggregation of 44 generators into 21 coherent generators.

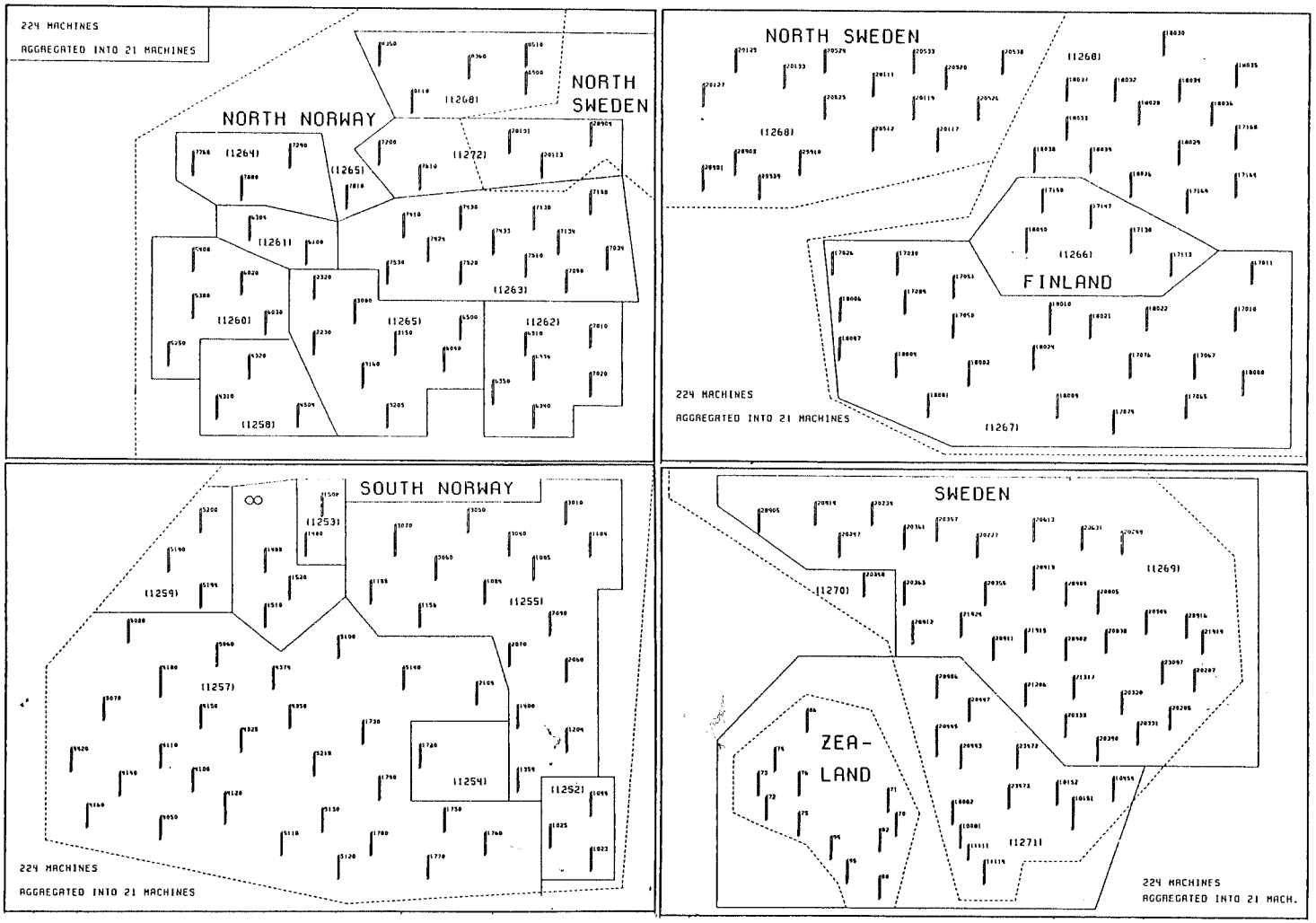

Figure E.3 Aggregation of 224 generators into 21 coherent generators.

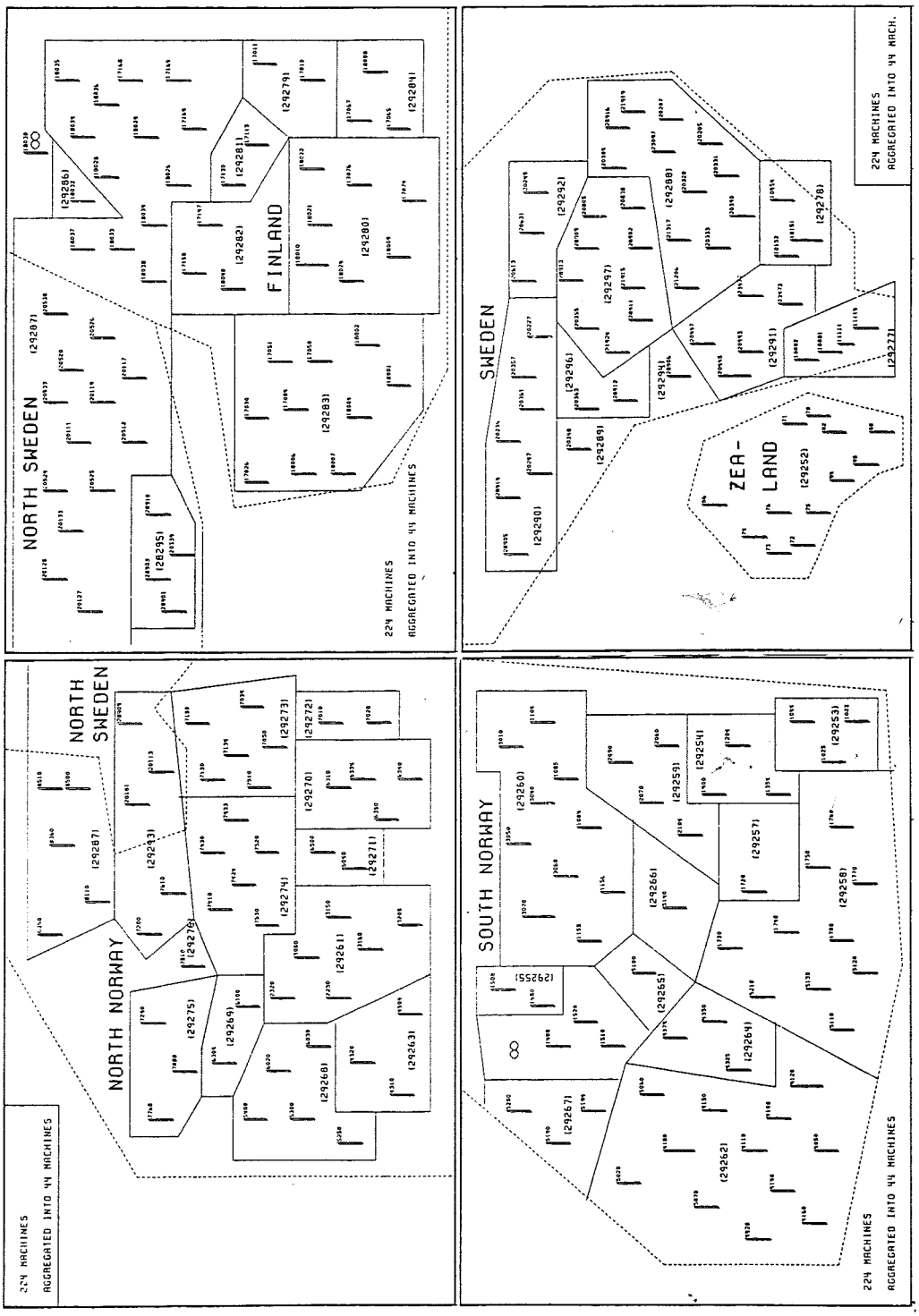

Figure E.4 Aggregation of 224 generators into 44 coherent generators.